Critical Fields in Heavy Nuclei and Massive Nuclear Cores

Contents

1. Topics

- On the gravitational and electrodynamical stability of nuclear matter cores
- Electrodynamics for Nuclear Matter in Bulk
- On the Charge to Mass ratio of Neutron Cores and Heavy Nuclei
- Supercritical fields on the surface of massive nuclear cores: neutral core v.s. charged core
- The extended nuclear matter model with smooth transition surface
- Electron-positron pairs production in an electric potential of massive cores
- On the General Relativistic Thomas-Fermi Model for Neutron Star Cores
- The Crust of Neutron Stars and its connection with the Fireshell Model of GRBs

2. Participants

2.1. ICRANet participants

- D. Arnett (Steward Observatory, University of Arizona, USA)
- W. Greiner (Institut für Theoretical Physics Johann Wolfgang Goethe-Universität, Frankfurt am Main)
- H. Kleinert (Free University of Berlin , Germany)
- V. Popov (ITEP, Moscow, Russia)
- M. Rotondo (ICRANet, University of Rome, Italy)
- R. Ruffini (ICRANet, University of Rome, Italy)
- G.'t Hooft (Institute for Theoretical Physic Universiteit Utrecht)
- S.-S. Xue (ICRANet)

2.2. Past collaborators

- L. Stella (Rome Astronomical Observatory, Italy)

2.3. On going collaborations

2.4. Ph.D. and M.S. Students

- B. Patricelli (ICRANet, University of Rome, Italy)
- J. A. Rueda Hernandez (ICRANet, University of Rome, Italy)
- R. Belvedere (ICRANet, University of Rome, Italy)
- D. Pugliese (ICRANet, University of Rome, Italy)

3. Introduction

One of the most active field of research has been to analyse a general approach to Neutron Stars based on the Thomas-Fermi ultrarelativistic equations amply adopted in the study of superheavy nuclei. The aim is to have a unified approach both to superheavy nuclei, up to atomic numbers of the order of 10^5–10^6, and to what we have called Massive Nuclear Cores. These Massive Nuclear Cores are

- characterized by atomic number of the order of 10^{57};
- composed by neutrons, protons and electrons in β–equilibrium;
- expected to be kept at nuclear density by self gravity.

The analysis of superheavy nuclei has historically represented a major field of research, guided by Prof. V. Popov and Prof. W. Greiner and their schools. This same problem was studied in the context of the relativistic Thomas-Fermi equation also by R. Ruffini and L. Stella, already in the 80s. The recent approach was started with the Ph.D. Thesis of M. Rotondo and has shown the possibility to extrapolate this treatment of superheavy nuclei to the case of Massive Nuclear Cores. The very unexpected result has been that also around these massive cores there is the distinct possibility of having an electromagnetic field close to the critical value $E_c = \frac{m_e^2 c^3}{e\hbar}$, although localized in a very narrow shell of the order of the electron Compton wavelength (see Fig. 3.1, 3.2).

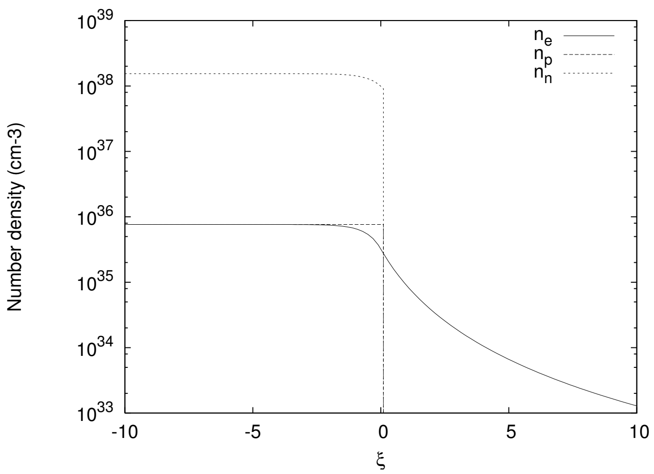

Figure 3.1.: Number density of electrons, protons and neutrons.

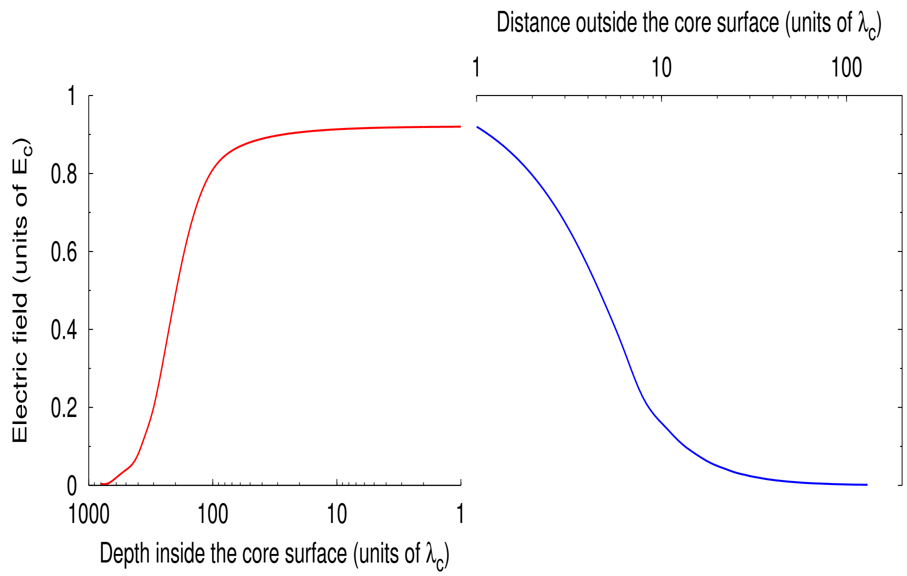

Figure 3.2.: Electric Field in units of the critical field.

The welcome result has been that all the analytic work developed by Prof. Popov and the Russian school can be straightforwardly applied to the case of massive cores, if the β–equilibrium condition is properly taken into account. This has been the result obtained and published by Ruffini, Xue and Rotondo already in 2007. Since then, a large variety of problems has emerged, which have seen the direct participation at ICRANet of Prof. Greiner, Prof. Popov, and Prof. 't Hooft. The crucial issue to be debated is the stability of such cores under the competing effects of self gravity and Coulomb repulsion. In order to probe this stability, we have started a new approach to the problem within the framework of general relativity. The object of the work by Patricelli and Rueda is the generalization of the Tolman-Oppenheimer-Volkoff equation duly taking into account the elecrodynamical contribution. The major scientific issue here is to have a unified approach solving the coupled system of the general relativistic self gravitating electrodynamical problem with the corresponding formulation of the Thomas-Fermi equation in the framework of general relativity. Prof. 't Hooft, in a series of lectures, has forcefully expressed the opinion that necessarily, during the process of gravitational collapse, it should occur a more extended distribution of the electromagnetic field to the entire core of the star and not only confined to a thin shell. This is a necessary condition in order to transmit the gravitational energy of the collapse to the electrodynamical component of the field giving possibly rise to large pair creation processes. This crucial idea is currently being pursued by the application to this system of a classical work of Feynmann-Metropolis and Teller, who considered in relativistic Thomas-Fermi the crucial role of non-degeneracy.

4. Brief description

4.1. On the gravitational and electrodynamical stability of nuclear matter cores

Using an explicit analytic solution of the relativistic Thomas-Fermi equation we show that a core of neutrons, protons and electrons in beta equilibrium at nuclear densities has stable configurations both in the limit of superheavy nuclei with mass number $A \approx 10^4$–10^6 and in the limit of massive cores with $A \approx (m_{Planck}/m_n)^3 \sim 10^{57}$. These are globally neutral configurations which have a maximum value of the electric field $E_{max} = 0.95\sqrt{\alpha} m_\pi^2 c^3/e\hbar$ near the core surface. This electric field, the value of which is below the critical value for muon and pion production but well above the critical value $E_c = m_e^2 c^3/e\hbar$ for electron-positron pair creation, is stabilized against pair creation by the degenerate electrons present in the configuration (Pauli blocking). On the one extreme, superheavy nuclei are bound together by the strong interactions, while on the other extreme we show that globally neutral massive cores can be gravitationally bound. The value of the charge-to-mass ratios predicted at the surface of massive cores coincides with the range of values expected in astrophysical scenarios for Kerr-Newman black holes (see Appendix A.1).

4.2. Electrodynamics for Nuclear Matter in Bulk

A general approach to analyze the electrodynamics of nuclear matter in bulk is presented using the relativistic Thomas-Fermi equation generalizing to the case of $N \simeq (m_{\text{Planck}}/m_n)^3$ nucleons of mass m_n the approach well tested in very heavy nuclei ($Z \simeq 10^6$). Particular attention is given to implement the condition of charge neutrality globally on the entire configuration, versus the one usually adopted on a microscopic scale. As the limit $N \simeq (m_{\text{Planck}}/m_n)^3$ is approached the penetration of electrons inside the core increases and a relatively small tail of electrons persists leading to a significant electron density outside the core. Within a region of 10^2 electron Compton wavelength near the core surface electric fields close to the critical value for pair creation by vacuum polarization effect develop. These results can have important consequences on the understanding of physical process in neutron stars structures as well as on the initial conditions leading to the process of gravitational collapse to a black hole (see Appendix A.2).

4.3. On the Charge to Mass ratio of Neutron Cores and Heavy Nuclei

We determine theoretically the relation between the total number of protons N_p and the mass number A (the charge to mass ratio) of nuclei and neutron cores with the model recently proposed by Ruffini et al. (2007) and we compare it with other N_p versus A relations: the empirical one, related to the Periodic Table, and the semi-empirical relation, obtained by minimizing the Weizsäcker mass formula. We find that there is a very good agreement between all the relations for values of A typical of nuclei, with differences of the order of per cent. Our relation and the semi-empirical one are in agreement up to $A \approx 10^4$ for higher values, we find that the two relations differ. We interpret the different behavior of our theoretical relation as a result of the penetration of electrons (initially confined in an external shell) inside the core, that becomes more and more important by increasing A; these effects are not taken into account in the semi-empirical mass-formula (see Appendix A.3).

4.4. Supercritical fields on the surface of massive nuclear cores: neutral core v.s. charged core

Based on the Thomas-Fermi approach, we describe and distinguish the electron distributions around extended nuclear cores: (i) in the case that cores are neutral for electrons bound by protons inside cores and proton and electron numbers are the same; (ii) in the case that super charged cores are bare, electrons (positrons) produced by vacuum polarization are bound by (fly into) cores (infinity) (see Appendix A.4).

4.5. The extended nuclear matter model with smooth transition surface

The existence of electric fields close to their critical value $E_c = \frac{m_e^2 c^3}{e\hbar}$ has been proved for massive cores of 10^7 up to 10^{57} nucleons using a distribution of constant nuclear density and a sharp step function at its boundary. We explore the modifications of this effect by considering a smoother density profile with a proton distribution fulfilling a Wood-Saxon dependence. The occurrence of a critical field has been confirmed. We discuss how the location of the maximum of the electric field as well as its magnitude is modified by the smoother distribution (see Appendix A.5).

4.6. Electron-positron pairs production in an electric potential of massive cores

Classical and semi-classical energy states of relativistic electrons bounded by a massive and charged core with the charge-mass-radio Q/M and macroscopic radius R_c are discussed. We show that the energies of semi-classical (bound) states can be much smaller than the negative electron mass-energy ($-mc^2$), and energy-level crossing to negative energy continuum occurs. Electron $-$ positron pair production takes place by quantum tunneling, if these bound states are not occupied. Electrons fill into these bound states and positrons go to infinity. We explicitly calculate the rate of pair-production, and compare it with the rates of electron-positron production by the Sauter-Euler-Heisenberg-Schwinger in a constant electric field. In addition, the pair-production rate for the electro-gravitational balance ratio $Q/M = 10^{-19}$ is much larger than the pair-production rate due to the Hawking processes. We point out that in neutral cores with equal proton and electron numbers, the configuration of relativistic electrons in these semi-classical (bound) states should be stabilized by photon emissions (see Appendix B).

4.7. On the General Relativistic Thomas-Fermi Model for Neutron Star Cores

The connection between the generalized Tolman-Oppenheimer-Volkoff (TOV) equation for charged fluids and the Thomas-Fermi approach for atoms is used to formulate a general relativistic model for neutron star cores composed by degenerate electrons, protons and neutrons. We show that the TOV equation can be reduced to a "conservation" equation for the general relativistic Fermi energies of the particles. In fact, by assuming the Thomas-Fermi equilibrium condition for the electron gas ($E_e^F = 0$) and the $\beta-$equilibrium we find that the Fermi energy of each component of the gas is constant on the whole configuration. We demonstrate analytically that the system does not satisfy the local charge neutrality, which is generally assumed, but instead it acquires a small net charge. Following Ruffini et al. (2007) we show that in order to neutralize the system a critical electric field on the core surface should exist(see Appendix C).

4.8. The Crust of Neutron Stars and its connection with the Fireshell Model of GRBs

We study the characteristics of the Outer Crust of Neutron Stars, that is the region of Neutron Stars characterized by a mass density less than the "neutron drip" density and composed by White Dwarf - like material (fully ionized nuclei and free electrons). In particular, we calculate its mass and its thickness (M_{crust} and ΔR_{crust} respectively) with a general relativistic model, finding that the Outer Crust is smaller in mass and in radial extension for stars with more compact Cores. We also propose a correlation with the Fireshell Model of GRBs, that assumes that GRBs originates from the gravitational collapse to a black hole. One of the parameters used in this model is the baryon loading B of the electron - positron plasma, related to the mass of the baryonic remnant of the star progenitor M_B. We propose that B originates from the Crust of Neutron Stars and we compare M_{crust} with the values of M_B used to reproduce the observed data, finding that they are compatible (see Appendix D).

4.9. The Role of Thomas Fermi approach in Neutron Star Matter

The role of the Thomas-Fermi approach in Neutron Star matter cores is presented and discussed with special attention to solutions globally neutral and not fulfilling the traditional condition of local charge neutrality. A new stable and energetically favorable configuration is found. This new solution can be of relevance in understanding unsolved issues of the gravitational collapse processes and their energetics (see Appendix E).

5. Publications (before 2007)

1. J. Ferreirinho, R. Ruffini and L. Stella, “On the relativistic Thomas-Fermi model”, Phys. Lett. B 91, (1980) 314. The relativistic generalization of the Thomas-Fermi model of the atom is derived. It approaches the usual nonrelativistic equation in the limit $Z \ll Z_{\mathrm{crit}}$, where Z is the total number of electrons of the atom and $Z_{\mathrm{crit}} = (3\pi/4)^{1/2}\alpha^{-3/2}$ and α is the fine structure constant. The new equation leads to the breakdown of scaling laws and to the appearance of a critical charge, purely as a consequence of relativistic effects. These results are compared and contrasted with those corresponding to N self-gravitating degenerate relativistic fermions, which for $N \approx N_{\mathrm{crit}} = (3\pi/4)^{1/2}(m/m_p)^3$ give rise to the concept of a critical mass against gravitational collapse. Here m is the mass of the fermion and $m_p = (\hbar c/G)^{1/2}$ is the Planck mass.

2. R. Ruffini and L. Stella,“Some comments on the relativistic Thomas-Fermi model and the Vallarta-Rosen equation”, Phys. Lett. B 102 (1981) 442. Some basic differences between the screening of the nuclear charge due to a relativistic cloud of electrons in a neutral atom and the screening due to vacuum polarization effects induced by a superheavy ion are discussed.

6. Publications (2007-2008)

1. R. Ruffini, M. Rotondo and S.-S. Xue,"Electrodynamics for Nuclear Matter in Bulk ", Int. Journ. Mod. Phys. D Vol. 16, No. 1 (2007) 1-9.

   A general approach to analyze the electrodynamics of nuclear matter in bulk is presented using the relativistic Thomas-Fermi equation generalizing to the case of $N \simeq (m_{\rm Planck}/m_n)^3$ nucleons of mass m_n the approach well tested in very heavy nuclei ($Z \simeq 10^6$). Particular attention is given to implement the condition of charge neutrality globally on the entire configuration, versus the one usually adopted on a microscopic scale. As the limit $N \simeq (m_{\rm Planck}/m_n)^3$ is approached the penetration of electrons inside the core increases and a relatively small tail of electrons persists leading to a significant electron density outside the core. Within a region of 10^2 electron Compton wavelength near the core surface electric fields close to the critical value for pair creation by vacuum polarization effect develop. These results can have important consequences on the understanding of physical process in neutron stars structures as well as on the initial conditions leading to the process of gravitational collapse to a black hole.

2. R. Ruffini, M. Rotondo and S.-S. Xue, "On the gravitational and electrodynamical stability of nuclear matter in bulk", submitted to Phy. Rev. Lett.

   Using an explicit analytic solution of the relativistic Thomas-Fermi equation we show that a core of neutrons, protons and electrons in beta equilibrium at nuclear densities has stable configurations both in the limit of superheavy nuclei with mass number $A \approx 10^4$–10^6 and in the limit of massive cores with $A \approx (m_{Planck}/m_n)^3 \sim 10^{57}$. These are globally neutral configurations which have a maximum value of the electric field $E_{max} = 0.95\sqrt{\alpha}m_\pi^2 c^3/e\hbar$ near the core surface. This electric field, the value of which is below the critical value for muon and pion production but well above the critical value $E_c = m_e^2 c^3/e\hbar$ for electron-positron pair creation, is stabilized against pair creation by the degenerate electrons present in the configuration (Pauli blocking). On the one extreme, superheavy nuclei are bound together by the strong interactions, while on the other extreme we show that globally neutral massive cores can be gravitationally bound. The value of the charge-to-mass ratios predicted at the surface of massive cores coincides with the range of values expected in astrophysical scenarios for Kerr-Newman black holes.

3. R. Ruffini, M. Rotondo and S.-S. Xue, "Neutral nuclear core vs super

charged one ”, in Proceedings of the Eleventh Marcel Grossmann Meeting, R. Jantzen, H. Kleinert, R. Ruffini (eds.), (World Scientific, Singapore, 2008).

Based on the Thomas-Fermi approach, we describe and distinguish the electron distributions around extended nuclear cores: (i) in the case that cores are neutral for electrons bound by protons inside cores and proton and electron numbers are the same; (ii) in the case that super charged cores are bare, electrons (positrons) produced by vacuum polarization are bound by (fly into) cores (infinity).

4. R. Ruffini and S.-S. Xue, “Electron-positron pairs production in an electric potential of massive cores ”, to be submitted to Phys. Lett. B

   Classical and semi-classical energy states of relativistic electrons bounded by a massive and charged core with the charge-mass-radio Q/M and macroscopic radius R_c are discussed. We show that the energies of semi-classical (bound) states can be much smaller than the negative electron mass-energy ($-mc^2$), and energy-level crossing to negative energy continuum occurs. Electron-positron pair production takes place by quantum tunneling, if these bound states are not occupied. Electrons fill into these bound states and positrons go to infinity. We explicitly calculate the rate of pair-production, and compare it with the rates of electron-positron production by the Sauter-Euler-Heisenberg-Schwinger in a constant electric field. In addition, the pair-production rate for the electro-gravitational balance ratio $Q/M = 10^{-19}$ is much larger than the pair-production rate due to the Hawking processes. We point out that in neutral cores with equal proton and electron numbers, the configuration of relativistic electrons in these semi-classical (bound) states should be stabilized by photon emissions.

5. B. Patricelli, M. Rotondo and R. Ruffini, “On the Charge to Mass Ratio of Neutron Cores and Heavy Nuclei”, AIP Conference Proceedings, Vol. 966 (2008), pp. 143-146.

   We determine theoretically the relation between the total number of protons N_p and the mass number A (the charge to mass ratio) of nuclei and neutron cores with the model recently proposed by Ruffini et al. (2007) and we compare it with other N_p versus A relations: the empirical one, related to the Periodic Table, and the semi-empirical relation, obtained by minimizing the Weizsäcker mass formula. We find that there is a very good agreement between all the relations for values of A typical of nuclei, with differences of the order of per cent. Our relation and the semi-empirical one are in agreement up to $A \approx 10^4$ for higher values, we find that the two relations differ. We interpret the different behavior of our theoretical relation as a result of the penetration of electrons (initially confined in an external shell) inside the core, that becomes more and more important by increasing A; these effects are not taken into account in the semi-empirical mass-formula.

6. M. Rotondo, R. Ruffini and S.-S Xue, "On the Electrodynamical properties of Nuclear matter in bulk", AIP Conference Proceedings, Vol. 966 (2008), pp. 147-152.

   We analyze the properties of solutions of the relativistic Thomas-Fermi equation for globally neutral cores with radius of the order of $R \approx 10$ Km, at constant densities around the nuclear density. By using numerical tecniques as well as well tested analytic procedures developed in the study of heavy ions, we confirm the existence of an electric field close to the critical value $E_c = m_e^2 c^3/e\hbar$ in a shell $\Delta R \approx 10^4 \hbar/m_\pi c$ near the core surface. For a core of ≈ 10 Km the difference in binding energy reaches 10^{49} ergs. These results can be of interest for the understanding of very heavy nuclei as well as physics of neutron stars, their formation processes and further gravitational collapse to a black hole.

7. B. Patricelli, M. Rotondo, J. A. Rueda H. and R. Ruffini, "The Electrodynamics of the Core and the Crust components in Neutron Stars", AIP Conference Proceedings, Vol. 1059 (2008), pp. 68-71.

   We study the possibility of having a strong electric field (E) in Neutron Stars. We consider a system composed by a core of degenerate relativistic electrons, protons and neutrons, surrounded by an oppositely charged leptonic component and show that at the core surface it is possible to have values of E of the order of the critical value for electron-positron pair creation, depending on the mass density of the system. We also describe Neutron Stars in general relativity, considering a system composed by the core and an additional component: a crust of white dwarf - like material. We study the characteristics of the crust, in particular we calculate its mass M_{crust}. We propose that, when the mass density of the star increases, the core undergoes the process of gravitational collapse to a black hole, leaving the crust as a remnant; we compare M_{crust} with the mass of the baryonic remnant considered in the fireshell model of GRBs and find that their values are compatible.

8. R. Ruffini, "The Role of Thomas Fermi approach in Neutron Star Matter", to be published in the Proceedings of the 9^{th} International Conference "Path Integrals - New trends and perspectives", Max Planck Institute for the Physics of Complex Systems, Dresden, Germany, Semptember 23 - 28 2007, World Scientific 207 - 218 (2008), eds. W. Janke and A. Pelster

   The role of the Thomas-Fermi approach in Neutron Star matter cores is presented and discussed with special attention to solutions globally neutral and not fulfilling the traditional condition of local charge neutrality. A new stable and energetically favorable configuration is found. This new solution can be of relevance in understanding unsolved issues of the gravitational collapse processes and their energetics.

7. Invited talks in international conferences

1. XI Marcel Grossmann Meeting on General Relativity, July 23-29 2006, Berlin (Germany).
2. APS April meeting, April 14-17 2007, Jacksonville (USA).
3. Path Integrals - New Trends and Perspectives, September 23 - 28 2007, Dresden (Germany)
4. APS April meeting, April 12-15 2008, Saint Louis (USA).
5. V Italian-Sino Workshop, May 28- June 1 2008, Taipei (Taiwan).
6. III Stueckelberg Workshop, July 8-18 2008, Pescara (Italy).
7. XIII Brazilian School of Cosmology and Gravitation, July 20-August 2 2008, Rio de Janeiro (Brazil).
8. Probing stellar populations out to the distant universe, September 7-19 2008, Cefalù (Italy).

8. APPENDICES

A. Solution to Thomas-Fermi Equation for large nuclear cores

A.1. On the gravitational and electrodynamical stability of nuclear matter cores

Having proposed a relativistic Thomas-Fermi model for a unified treatment of globally neutral systems ranging from atoms with superheavy nuclei to supermassive cores at nuclear densities (1), we were naturally interested in the proposal by Jes Madsen (2) of a relation between the maximum charge and radius of any static, spherically symmetric maximally charged object ranging from superheavy nuclei to neutron stars and black holes, based on the relativistic Thomas-Fermi model. At present the observations of neutron stars in millisecond binary pulsars (3; 4) lead to estimates of their masses approaching but not exceeding the absolute upper limit for the mass of a neutron star (5), and which are sufficiently close to that limit to exclude all known equations of state (EOS) (6). The problem of the emission of a remnant during the gravitational collapse which leads to the formation of a neutron star is still unresolved (7). Equally challenging is the identification of the electrodynamical process around neutron stars taking place during the gravitational collapse phase which generates the copious e^+e^- electron-positron pair production powering Gamma-Ray Bursts (8). The fundamental understanding reachable by a rigorous analysis of the relativistic Thomas-Fermi model, important in its own right, can therefore identify new physical effects to be accounted for using a more complete EOS and consequently overcome these difficulties and address the new challenges.

We therefore present here some results complementary to those of Madsen in addition to the ones we have already obtained numerically (1), now made possible by a particular explicit analytic solution of the Thomas-Fermi equations, a solution with boundary conditions which are physically quite different from those used by Madsen. This analytic solution describes a system of neutrons, protons and electrons in beta equilibrium at nuclear densities having a mass number $A \approx 10^4$–10^6 in the limit of atoms with superheavy nuclei and $A \approx (m_{Planck}/m_n)^3 \sim 10^{57}$ in the limit of massive cores. The former case generalizes the classic results of Greiner (9; 10; 11) and Popov (12; 13; 14), while in the latter case the analytic expression agrees with previous numerical solutions (1). In both cases a supercritical field exists in a shell of thickness $\approx 10^2\hbar/m_\pi c$ at the core surface, and a charged lepton-baryonic core is surrounded by an oppositely charged leptonic component. Such massive cores appear to be stable both with respect to gravity and to Coulomb repulsion of the proton component. Thus while superheavy nuclei for small A are stabilized by the effect of strong interactions at least in limited charge range (9; 10; 11; 12; 13; 14), the gravitational interaction alone appears to be sufficient for the stability of the massive cores. A direct comparison is made below between our globally neutral solutions and the charged ones recently discussed by Madsen.

The analytic solution representing a core of degenerate neutrons, protons and electrons is obtained by assuming N_p protons are distributed at a constant density n_p within a radius

$$R_c = \Delta \frac{\hbar}{m_\pi c} N_p^{1/3}\,, \tag{A.1.1}$$

where m_π is the pion mass and Δ is a parameter such that the condition $\Delta \approx 1$ ($\Delta < 1$), when applied to ordinary nuclei, corresponds to nuclear (supranuclear) densities. The overall Coulomb potential satisfies the Poisson equation

$$\nabla^2 V(r) = -4\pi e \left[n_p(r) - n_e(r)\right] \tag{A.1.2}$$

with the boundary conditions $V(\infty) = 0$ (due to the global charge neutrality of the system) and $V(0) =$ finite. The density of the electrons of mass m_e and charge -e is determined by the Fermi energy condition

$$E_e^F = [(P_e^F c)^2 + m_e^2 c^4]^{1/2} - m_e c^2 - eV(r) = 0\,, \tag{A.1.3}$$

or

$$n_e(r) = \frac{1}{3\pi^2\hbar^3 c^3}\left[e^2V^2(r) + 2m_e c^2 eV(r)\right]^{3/2}. \tag{A.1.4}$$

By introducing the dimensionless quantities $x = r/[\hbar/m_\pi c]$, $x_c = R_c/[\hbar/m_\pi c]$ and $\chi/r = eV(r)/c\hbar$, the relativistic Thomas-Fermi equation takes the form

$$\frac{1}{3x}\frac{d^2\chi(x)}{dx^2} = -\frac{\alpha}{\Delta^3}\theta(x_c - x) + \frac{4\alpha}{9\pi}\left[\frac{\chi^2(x)}{x^2} + 2\frac{m_e}{m_\pi}\frac{\chi}{x}\right]^{3/2} \tag{A.1.5}$$

where as usual $\alpha = e^2/(\hbar c)$ and $\chi(0) = 0, \chi(\infty) = 0$. In the current literature phenomenological expressions have been assumed both for the radius $R_c \approx 1.5 \times 10^{-13} A^{1/3}$ cm of the core as a function of the mass number A, and for the relation between A and N_p (11; 14; 15)

$$N_p \simeq \frac{A}{2}, \tag{A.1.6}$$

or

$$N_p \simeq \left[\frac{2}{A} + \frac{3}{200}\frac{1}{A^{1/3}}\right]^{-1}. \tag{A.1.7}$$

Instead of these phenomenological expressions, Eq. (A.4.1) and the condition of beta equilibrium have been adopted in our treatment. The neutron density $n_n(r)$ is determined by the Fermi energy condition on their Fermi momentum P_n^F imposed by beta equilibrium

$$\begin{aligned} E_n^F &= [(P_n^F c)^2 + m_n^2 c^4]^{1/2} - m_n c^2 \\ &= [(P_p^F c)^2 + m_p^2 c^4]^{1/2} - m_p c^2 + eV(r) \end{aligned} \tag{A.1.8}$$

which in turn is related to the proton and electron densities by Eqs. (A.4.7), (A.1.4) and (E.0.12).

These equations have been integrated numerically (1), and a new generalized relation between A and N_p has been derived for any value of A which agrees remarkably well with the phenomenological relations given by Eqs. (E.0.7) and (A.1.7) in the limit of $A < 300$ (see Fig. A.1).

The ultrarelativistic case for massive cores is the relevant one for studying the onset of gravitational collapse. In this limit, as in the case of heavy nuclei (14), the relativistic Thomas-Fermi equation admits an analytic solution. Introducing the new function ϕ defined by

$$\phi = \Delta\left[\frac{4}{9\pi}\right]^{1/3}\frac{\chi}{x},$$

and the new variables $\hat{x} = (12/\pi)^{1/6}\sqrt{\alpha}\Delta^{-1}x$, $\xi = \hat{x} - \hat{x}_c$, where $\hat{x}_c = (12/\pi)^{1/6}\sqrt{\alpha}\Delta^{-1}x_c$, then Eq. (5) becomes

$$\frac{d^2\hat{\phi}(\xi)}{d\xi^2} = -\theta(-\xi) + \hat{\phi}(\xi)^3, \tag{A.1.9}$$

where $\hat{\phi}(\xi) = \phi(\xi + \hat{x}_c)$. The boundary conditions on $\hat{\phi}$ are: $\hat{\phi}(\xi) \to 1$ as $\xi \to -\hat{x}_c \ll 0$ (at the massive core center) and $\hat{\phi}(\xi) \to 0$ as $\xi \to \infty$. The function $\hat{\phi}$ and its first derivative $\hat{\phi}'$ must be continuous at the surface $\xi = 0$

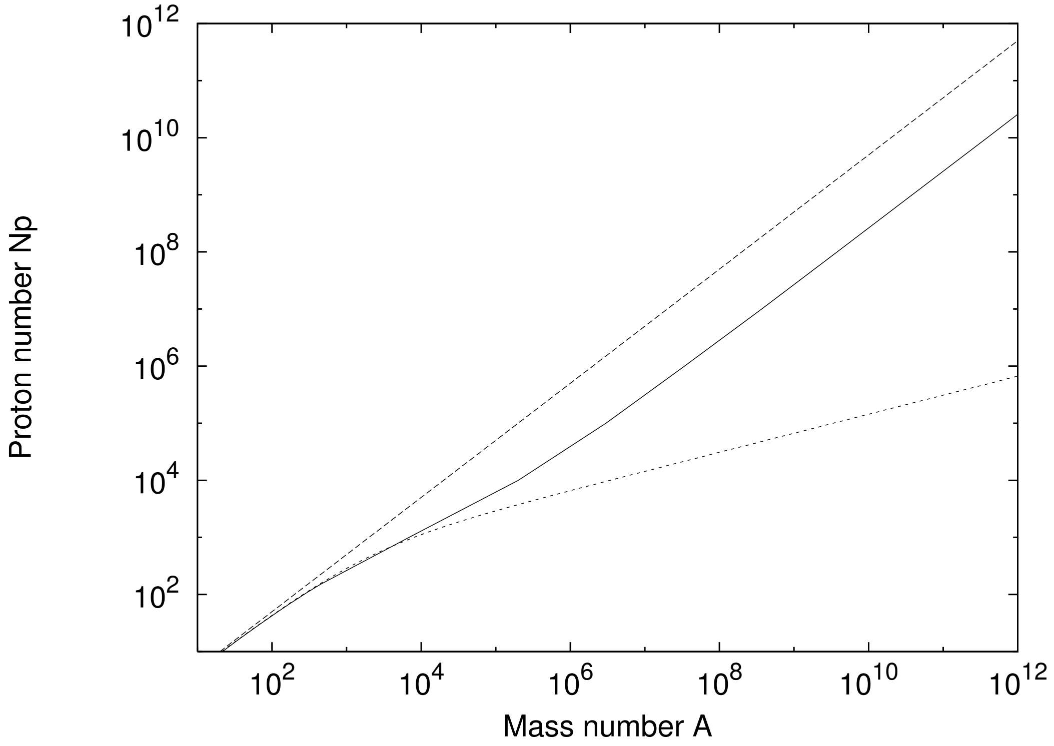

Figure A.1.: Our A-N_p relation at nuclear density (solid line) obtained from first principles compared with the phenomenological expressions given by Eq. (E.0.7) (dashed line) and Eq. (A.1.7) (dotted line).

of the massive core. Eq. (E.0.15) admits an exact solution

$$\hat{\phi}(\xi) = \begin{cases} 1 - 3\left[1 + 2^{-1/2}\sinh(a - \sqrt{3}\xi)\right]^{-1}, & \xi < 0, \\ \dfrac{\sqrt{2}}{(\xi + b)}, & \xi > 0, \end{cases}$$

where the integration constants a and b have the values $a = \mathrm{arcsinh}(11\sqrt{2}) = 3.439$, $b = (4/3)\sqrt{2} = 1.886$. We can next evaluate the Coulomb potential energy function

$$eV(\xi) = \left(\frac{9\pi}{4}\right)^{1/3} \frac{1}{\Delta} m_\pi c^2 \hat{\phi}(\xi), \tag{A.1.10}$$

and by differentiation, the electric field

$$E(\xi) = \left(\frac{3\pi}{4}\right)^{1/6} \frac{1}{\Delta^2} \frac{m_\pi^2 c^4}{(\hbar c)^{3/2}} \hat{\phi}'(\xi). \tag{A.1.11}$$

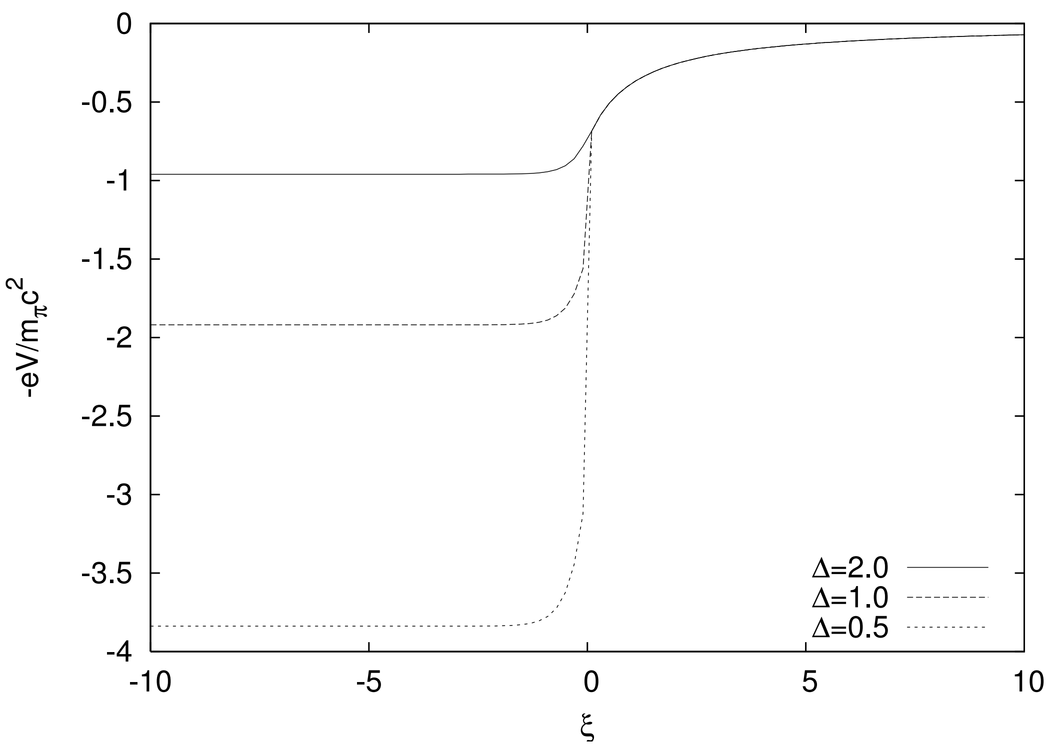

Figure A.2.: The electron Coulomb potential energy $-eV$, in units of pion mass m_π is plotted as a function of the radial coordinate $\xi = \hat{x} - \hat{x}_c$, for selected values of the density parameter Δ.

Details are given in Figs. E.5 and A.3.

Next we can estimate two crucial quantities: the Coulomb potential at the center of the configuration and the electric field at the surface of the core

$$eV(0) \approx \left(\frac{9\pi}{4}\right)^{1/3} \frac{1}{\Delta} m_\pi c^2 \,, \tag{A.1.12}$$

$$E_{max} \approx 0.95\sqrt{\alpha}\frac{1}{\Delta^2}\frac{m_\pi^2 c^3}{e\hbar} \,. \tag{A.1.13}$$

Most remarkably these two quantities are functions only of the pion mass m_π, the density parameter Δ and of course the fine constant structure α and their formulas apply over the entire range from superheavy nuclei with $N_p \leq 10^3$ all the way to massive cores with $N_p \approx (m_{Planck}/m_n)^3$.

This critical field E_{max} is totally analogous to the one considered by Heisenberg and Euler in the context of elementary particles differing only by the replacement of the pion mass by the electron mass (16). Having established

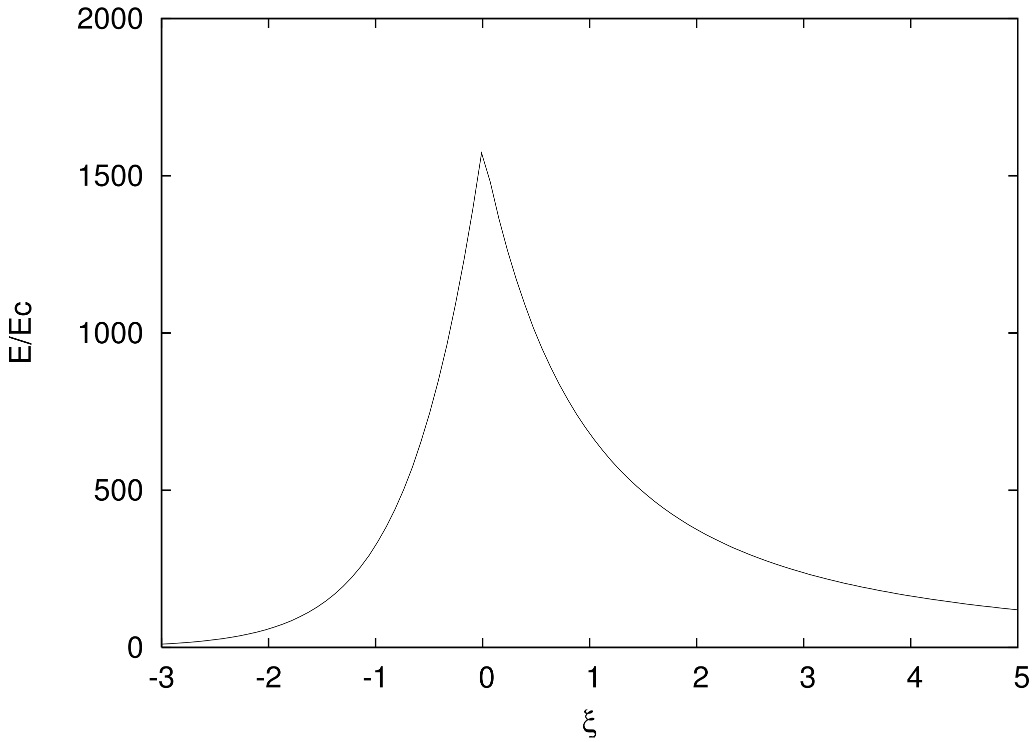

Figure A.3.: The electric field, in units of the critical field E_c, is plotted as a function of the radial coordinate ξ for Δ=2.

the validity of the above equations both for superheavy nuclei and for massive cores, we now outline some fundamental differences between these two systems. We find the charge-to-mass ratio

$$\frac{Q}{\sqrt{G}M} \approx \frac{E_{max}R_c^2}{\sqrt{G}m_n A} \approx \left(\frac{m_{Planck}}{m_n}\right)\left(\frac{1}{N_p}\right)^{1/3}\frac{N_p}{A} \tag{A.1.14}$$

for the effective charge Q at the core surface and the mass M, where m_n is the nucleon mass. We see immediately that for superheavy nuclei with $N_p < 10^3$ and $N_p/A = 1/2$, this charge-to-mass ratio for the nucleus is always larger than 1/20 of the Planck mass ratio $m_{Planck}/m_n \sim 10^{18}$. This means that the gravitational interaction can be safely neglected and the strong interactions must be properly taken into account to keep the nucleus confined within a core radius given by Eq. (A.4.1) (17). Instead for massive cores where $N_p \approx (m_{Planck}/m_n)^3$, the ratio $Q/\sqrt{G}M$ given by Eq. (A.1.14) is simply

$$\frac{Q}{\sqrt{G}M} \approx \frac{N_p}{A} \tag{A.1.15}$$

which is of the order of and smaller than $1/10$. Thus the massive core is gravitationally stable and bound. This is a very significant conceptual simplification of the problem: it is possible to formulate a consistent model of massive cores only in terms of gravitational, electromagnetic and weak interactions and quantum statistics. We can also see the same constraint on the gravitational stability of neutron cores from a different point of view: from Eq. (A.1.12) it is clear that the repulsive Coulomb potential of the proton can indeed be balanced by the gravitational potential of the massive core since for $A \approx (m_{Planck}/m_n)^3$, the gravitational potential can be as large as $0.1 m_p c^2$. This is consistent with the existence of gravitationally bound massive cores and supercritical fields with values given by Eq. (A.1.11); see also Fig. (3). Thus all the arguments often quoted in the literature and in textbooks concerning limits on the electric fields of an astrophysical system based on a free test particle approximation given by equations like

$$E_{max} \approx \frac{m_e}{e} \frac{m_n c^3}{\hbar} \frac{m_n}{m_{Planck}} \tag{A.1.16}$$

$$\frac{Q}{\sqrt{G}M} \approx \sqrt{G}\frac{m_e}{e} = \frac{1}{\sqrt{\alpha}} \frac{m_e}{m_{Planck}}\,, \tag{A.1.17}$$

appear to be inapplicable when the collective effects of the quantum statistics are present and properly taken into account as in the relativistic Thomas-Fermi model, which instead leads to the corresponding Eqs. (A.1.13), (A.1.14).

We now compare in Fig. A.4 our globally neutral solutions with the charged ones considered by Madsen (see also (18)). The solutions for the electron distributions inside the core are practically identical and the only slightly difference occurs in the electron distribution outside the core. In the Madsen case, it is confined to a region within $\approx 10^2$ pion Compton wavelengths of the core surface, while in the globally neutral case it extends out to infinity, although it decays sharply with the distance. Madsen correctly points out that the result for massive cores closely resembles the parameters used by Damour and Ruffini within the general relativistic treatment of charged black holes described by the Kerr-Newman solution (19). Already in 1975 it was recognized that such a result "leads to a most simple model for the explanation of the recently discovered γ-rays bursts" (19). These results are confirmed by our treatment and by Eqs. (A.1.13), (A.1.14).

From our analysis we can infer three general conclusions. 1) By imposing the condition of beta decay equilibrium, in addition to the solution of the relativistic Thomas-Fermi equation, we obtain from first principles a relation between the mass number A and the proton number N_p in the entire mass range from superheavy nuclei with mass number $A \approx 10^4$–10^6 up to massive cores with $A \approx (m_{Planck}/m_n)^3 \sim 10^{57}$. This relation reproduces accurately the phe-

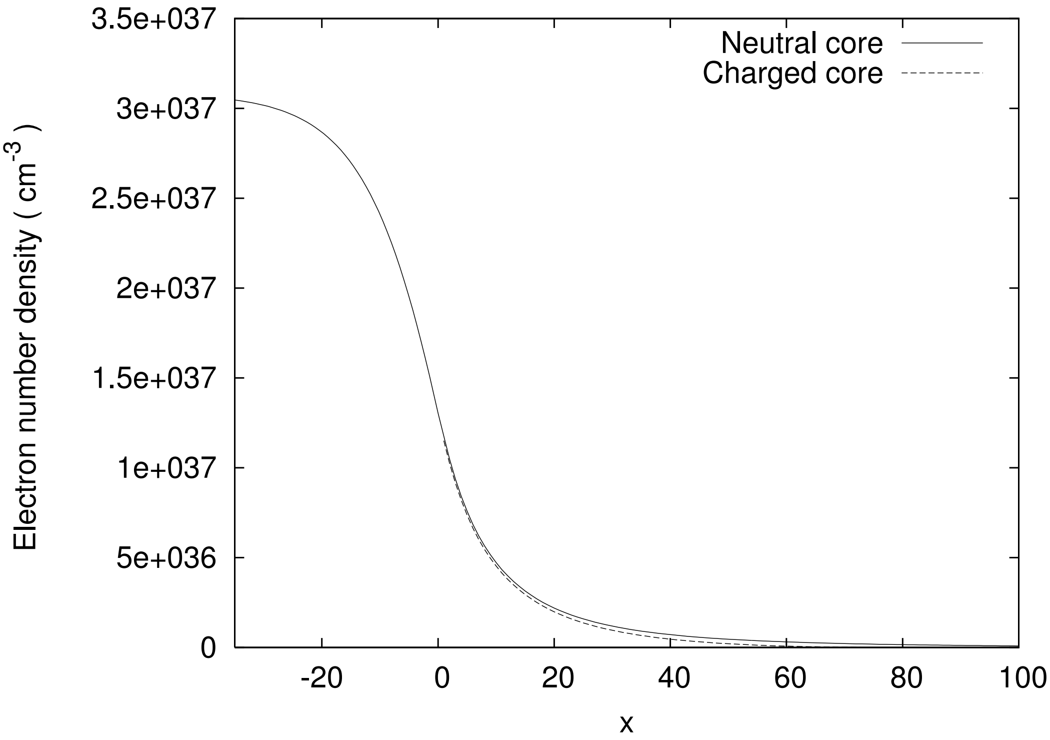

Figure A.4.: Electron number density in a neutral core (solid line) and in a charged one (dotted line) as a function of the pion Compton wavelength for $\Delta \approx 1$.

nomenological relation adopted for superheavy nuclei (17). 2) The collective effects of the ground state due to the relativistic quantum statistics reflected in any solution of the relativistic Thomas-Fermi equation clearly allow stable configurations with electric fields much larger than the ones suggested by test particle approximations. This has clear conceptual implications in astrophysics. 3) The existence of two 'island' of stability. The explicit solution for the electric potential of the relativistic Thomas-Fermi equation for superheavy nuclei implies the existence of stable configurations, up to some critical value of N_p (9; 10; 11; 12; 13; 14), once the confining effects of strong interactions are taken into account. In the opposite case of massive cores we have uncovered the theoretical appealing possibility that stable configurations exist based solely on gravitational, electromagnetic and weak interactions and relativistic quantum statistics. This novel result is interesting in its own right and opens up a whole new scenario for the study of neutron star configurations close to their critical mass and the subsequent approach to the process of gravitational collapse to a Kerr-Newman black hole (20). It also offers an unprecedented arena to study self-gravitating configurations in the framework of tested field theories in their complete range of validity . This will also foster the understanding of the vacuum polarization during the formation process of a black hole (19) and of the thermalisation of the electron-positron plasma created there (21).

We finally outline some consequences of our results for neutron stars. In the classic work of Oppenheimer and collaborators (22), neutron stars are described by a Schwarzchild spacetime whose source is composed of only neutrons and find $M_{\rm crit} \approx 0.7 M_{\odot}$. Harrison and Wheeler (23) introduced an important step forward by considering the presence of neutrons, protons and electrons in beta equilibrium, but imposing local charge neutrality. These considerations were further extended by evaluating the neutron, proton, and electron core melting density at $3 \times 10^{14}\ gcm^{-3}$ (24). These last two studies lead to identify two sharply separated components in a neutron star across the above melting density : a core composed of neutrons, protons and electrons with a pressure mainly due to the neutrons and a crust component consisting of white-dwarf-like material with a pressure due mainly to the electrons (25; 26).

The present work clearly applies only to the inner core of the neutron star and our considerations for a core of constant density apply as well to the case of neutron star cores where the density monotonically increases from the surface to the center. We have shown elsewhere (27) by explicit computation that such a monotonic density increase leads to an enhancement of the electric field at the core surface. Moreover these electrodynamical effects are expected to be especially important for configurations close to the critical value of the mass where the process of gravitational collapse takes place. Such conditions occur at supra-nuclear densities and correspond to values of $\Delta \approx 0.4 - 1$. The electromagnetic structure considered above represents a conceptually new component in neutron star physics, implying the need to use a Reissner-Nordström and possibly a Kerr-Newman geometry for the description of the inner core instead of a Schwarzchild geometry, while still maintaining the overall charge neutrality of the star. This may very well affect the neutron star mass-radius relation and the value of $M_{\rm crit}$ (28). These considerations clearly also modify the description of the gravitational collapse of the baryonic component of the massive core, triggered when protons and neutrons become ultrarelativistic as the mass nears the critical value. This situation characterizes the initial value problem for a gravitational collapse which leads to an electromagnetic Kerr-Newman black hole.

A.2. Electrodynamics for Nuclear Matter in Bulk

It is well know that the Thomas-Fermi equation is the exact theory for atoms, molecules and solids as $Z \to \infty$ (29). We show in this letter that the relativistic Thomas-Fermi theory developed for the study of atoms for heavy nuclei with $Z \simeq 10^6$ (9), (10), (11), (12), (13),(15), (18), (30), (31), (32), (33) gives important basic new information on the study of nuclear matter in bulk in the limit of $N \simeq (m_{\rm Planck}/m_n)^3$ nucleons of mass m_n and on its electrodynamic properties. The analysis of nuclear matter bulk in neutron stars composed of degenerate gas of neutrons, protons and electrons, has traditionally been approached by implementing microscopically the charge neutrality condition by requiring the electron density $n_e(x)$ to coincide with the proton density $n_p(x)$,

$$n_e(x) = n_p(x). \tag{A.2.1}$$

It is clear however that especially when conditions close to the gravitational collapse occur, there is an ultra-relativistic component of degenerate electrons whose confinement requires the existence of very strong electromagnetic fields, in order to guarantee the overall charge neutrality of the neutron star. Under these conditions equation (A.2.1) will be necessarily violated. We are going to show in this letter that they will develop electric fields close to the critical value E_c introduced by Sauter (34), Heisenberg and Euler (16), and by Schwinger (35)

$$E_c = \frac{m^2c^3}{e\hbar}. \tag{A.2.2}$$

Special attention for the existence of critical electric fields and the possible condition for electron-positron (e^+e^-) pair creation out of the vacuum in the case of heavy bare nuclei, with the atomic number $Z \geq 173$, has been given by Pomeranchuk and Smorodinsky (30), Gershtein and Zel'dovich (31), Popov (12), Popov and Zel'dovich (13), Greenberg and Greiner (10), Muller, Peitz, Rafelski and Greiner (11). They analyzed the specific pair creation process of an electron-positron pair around both a point-like and extended bare nucleus by direct integration of Dirac equation. These considerations have been extrapolated to much heavier nuclei $Z \gg 1600$, implying the creation of a large number of e^+e^- pairs, by using a statistical approach based on the relativistic Thomas-Fermi equation by Muller and Rafelski (32), Migdal, Voskresenskii and Popov (33). Using substantially the same statistical approach based on the relativistic Thomas-Fermi equation, Ferreirinho et al. (15), Ruffini and Stella (18) have analyzed the electron densities around an extended nucleus in a neutral atom all the way up to $Z \simeq 6000$. They have shown the effect of penetration of the electron orbitals well inside the nucleus, leading to a screening of the nuclei positive charge and to the concept of an "effective" nuclear charge distribution. All the above works assumed for the radius of the extended nucleus the semi-empirical formulae (17),

$$R_c \approx r_0 A^{1/3}, \quad r_0 = 1.2 \cdot 10^{-13}\text{cm}, \tag{A.2.3}$$

where the mass number $A = N_n + N_p$, N_n and N_p are the neutron and proton numbers. The approximate relation between A and the atomic number $Z = N_p$,

$$Z \simeq \frac{A}{2}, \tag{A.2.4}$$

was adopted in Refs. (32; 33), or the empirical formulae

$$Z \simeq [\frac{2}{A} + \frac{3}{200}\frac{1}{A^{1/3}}]^{-1}, \tag{A.2.5}$$

was adopted in Refs. (15; 18).

The aim of this letter is to outline an alternative approach of the description of nuclear matter in bulk: it generalizes, to the case of $N \simeq (m_{\rm Planck}/m_n)^3$ nucleons, the above treatments, already developed and tested for the study of heavy nuclei. This more general approach differs in many aspects from the ones in the current literature and recovers, in the limiting case of A smaller than 10^6, the above treatments. We shall look for a solution implementing the condition of overall charge neutrality of the star as given by

$$N_e = N_p, \tag{A.2.6}$$

which significantly modifies Eq. (A.2.1), since now $N_e(N_p)$ is the total number of electrons (protons) of the equilibrium configuration. Here we present only a simplified prototype of this approach. We outline the essential relative role of the four fundamental interactions present in the neutron star physics: the gravitational, weak, strong and electromagnetic interactions. In addition, we also implement the fundamental role of Fermi-Dirac statistics and the phase space blocking due to the Pauli principle in the degenerate configuration. The new results essentially depend from the coordinated action of the five above theoretical components and cannot be obtained if any one of them is neglected. Let us first recall the role of gravity. In the case of neutron stars, unlike in the case of nuclei where its effects can be neglected, gravitation has the fundamental role of defining the basic parameters of the equilibrium configuration. As pointed out by Gamow (36), at a Newtonian level and by Oppenheimer and Volkoff (37) in general relativity, configurations of equilibrium exist at approximately one solar mass and at an average density around the nuclear density. This result is obtainable considering only the gravitational interaction of a system of Fermi degenerate self-gravitating neutrons, neglecting all other particles and interactions. It can be formulated within a Thomas-Fermi self-gravitating model (see e.g. (38)). In the present case of our simplified prototype model directed at evidencing new electrodynamic properties, the role of gravity is simply taken into account by considering, in line with the generalization of the above results, a mass-radius relation for the baryonic core

$$R^{NS} = R_c \approx \frac{\hbar}{m_\pi c}\frac{m_{\rm Planck}}{m_n}. \tag{A.2.7}$$

This formula generalizes the one given by Eq. (A.2.3) extending its validity to $N \approx (m_{\rm Planck}/m_n)^3$, leading to a baryonic core radius $R_c \approx 10$km. We also recall that a more detailed analysis of nuclear matter in bulk in neutron stars (see e.g. Bethe et al. (39) and Cameron (40)) shows that at mass densities larger than the "melting" density of

$$\rho_c = 4.34 \cdot 10^{13} g/cm^3, \tag{A.2.8}$$

all nuclei disappear. In the description of nuclear matter in bulk we have to consider then the three Fermi degenerate gas of neutrons, protons and electrons. In turn this naturally leads to consider the role of strong and weak interactions among the nucleons. In the nucleus, the role of the strong and weak interaction, with a short range of one Fermi, is to bind the nucleons, with a binding energy of 8 MeV, in order to balance the Coulomb repulsion of the protons. In the neutron star case we have seen that the neutrons confinement is due to gravity. We still assume that an essential role of the strong interactions is to balance the effective Coulomb repulsion due to the protons, partly screened by the electrons distribution inside the neutron star core. We shall verify, for self-consistency, the validity of this assumption on the final equilibrium solution we are going to obtain. We now turn to the essential weak interaction role in establishing the relative balance between neutrons, protons and electrons via the direct and inverse β-decay

$$p + e \longrightarrow n + \nu_e, \tag{A.2.9}$$

$$n \longrightarrow p + e + \bar{\nu}_e. \tag{A.2.10}$$

Since neutrinos escape from the star and the Fermi energy of the electrons is null, as we will show below, the only non-vanishing terms in the equilibrium condition given by the weak interactions are:

$$[(P_n^F c)^2 + M_n^2 c^4]^{1/2} - M_n c^2 = [(P_p^F c)^2 + M_p^2 c^4]^{1/2} - M_p c^2 + |e|V_{\rm coul}^p, \tag{A.2.11}$$

where P_n^F and P_p^F are respectively, the neutron and proton Fermi momenta, and $V_{\rm coul}^p$ is the Coulomb potential of protons. At this point, having fixed all these physical constraints, the main task is to find the electrons distributions fulfilling in addition to the Dirac-Fermi statistics also the Maxwell equations for the electrostatic. The condition of equilibrium of the Fermi degenerate electrons implies the null value of the Fermi energy:

$$[(P_e^F c)^2 + m^2 c^4]^{1/2} - mc^2 + eV_{\rm coul}(r) = 0, \tag{A.2.12}$$

where P_e^F is the electron Fermi momentum and $V_{\rm coul}(r)$ the Coulomb potential. In line with the procedure already followed for the heavy atoms (15),(18) we here adopt the relativistic Thomas-Fermi Equation:

$$\frac{1}{x}\frac{d^2\chi(x)}{dx^2} = -4\pi\alpha \left\{ \theta(x - x_c) - \frac{1}{3\pi^2}\left[\left(\frac{\chi(x)}{x} + \beta \right)^2 - \beta^2 \right]^{3/2} \right\}, \tag{A.2.13}$$

where $\alpha = e^2/(\hbar c)$, $\theta(x - x_c)$ represents the normalized proton density distribution, the variables x and χ are related to the radial coordinate and the electron Coulomb potential $V_{\rm coul}$ by

$$x = \frac{r}{R_c}\left(\frac{3N_p}{4\pi}\right)^{1/3}; \quad eV_{\rm coul}(r) \equiv \frac{\chi(r)}{r}, \tag{A.2.14}$$

and the constants $x_c(r = R_c)$ and β are respectively

$$x_c \equiv \left(\frac{3N_p}{4\pi}\right)^{1/3}; \quad \beta \equiv \frac{mcR_c}{\hbar}\left(\frac{4\pi}{3N_p}\right)^{1/3}. \tag{A.2.15}$$

The solution has the boundary conditions

$$\chi(0) = 0; \quad \chi(\infty) = 0, \tag{A.2.16}$$

with the continuity of the function χ and its first derivative χ' at the boundary of the core R_c. The crucial point is the determination of the eigenvalue of the first derivative at the center

$$\chi'(0) = \text{const.}, \tag{A.2.17}$$

which has to be determined by fulfilling the above boundary conditions (A.2.16) and constraints given by Eq. (E.0.14) and Eq. (A.2.6). The difficulty of the integration of the Thomas-Fermi Equations is certainly one of the most celebrated chapters in theoretical physics and mathematical physics, still challenging a proof of the existence and uniqueness of the solution and strenuously avoiding the occurrence of exact analytic solutions. We recall after the original papers of Thomas (41) and Fermi (42), the works of Scorza Dragoni (43), Sommerfeld (44), Miranda (45) all the way to the many hundredth papers reviewed in the classical articles of Lieb and Simon (29), Lieb (46) and Spruch (47). The situation here is more difficult since we are working on the special relativistic generalization of the Thomas-Fermi Equation. Also in this case, therefore, we have to proceed by numerical integration. The difficulty of this numerical task is further enhanced by a consistency check in order to fulfill all different constraints. It is so that we start the computations by assuming a total number of protons and a value of the core radius R_c. We integrate the Thomas-Fermi Equation and we determine the number of neutrons from the Eq. (E.0.14). We iterate the procedure until a value of A is reached consistent with our choice of the core radius. The paramount difficulty of the problem is the numerical determination of the eigenvalue in Eq. (A.2.17) which already for $A \approx 10^4$ had presented remarkable numerical difficulties (15). In the present context we have been faced for a few months by an apparently unsurmountable numerical task: the determination of the eigenvalue seemed to necessitate a significant number of decimals in the first derivative (A.2.17) comparable to the number of the electrons in the problem! We shall discuss elsewhere the way we overcame the difficulty by splitting the problem on the ground of the physical interpretation of the solution (48). The solution is given in Fig. (A.5) and Fig. (E.4).

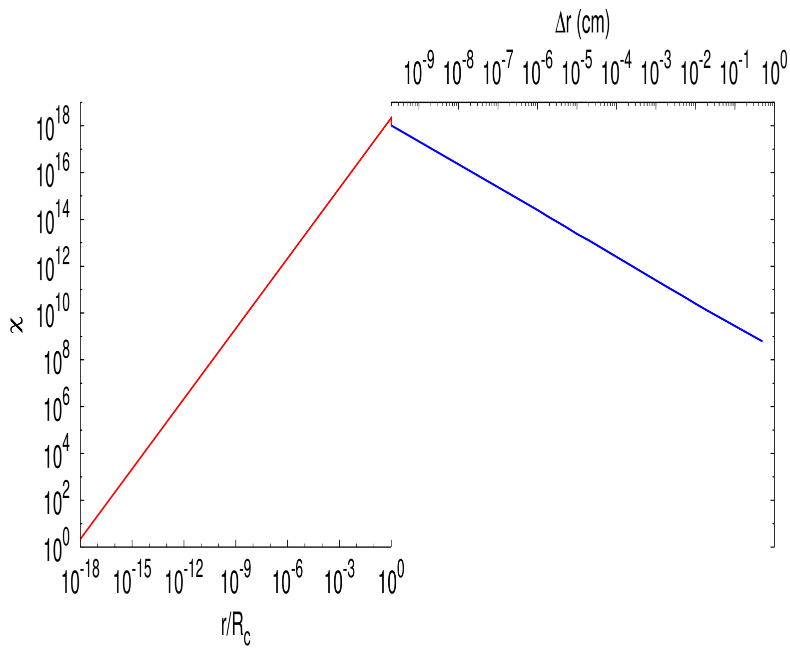

Figure A.5.: The solution χ of the relativistic Thomas-Fermi Equation for $A = 10^{57}$ and core radius $R_c = 10$km, is plotted as a function of radial coordinate. The left red line corresponds to the internal solution and it is plotted as a function of radial coordinate in unit of R_c in logarithmic scale. The right blue line corresponds to the solution external to the core and it is plotted as function of the distance Δr from the surface in the logarithmic scale in centimeter.

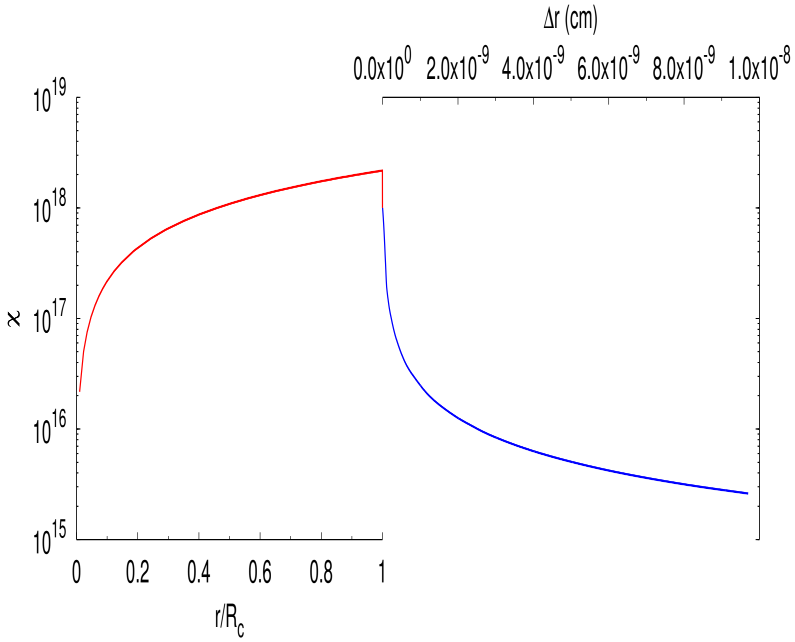

Figure A.6.: The same as Fig. (A.5): enlargement around the core radius R_c showing explicitly the continuity of function χ and its derivative χ' from the internal to the external solution.

A relevant quantity for exploring the physical significance of the solution is given by the number of electrons within a given radius r:

$$N_e(r) = \int_0^r 4\pi(r')^2 n_e(r')dr'. \tag{A.2.18}$$

This allows to determine, for selected values of the A parameter, the distribution of the electrons within and outside the core and follow the progressive penetration of the electrons in the core at increasing values of A [see Fig. (A.7)]. We can then evaluate, generalizing the results in (15), (18) , the net charge inside the core

$$N_{\rm net} = N_p - N_e(R_c) < N_p, \tag{A.2.19}$$

and consequently determine of the electric field at the core surface, as well as within and outside the core [see Fig. (E.5)] and evaluate as well the Fermi degenerate electron distribution outside the core [see Fig. (A.9)]. It is interesting to explore the solution of the problem under the same conditions and constraints imposed by the fundamental interactions and the quantum statistics and imposing instead of Eq. (A.2.1) the corresponding Eq. (A.2.6). Indeed a solution exist and is much simpler

$$n_n(x) = n_p(x) = n_e(x) = 0, \quad \chi = 0. \tag{A.2.20}$$

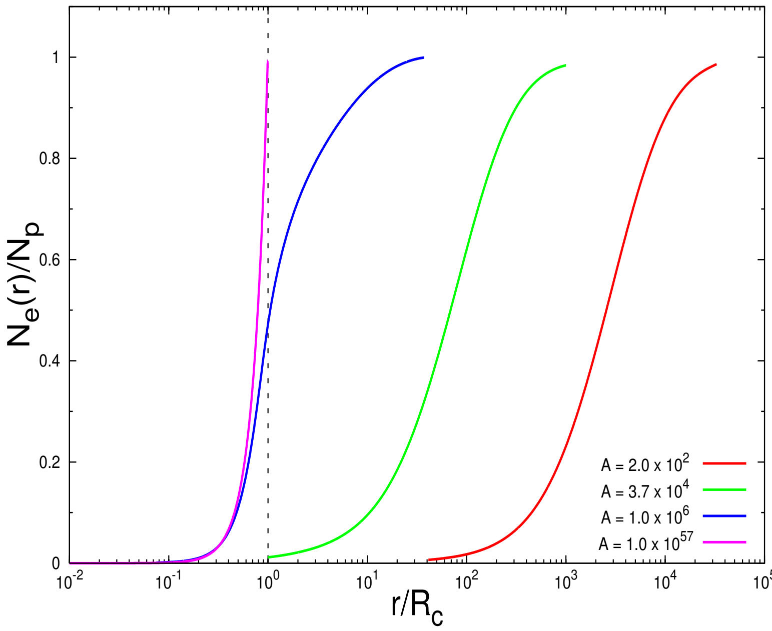

Figure A.7.: The electron number (A.2.18) in the unit of the total proton number N_p, for selected values of A, is given as function of radial distance in the unit of the core radius R_c, again in logarithmic scale. It is clear how by increasing the value of A the penetration of electrons inside the core increases. The detail shown in Fig. (E.5) and Fig. (A.9) demonstrates how for $N \simeq (m_{\text{Planck}}/m_n)^3$ a relatively small tail of electron outside the core exists and generates on the baryonic core surface an electric field close to the critical value given in . A significant electron density outside the core is found.

Before concluding as we announce we like to check on the theoretical consistency of the solution. We obtain an overall neutral configuration for the nuclear matter in bulk, with a positively charged baryonic core with

$$N_{\text{net}} = 0.92 \left(\frac{m}{m_\pi}\right)^2 \left(\frac{e}{m_n\sqrt{G}}\right)^2 \left(\frac{1}{\alpha}\right)^2, \tag{A.2.21}$$

and an electric field on the baryonic core surface (see Fig. (E.5))

$$\frac{E}{E_c} = 0.92. \tag{A.2.22}$$

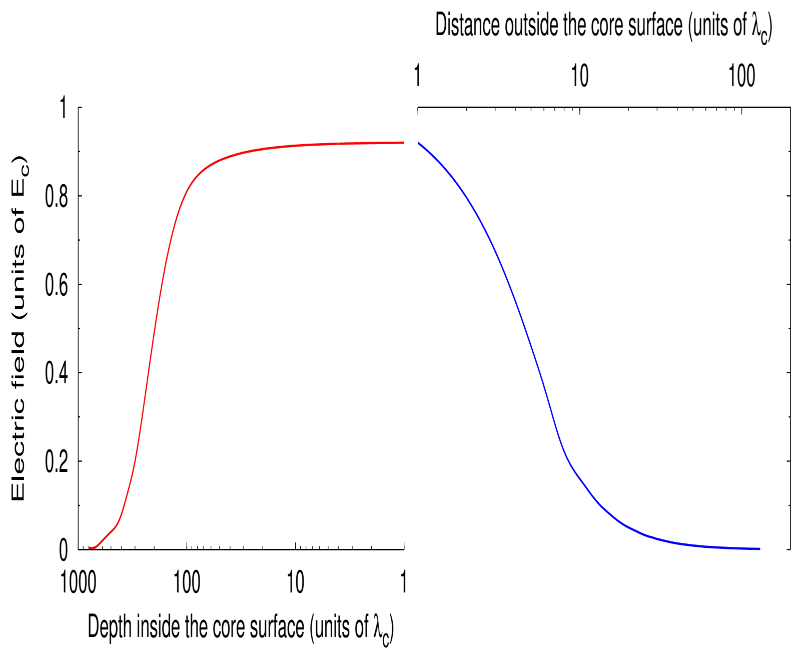

Figure A.8.: The electric field in the unit of the critical field E_c is plotted around the core radius R_c. The left (right) diagram in the red (blue) refers the region just inside (outside) the core radius plotted logarithmically. By increasing the density of the star the field approaches the critical field.

The corresponding Coulomb repulsive energy per nucleon is given by

$$U_{\text{coul}}^{\text{max}} = \frac{1}{2\alpha}\left(\frac{m}{m_\pi}\right)^3 mc^2 \approx 1.78 \cdot 10^{-6}(\text{MeV}), \tag{A.2.23}$$

well below the nucleon binding energy per nucleon. It is also important to verify that this charge core is gravitationally stable. We have in fact

$$\frac{Q}{\sqrt{G}M} = \alpha^{-1/2}\left(\frac{m}{m_\pi}\right)^2 \approx 1.56 \cdot 10^{-4}. \tag{A.2.24}$$

The electric field of the baryonic core is screened to infinity by an electron distribution given in Fig. (A.9). As usual any new solution of Thomas-Fermi systems has relevance and finds its justification in the theoretical physics and mathematical physics domain. We expect that as in the other solutions previously obtained in the literature of the relativistic Thomas-Fermi equations also this one we present in this letter will find important applications in physics and astrophysics. There are a variety of new effects that such a generalized approach naturally leads to: (1) the mass-radius relation of neutron star may be affected; (2) the electrodynamic aspects of neutron stars and

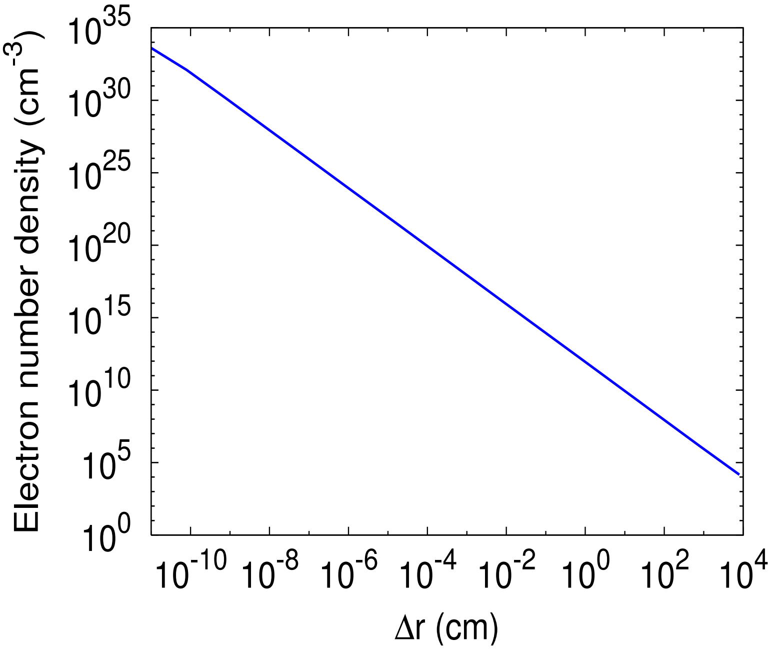

Figure A.9.: The density of electrons for $A = 10^{57}$ in the region outside the core; both scale are logarithmically.

pulsars will be different; (3) we expect also important consequence in the initial conditions in the physics of gravitational collapse of the baryonic core as soon as the critical mass for gravitational collapse to a black hole is reached. The consequent collapse to a black hole will have very different energetics properties.

A.3. On the Charge to Mass Ratio of Neutron Cores and Heavy Nuclei

Introduction. It is well known that stable nuclei are located, in the N_n-N_p plane (where N_n and N_p are the total number of neutrons and protons respectively), in a region that, for small values of N_p, is almost a line well described by the relation $N_n = N_p$.

In the past, several efforts have been made to explain theoretically this property, for example with the liquid drop model of atoms, that is based on two properties common to all nuclei: their mass densities and their binding energies for nucleons are almost indipendent from the mass number $A = N_n + N_p$ (17). This model takes into account the strong nuclear force and the Coulombian repulsion between protons and explains different properties of nuclei, for example the relation between N_p and A (the charge to mass ratio).

In this work (66) we derive theoretically the charge to mass ratio of nuclei and extend it to neutron cores (characterized by higher values of A) with the model of Ruffini et al. (1). We consider systems composed of degenerate neutrons, protons and electrons and we use the relativistic Thomas-Fermi equation and the equation of β-equilibrium to determine the number density and the total number of these particles, from which we obtain the relation between N_p and A.

The theoretical model. Following the work of Ruffini et al. (1), we describe nuclei and neutron cores as spherically symmetric systems composed of degenerate protons, electrons and neutrons and impose the condition of global charge neutrality.
We assume that the proton's number density $n_p(r)$ is constant inside the core ($r \leq R_C$) and vanishes outside the core ($r > R_C$):

$$n_p(r) = \left(\frac{3N_p}{4\pi R_C^3}\right)\theta(R_C - r), \tag{A.3.1}$$

where Np is the total number of protons and R_C is the core-radius, parametrized as:

$$R_C = \Delta\frac{\hbar}{m_\pi c}N_p^{1/3}. \tag{A.3.2}$$

We choose Δ in order to have $\rho \sim \rho_N$, where ρ and ρ_N are the mass density of the system and the nuclear density respectively ($\rho_N = 2.314 \cdot 10^{14} g\, cm^{-3}$).
The electron number density $n_e(r)$ is given by:

$$n_e(r) = \frac{1}{3\pi^2\hbar^3}\left[p_e^F(r)\right]^3, \tag{A.3.3}$$

where $p_e^F(r)$ is the electron Fermi momentum. It can be calculated from the condition of equilibrium of Fermi degenerate electrons, that implies the null value of their Fermi energy $\epsilon_e^F(r)$:

$$\epsilon_e^F(r) = \sqrt{[p_e^F(r)c]^2 + m_e^2c^4} - m_ec^2 + V_c(r) = 0, \tag{A.3.4}$$

where $V_c(r)$ is the Coulomb potential energy of electrons.

From this condition we obtain:

$$p_e^F(r) = \frac{1}{c}\sqrt{V_c^2(r) - 2m_ec^2V_c(r)}, \tag{A.3.5}$$

hence the electron number density is:

$$n_e(r) = \frac{1}{3\pi^2\hbar^3c^3}\left[V_c^2(r) - 2m_ec^2V_c(r)\right]^{3/2}. \tag{A.3.6}$$

The Coulomb potential energy of electrons, necessary to derive $n_e(r)$, can be determined as follows. Based on the Gauss law, $V_c(r)$ obeys the following Poisson equation:

$$\nabla^2 V_c(r) = -4\pi e^2 [n_e(r) - n_p(r)], \quad \text{(A.3.7)}$$

with the boundary conditions $V_c(\infty) = 0$, $V_c(0) = finite$. Introducing the dimensionless function $\chi(r)$, defined by the relation:

$$V_c(r) = -\hbar c \frac{\chi(r)}{r}, \quad \text{(A.3.8)}$$

and the new variable $x = rb^{-1} = r\left(\frac{\hbar}{m_\pi c}\right)^{-1}$, from eq. (A.3.7) we obtain the relativistic Thomas-Fermi equation:

$$\frac{1}{3x}\frac{d^2\chi(x)}{dx^2} = -\alpha \left\{ \frac{1}{\Delta^3}\theta(x_c - x) - \frac{4}{9\pi}\left[\frac{\chi^2(x)}{x^2} + 2\frac{m_e}{m_\pi}\frac{\chi(x)}{x}\right]^{3/2} \right\}. \quad \text{(A.3.9)}$$

The boundary conditions for the function $\chi(x)$ are:

$$\chi(0) = 0, \qquad \chi(\infty) = 0, \quad \text{(A.3.10)}$$

as well as the continuity of $\chi(x)$ and its first derivative $\chi^{'}(x)$ at the boundary of the core.
The number density of neutrons $n_n(r)$ is:

$$n_n(r) = \frac{1}{3\pi^2\hbar^3}\left[p_n^F(r)\right]^3, \quad \text{(A.3.11)}$$

where $p_n^F(r)$ is the neutron Fermi momentum. It can be calculated with the condition of equilibrium between the processes

$$e^- + p \rightarrow n + \nu_e; \quad \text{(A.3.12)}$$

$$n \rightarrow p + e^- + \bar{\nu}_e, \quad \text{(A.3.13)}$$

Assuming that neutrinos escape from the core as soon as they are produced, this condition (condition of β-equilibrium) is

$$\epsilon_e^F(r) + \epsilon_p^F(r) = \epsilon_n^F(r). \quad \text{(A.3.14)}$$

Eq. (A.3.14) can be explicitly written as:

$$\sqrt{[p_p^F(r)c]^2 + m_p^2c^4} - m_p c^2 - V_c(r) = \sqrt{[p_n^F(r)c]^2 + m_n^2c^4} - m_n c^2. \quad \text{(A.3.15)}$$

N_p versus A relation. Using the previous equations, we derive $n_e(r)$, $n_n(r)$

and $n_p(r)$ and, by integrating these, we obtain the N_e, N_n and N_p. We also derive a theoretical relation between N_p and A and we compare it with the data of the Periodic Table and with the semi-empirical relation:

$$N_p = \left(\frac{A}{2}\right) \cdot \frac{1}{1 + \left(\frac{3}{400}\right) \cdot A^{2/3}} \tag{A.3.16}$$

that, in the limit of low A, gives the well known relation $N_p = A/2$ (17).
Eq. (A.3.16) can be obtained by minimizing the semi-empirical mass formula, that was first formulated by Weizsäcker in 1935 and is based on empirical measurements and on theory (the liquid drop model of atoms).
The liquid drop model approximates the nucleus as a sphere composed of protons and neutrons (and not electrons) and takes into account the Coulombian repulsion between protons and the strong nuclear force. Another important characteristic of this model is that it is based on the property that the mass densities of nuclei are approximately the same, indipendently from A (67). In fact, from scattering experiments it was found the following expression for the nuclear radius R_N:

$$R_N = r_0 A^{1/3}, \tag{A.3.17}$$

with $r_0 = 1.2$ fm. Using eq. (A.3.17) the nuclear density can be write as follows:

$$\rho_N = \frac{A m_N}{V} = \frac{3 A m_N}{4\pi r_0^3 A} = \frac{3 m_N}{4\pi r_0^3}, \tag{A.3.18}$$

where m_N is the nucleon mass. From eq. (A.3.18) it is clear that nuclear density is indipendent from A, so it is constant for all nuclei.
The property of constant density for all nuclei is a common point with our model: in fact, we choose Δ in order to have the same mass density for every value of A; in particular we consider the case $\rho \sim \rho_N$, as previously said.

In table (A.1) are listed some values of A obtained with our model and the semi-empirical mass formula, as well as the data of the Periodic Table; in fig. (A.10) and (A.11) it is shown the comparison between the various $N_p - A$ relations. It is clear that there is a good agreement between all the relations for values of A typical of nuclei, with differences of the order of per cent. Our relation and the semi-empirical one are in agreement up to $A \sim 10^4$; for higher values, we find that the two relations differ. We interprete these differences as due to the effects of penetration of electrons inside the core [see fig. (A.12)]: in our model we consider a system composed of degenerate protons, neutrons and electrons. For the smallest values of A, all the electrons are in a shell outside the core; by increasing A, they progressively penetrate into the core (1). These effects, which need the relativistic approach introduced in (1), are not taken into account in the semi-empirical mass formula.

We also note that the charge to mass ratio become constant for A greater

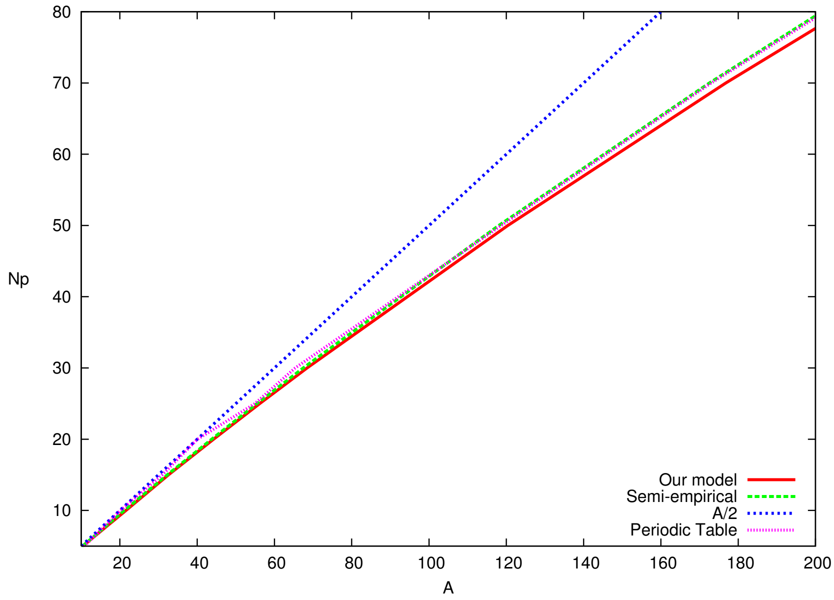

Figure A.10.: The $N_p - A$ relation obtained with our model and with the semi-empirical mass formula, the $N_p = A/2$ relation and the data of the Periodic Table; relations are plotted for values of A from 0 to 200.

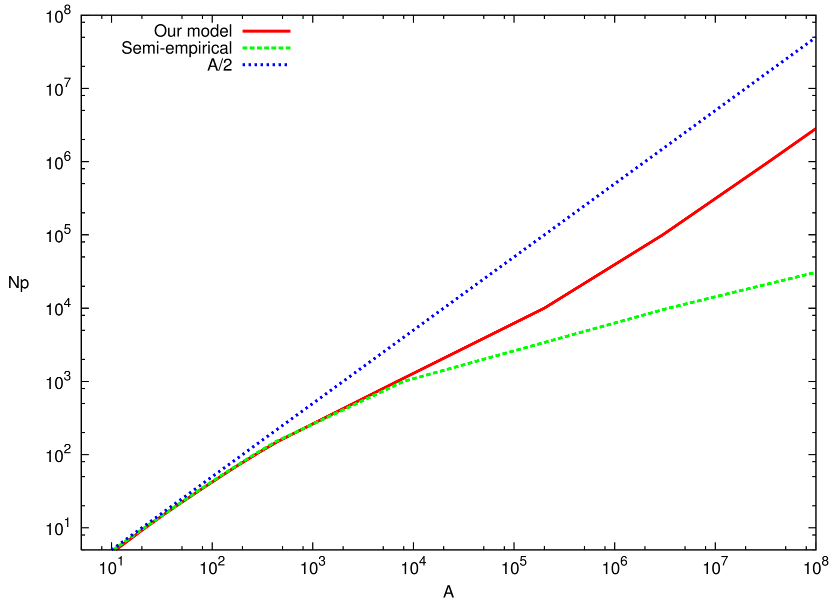

Figure A.11.: The $N_p - A$ relation obtained with our model and with the semi-empirical mass formula and the $N_p = A/2$ relation; relations are plotted for values of A from 0 to 10^8. It is clear how the semi-empirical relation and the one obtained with our model are in good agreement up to values of A of the order of 10^4; for greater values of A the two relation differ because our model takes into account the penetration of electrons inside the core, which is not considered in the semi-empirical mass formula.

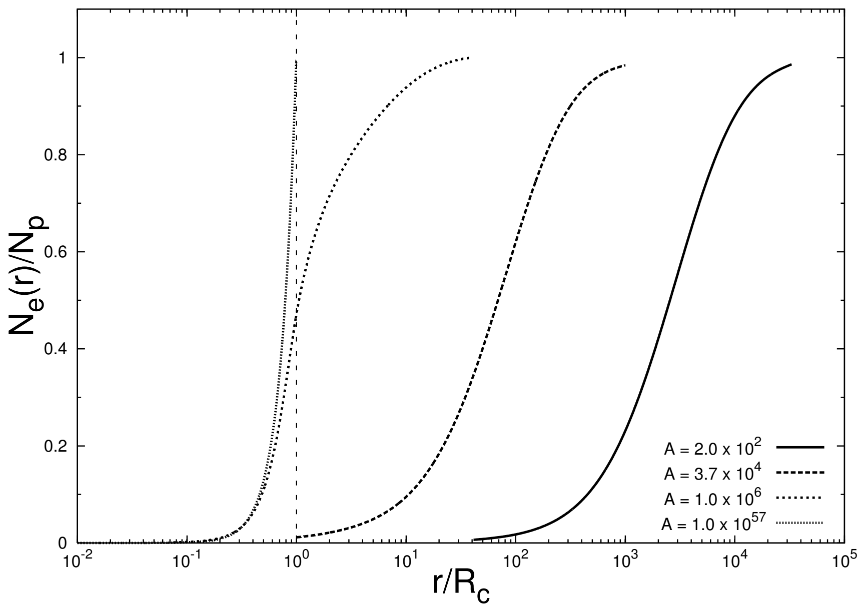

Figure A.12.: The electron number in units of the total proton number N_p as function of the radial distance in units of the core radius R_C, for different values of A. It is clear that, by increasing the value of A, the penetration of electrons inside the core increases. Figure from R. Ruffini, M. Rotondo and S. S. Xue (1).

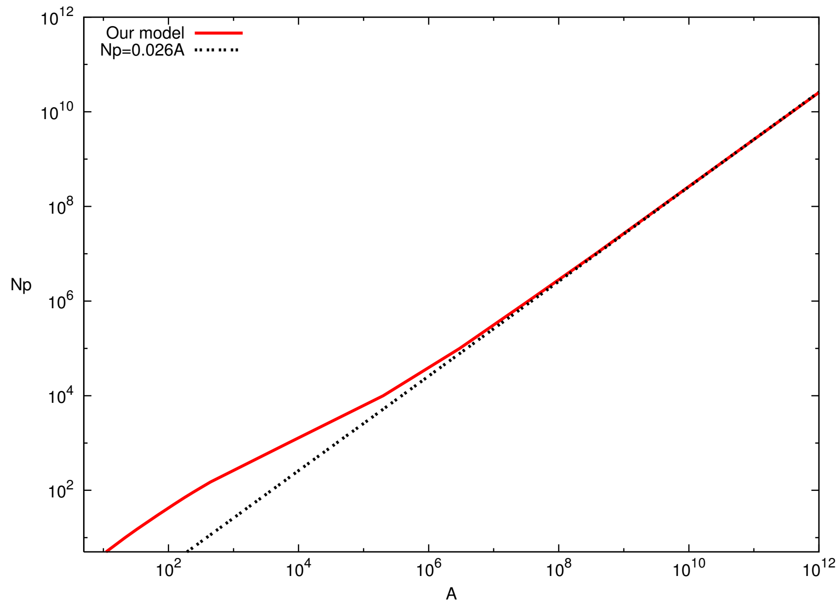

Figure A.13.: The $N_p - A$ relation obtained with our model and the asymptotic limit $N_p = 0.026A$

N_p	$\mathbf{A}_M$	$\mathbf{A}_{PT}$	$\mathbf{A}_{SE}$
5	10.40	10.811	10.36
10	21.59	20.183	21.15
15	32.58	30.9738	32.28
20	44.24	40.08	43.72
25	56.17	54.938	55.45
30	68.43	65.37	67.46
50	120.40	118.69	118.05
70	176.78	173.04	172.54
90	237.41	232.038	230.79
110	302.18	271	292.75
150	443.98		427.73
200	644.03		617.56
250	869.32		831.63
300	1119.71		1071.08
350	1395.12		1337.23
450	2019.48		1955.57
500	2367.77		2310.96
550	2739.60		2699.45
600	3134.28		3122.83
10^3	$6.9\cdot10^3$		$8\cdot10^3$
10^4	$2.0\cdot10^5$		$3.45\cdot10^6$
10^5	$3.0\cdot10^6$		$3.38\cdot10^9$
10^6	$3.4\cdot10^7$		$3.37\cdot10^{12}$
10^7	$3.7\cdot10^8$		$3.37\cdot10^{15}$
10^{10}	$3.9\cdot10^{11}$		$3.37\cdot10^{24}$

Table A.1.: Different values of N_p (column 1) and corresponding values of A from our model (A_M, column 2), the Periodic Table (A_{PT}, column 3) and the semi-empirical mass formula (A_{SE}, column 4).

that 10^7; in particular, it is well approximated by the relation $N_p = 0.026A$ [see fig. (A.13)].

Conclusions. In this work we have derived theoretically a relation between the total number of protons N_p and the mass number A for nuclei and neutron cores with the model recently proposed by Ruffini et al. (1)).
We have considered spherically symmetric systems composed of degenerate electrons, protons and neutrons having global charge neutrality and the same mass densities ($\rho \sim \rho_N$). By integrating the relativistic Thomas-Fermi equation and using the equation of β-equilibrium, we have determined the total number of protons, electrons and neutrons in the system and hence a theoretical relation between N_p and A.
We have compared this relation with the empirical data of the Periodic Table and with the semi-empirical relation, obtained by minimizing the Weizsäcker mass formula by considering systems with the same mass densities. We have shown that there's a good agreement between all the relations for values of A typical of nuclei, with differences of the order of per cent. Our relation and the semi-empirical one are in agreement up to $A \sim 10^4$; for higher values, we find that the two relations differ. We interprete the different behaviour of our theoretical relation as a result of the penetration of electrons (initially confined in an external shell) inside the core [see fig.(A.12)], that becomes more and more important by increasing A; these effects, which need the relativistic approach introduced in (1), are not taken into account in the semi-empirical mass-formula.

A.4. Supercritical fields on the surface of massive nuclear cores: neutral core v.s. charged core

Equilibrium of electron distribution in neutral cores. In Refs. (1; 15; 18), the Thomas-Fermi approach was used to study the electrostatic equilibrium of electron distributions $n_e(r)$ around extended nuclear cores, where total proton and electron numbers are the same $N_p = N_e$. Proton's density $n_p(r)$ is constant inside core $r \leq R_c$ and vanishes outside the core $r > R_c$,

$$n_p(r) = n_p \theta(R_c - r), \tag{A.4.1}$$

where R_c is the core radius and n_p proton density. Degenerate electron density,

$$n_e(r) = \frac{1}{3\pi^2\hbar^3}(P_e^F)^3, \tag{A.4.2}$$

where electron Fermi momentum P_e^F, Fermi-energy $\mathcal{E}_e(P_e^F)$ and Coulomb potential energy $V_{\rm coul}(r)$ are related by,

$$\mathcal{E}_e(P_e^F) = [(P_e^F c)^2 + m_e^2 c^4]^{1/2} - m_e c^2 - V_{\rm coul}(r). \tag{A.4.3}$$

The electrostatic equilibrium of electron distributions is determined by

$$\mathcal{E}_e(P_e^F) = 0, \tag{A.4.4}$$

which means the balance of electron's kinetic and potential energies in Eq. (A.4.3) and degenerate electrons occupy energy-levels up to $+m_e c^2$. Eqs. (A.4.2,A.4.3,A.4.4) give the relationships:

$$P_e^F = \frac{1}{c}\left[V_{\rm coul}^2(r) + 2m_e c^2 V_{\rm coul}(r)\right]^{1/2}; \tag{A.4.5}$$

$$n_e(r) = \frac{1}{3\pi^2(c\hbar)^3}\left[V_{\rm coul}^2(r) + 2m_e c^2 V_{\rm coul}(r)\right]^{3/2}. \tag{A.4.6}$$

The Gauss law leads the following Poisson equation and boundary conditions,

$$\Delta V_{\rm coul}(r) = 4\pi\alpha\left[n_p(r) - n_e(r)\right]; \quad V_{\rm coul}(\infty) = 0, \quad V_{\rm coul}(0) = \text{finite} \tag{A.4.7}$$

These equations describe a Thomas-Fermi model for neutral nuclear cores, and have numerically solved together with the empirical formula (15; 18) and β-equilibrium equation (1) for the proton number N_p and mass number $A = N_p + N_n$, where N_n is the neutron number.

Equilibrium of electron distribution in super charged cores In Ref. (32; 33), assuming that super charged cores of proton density (A.4.1) are bare, electrons (positrons) produced by vacuum polarization fall (fly) into cores (infinity), one studied the equilibrium of electron distribution when vacuum polarization process stop. When the proton density is about nuclear density, super charged core creates a negative Coulomb potential well $-V_{\rm coul}(r)$, whose depth is much more profound than $-m_e c^2$ (see Fig. [A.14]), production of electron-positron pairs take places, and electrons bound by the core and screen down its charge. Since the phase space of negative energy-levels $\epsilon(p)$

$$\epsilon(p) = [(pc)^2 + m_e^2 c^4]^{1/2} - V_{\rm coul}(r), \tag{A.4.8}$$

below $-m_e c^2$ for accommodating electrons is limited, vacuum polarization process completely stops when electrons fully occupy all negative energy-levels up to $-m_e c^2$, even electric field is still critical. Therefore an equilibrium of degenerate electron distribution is expected when the following condition is satisfied,

$$\epsilon(p) = [(pc)^2 + m_e^2c^4]^{1/2} - V_{\rm coul}(r) = -m_ec^2, \quad p = P_e^F, \tag{A.4.9}$$

and Fermi-energy

$$\mathcal{E}_e(P_e^F) = \epsilon(P_e^F) - m_ec^2 = -2m_ec^2, \tag{A.4.10}$$

which is rather different from Eq. (A.4.4). This equilibrium condition (A.4.10) leads to electron's Fermi-momentum and number-density (A.4.2),

$$P_e^F = \frac{1}{c}\left[V^2_{\rm coul}(r) - 2m_ec^2V_{\rm coul}(r)\right]^{1/2}; \tag{A.4.11}$$

$$n_e(r) = \frac{1}{3\pi^2(c\hbar)^3}\left[V^2_{\rm coul}(r) - 2m_ec^2V_{\rm coul}(r)\right]^{3/2}. \tag{A.4.12}$$

which have a different sign contracting to Eqs. (A.4.5,E.0.10). Eq. (A.4.7) remains the same. However, contracting to the neutrality condition $N_e = N_p$ and $n_e(r)|_{r\to\infty} \to 0$ in the case of neutral cores, the total number of electrons is given by

$$N_e^{\rm ion} = \int_0^{r_0} 4\pi r^2 dr n_e(r) < N_p, \tag{A.4.13}$$

where r_0 is the finite radius at which electron distribution $n_e(r)$ (A.4.12) vanishes: $n_e(r_0) = 0$, i.e., $V_{\rm coul}(r_0) = 2m_ec^2$, and $n_e(r) \equiv 0$ for the range $r > r_0$. $N^{\rm ion} < N_p$ indicates that such configuration is not neutral. These equations describe a Thomas-Fermi model for super charged cores, and have numerically (32) and analytically (33) solved with assumption $N_p = A/2$.

Ultra-relativistic solution In analytical approach (33; 48), the ultra-relativistic approximation is adopted for $V_{\rm coul}(r) \gg 2m_ec^2$, the term $2m_ec^2V_{\rm coul}(r)$ in Eqs. (A.4.5,E.0.10,A.4.11,A.4.12) is neglected. It turns out that approximated Thomas-Fermi equations are the same for both cases of neutral and charged cores, and solution $V_{\rm coul}(r) = \hbar c(3\pi^2 n_p)^{1/3}\phi(x)$,

$$\phi(x) = \left\{ \begin{array}{ll} 1 - 3\left[1 + 2^{-1/2}\sinh(3.44 - \sqrt{3}x)\right]^{-1}, & \text{for} \quad x < 0, \\ \frac{\sqrt{2}}{(x+1.89)}, & \text{for} \quad x > 0, \end{array} \right\}, \tag{A.4.14}$$

where $x = 2(\pi/3)^{1/6}\alpha^{1/2}n_p^{1/3}(r - R_c) \sim 0.1(r - R_c)/\lambda_\pi$ and the pion Compton length $\lambda_\pi = \hbar/(m_\pi c)$. At the core center $r = 0 (x \to -\infty)$, $V_{\rm coul}(0) = \hbar c(3\pi^2 n_p)^{1/3} \sim m_\pi c^2$. On core surface $r = R_c (x = 0)$, $V_{\rm coul}(R_c) = 3/4V_{\rm coul}(0) \gg m_ec^2$, indicating that the ultra-relativistic approximation is applicable for $r \lesssim R_c$. This approximation breaks down at $r \gtrsim r_0$. Clearly, it is impossible to determine the value r_0 out of ultra-relativistically approximated equation, and full Thomas-Fermi equation (A.4.7) with source terms Eq. (E.0.10) for the neutral case, and Eq. (A.4.12) for the charged case have to be solved.

For $r < r_0$ where $V_{\rm coul}(r) > 2m_e c^2$, we treat the term $2m_e c^2 V_{\rm coul}(r)$ in Eqs. (E.0.10,A.4.12) as a small correction term, and find the following inequality is always true

$$n_e^{\rm neutral}(r) > n_e^{\rm charged}(r), \quad r < r_0, \tag{A.4.15}$$

where $n_e^{\rm neutral}(r)$ and $n_e^{\rm charged}(r)$ stand for electron densities of neutral and super charged cores. For the range $r > r_0$, $n_e^{\rm charged}(r) \equiv 0$ in the case of super charged core, while $n_e^{\rm neutral}(r) \to 0$ in the case of neutral core, which should be calculated in non-relativistic approximation: the term $V^2_{\rm coul}(r)$ in Eq. (E.0.10) is neglected.

In conclusion, the physical scenarios and Thomas-Fermi equations of neutral and super charged cores are slightly different. When the proton density n_p of cores is about nuclear density, ultra-relativistic approximation applies for the Coulomb potential energy $V_{\rm coul}(r) \gg m_e c^2$ in $0 < r < r_0$ and $r_0 > R_c$, and approximate equations and solutions for electron distributions inside and around cores are the same. As relativistic regime $r \sim r_0$ and non-relativistic regime $r > r_0$ (only applied to neutral case) are approached, solutions in two cases are somewhat different, and need direct integrations.

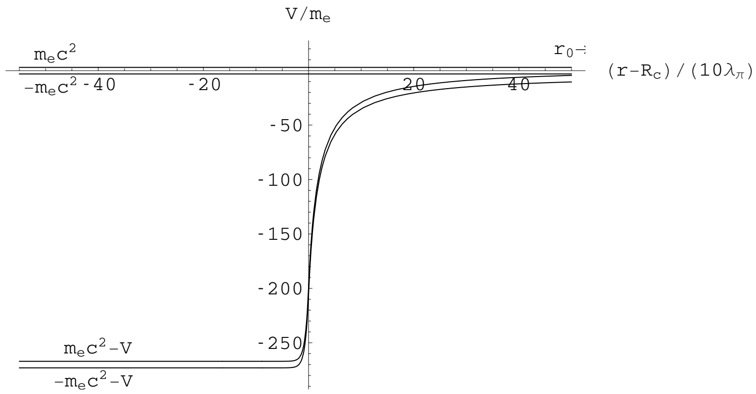

Figure A.14.: Potential energy-gap $\pm m_e c^2 - V_{\rm coul}(r)$ and electron mass-gap $\pm m_e c^2$ in the unit of $m_e c^2$ are plotted as a function of $(r - R_c)/(10\lambda_\pi)$. The potential depth inside core ($r < R_c$) is about pion mass $m_\pi c^2 \gg m_e c^2$ and potential energy-gap and electron mass-gap are indicated. The radius r_0 where electron distribution $n_e(r_0)$ vanishes in super charged core case is indicated as r_0-, since it is out of plotting range.

A.5. The Extended Nuclear Matter Model with Smooth Transition Surface

The Relativistic Thomas–Fermi Equation.

Let us to introduce the proton distribution function $f_p(x)$ by mean of $n_p(x) = n_p^c f_p(x)$, where n_p^c is the central number density of protons. We use the dimensionless unit $x = (r - b)/a$, with $a^{-1} = \sqrt{4\pi\alpha\lambda_e n_p^c}$, λ_e is the electron Compton wavelength, b the length where initial conditions are given ($x = 0$) and α is the fine structure constant.

Using the Poisson's equation and the equilibrium condition for the gas of electrons

$$E_F^e = m_e c^2 \sqrt{1 + x_e^2} - m_e c^2 - eV = 0\,, \tag{A.5.1}$$

where e is the fundamental charge, x_e the normalized electron Fermi momentum and V the electrostatic potential, we obtain the relativistic Thomas–Fermi equation

$$\xi_e''(x) + \left(\frac{2}{x + b/a}\right)\xi_e'(x) - \frac{[\xi_e^2(x) - 1]^{3/2}}{\mu} + f_p(x) = 0\,, \tag{A.5.2}$$

where $\mu = 3\pi^2\lambda_e^3 n_p^c$ and we have introduced the normalized electron chemical potential in absence of any field $\xi_e = \sqrt{1 + x_e^2}$. For a given distribution function $f_p(x)$ and a central number density of protons n_p^c, the above equation can be integrated numerically with the boundary conditions

$$\xi_e(0) = \sqrt{1 + \left[\mu\,\delta f_p(0)\right]^{2/3}}\,, \qquad \xi_e'(0) < 0\,, \tag{A.5.3}$$

where $\delta \equiv n_e(0)/n_p(0)$.

The Woods-Saxon–like Proton Distribution Function.

We simulate a monotonically decreasing proton distribution function fulfilling a Woods–Saxon dependence

$$f_p(x) = \frac{\gamma}{\gamma + e^{\beta x}}\,, \tag{A.5.4}$$

where $\gamma > 0$ and $\beta > 0$. In fig. A.15 we show the proton distribution function for a particular set of parameters.

Results of the Numerical Integration.

We have integrated numerically the eq.(A.5.2) for several sets of parameters and initial conditions. As an example, we show the results for the proton distribution function shown in fig. A.15, with $n_p^c = 1.38 \times 10^{36} (cm^{-3})$. This system was integrated with $N_e = N_p = 10^{54}$, mass number $A = 1.61 \times 10^{56}$ and $\delta \approx 0.967$.

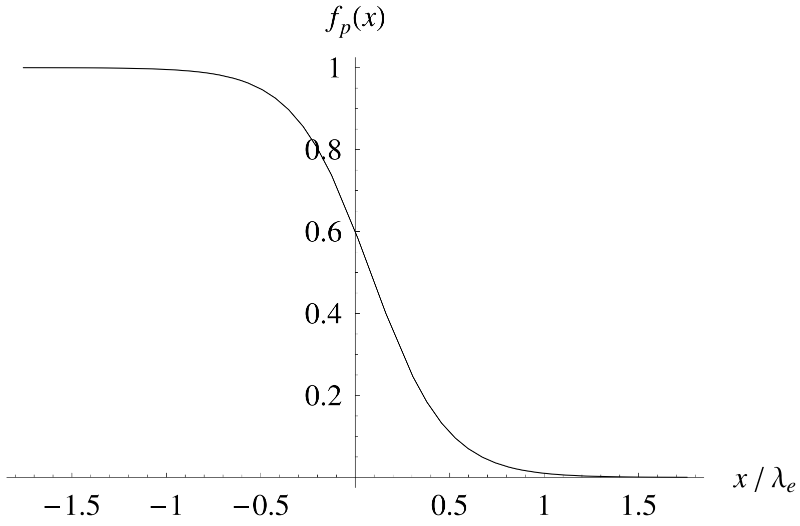

Figure A.15.: Proton distribution function for $\gamma = 1.5$, $\beta \approx 0.0585749$.

We summarize the principal features of our model in figures A.16 and A.17, where we have plotted the electric field in units of the critical field $E_c = \frac{m_e^2 c^3}{e\hbar}$, ($m_e$ and e are the electron mass and charge), and the normalized charge separation function

$$\Delta(x) = \frac{n_p(x) - n_e(x)}{n_p(0)} . \tag{A.5.5}$$

We see that the electric field is overcritical but smaller respect to the case of a sharp step proton distribution used in (1; 14). We have performed several numerical integrations expanding the transition surface and confirm the existence of overcritical fields but it is worth to mention that it could be subcritical expanding the width of the transition surface several orders of magnitude in electron Compton wavelength units.

We also see a displacement of the location of the maximum of intensity. This effect is due to the displacement of the point where $n_e = n_p$. After this point, the charge density becomes negative producing an effect of screening of the charged core up to global charged neutrality is achieved.

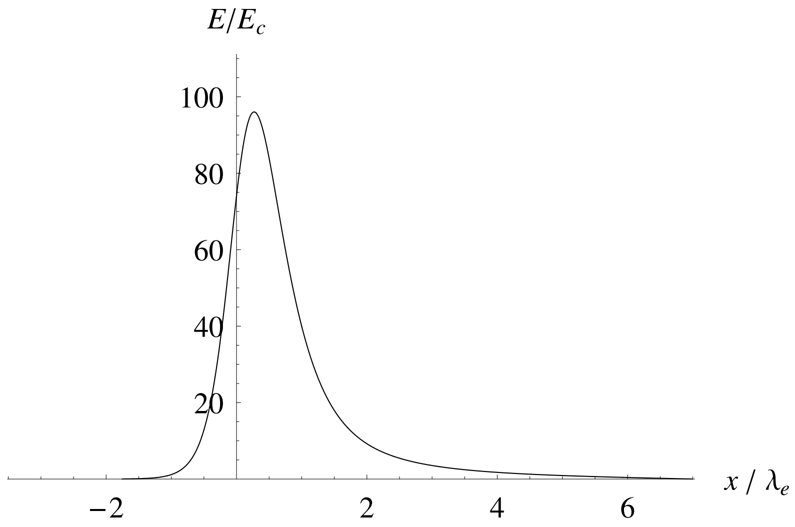

Figure A.16.: Electric field in units of the critical field E_c.

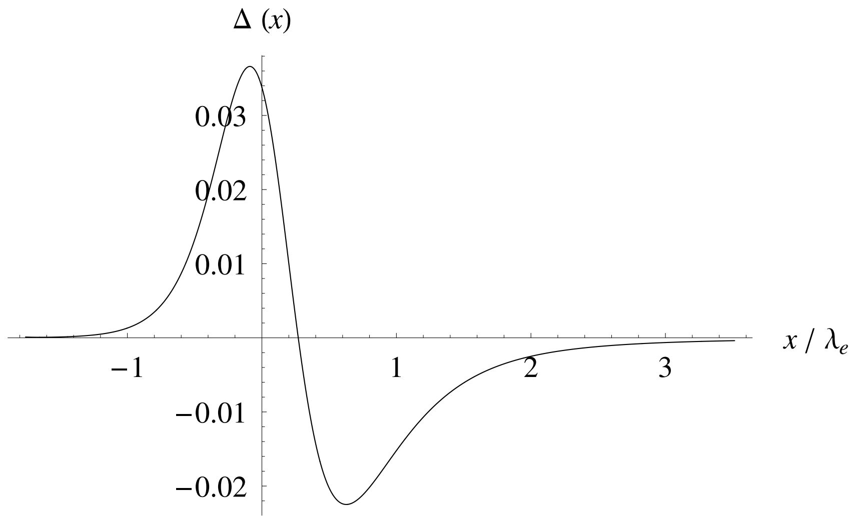

Figure A.17.: Charge separation function.

B. Electron-positron pairs production in an electric potential of massive cores

B.1. Introduction

Very soon after the Dirac equation for a relativistic electron was discovered (49; 50), Gordon (51) (for all $Z < 137$) and Darwin (52) (for $Z = 1$) found its solution in the point-like Coulomb potential $V(r) = -Z\alpha/r$, they obtained the well-known Sommerfeld's formula (53) for energy-spectrum,

$$\mathcal{E}(n,j) = mc^2 \left[1 + \left(\frac{Z\alpha}{n - |K| + (K^2 - Z^2\alpha^2)^{1/2}}\right)^2\right]^{-1/2}, \tag{B.1.1}$$

where the fine-structure constant $\alpha = e^2/\hbar c$, the principle quantum number $n = 1, 2, 3, \cdots$ and

$$K = \begin{cases} -(j+1/2) = -(l+1), & \text{if} \quad j = l + \frac{1}{2}, \quad l \geq 0 \\ (j+1/2) = l, & \text{if} \quad j = l - \frac{1}{2}, \quad l \geq 1 \end{cases} \tag{B.1.2}$$

$l = 0, 1, 2, \cdots$ is the orbital angular momentum corresponding to the upper component of Dirac bi-spinor, j is the total angular momentum. The integer values n and j label bound states whose energies are $\mathcal{E}(n,j) \in (0, mc^2)$. For the example, in the case of the lowest energy states, one has

$$\mathcal{E}(1S_{\frac{1}{2}}) = mc^2\sqrt{1 - (Z\alpha)^2}, \tag{B.1.3}$$

$$\mathcal{E}(2S_{\frac{1}{2}}) = \mathcal{E}(2P_{\frac{1}{2}}) = mc^2\sqrt{\frac{1 + \sqrt{1 - (Z\alpha)^2}}{2}}, \tag{B.1.4}$$

$$\mathcal{E}(2P_{\frac{3}{2}}) = mc^2\sqrt{1 - \frac{1}{4}(Z\alpha)^2}. \tag{B.1.5}$$

For all states of the discrete spectrum, the binding energy $mc^2 - \mathcal{E}(n,j)$ increases as the nuclear charge Z increases. No regular solution with $n = 1, l = 0, j = 1/2$ and $K = -1$ (the $1S_{1/2}$ ground state) is found for $Z > 137$, this was first noticed by Gordon in his pioneer paper (51). This is the problem so-called "$Z = 137$ catastrophe".

The problem was solved (13; 30; 54; 55; 56; 57; 58; 59) by considering the fact that the nucleus is not point-like and has an extended charge distribution, and the potential $V(r)$ is not divergent when $r \to 0$. The $Z = 137$ catastrophe disappears and the energy-levels $\mathcal{E}(n,j)$ of the bound states $1S$, $2P$ and $2S$, $\cdots$ smoothly continue to drop toward the negative energy continuum ($E_- < -mc^2$), as Z increases to values larger than 137. The critical values Z_{cr} for $\mathcal{E}(n,j) = -mc^2$ were found (13; 55; 57; 58; 59; 62; 63; 64): $Z_{cr} \simeq 173$ is a critical value at which the lowest energy-level of the bound state $1S_{1/2}$ encounters the negative energy continuum, while other bound states $2P_{1/2}, 2S_{3/2}, \cdots$ encounter the negative energy continuum at $Z_{cr} > 173$, thus energy-level-crossings and productions of electron and positron pair takes place, provided these bound states are unoccupied. We refer the readers to (13; 57; 58; 59; 60; 61; 62; 63; 64) for mathematical and numerical details.

The energetics of this phenomenon can be understood as follow. The energy-level of the bound state $1S_{1/2}$ can be estimated as follow,

$$\mathcal{E}(1S_{1/2}) = mc^2 - \frac{Ze^2}{\bar{r}} < -mc^2, \tag{B.1.6}$$

where $\bar{r}$ is the average radius of the $1S_{1/2}$ state's orbit, and the binding energy of this state $Ze^2/\bar{r} > 2mc^2$. If this bound state is unoccupied, the bare nucleus gains a binding energy $Ze^2/\bar{r}$ larger than $2mc^2$, and becomes unstable against the production of an electron-positron pair. Assuming this pair-production occur around the radius $\bar{r}$, we have energies of electron (ϵ_-) and positron (ϵ_+):

$$\epsilon_- = \sqrt{(c|\mathbf{p}_-|)^2 + m^2c^4} - \frac{Ze^2}{\bar{r}}; \quad \epsilon_+ = \sqrt{(c|\mathbf{p}_+|)^2 + m^2c^4} + \frac{Ze^2}{\bar{r}}, \tag{B.1.7}$$

where $\mathbf{p}_\pm$ are electron and positron momenta, and $\mathbf{p}_- = -\mathbf{p}_+$. The total energy required for a pair production is,

$$\epsilon_{-+} = \epsilon_- + \epsilon_+ = 2\sqrt{(c|\mathbf{p}_-|)^2 + m^2c^4}, \tag{B.1.8}$$

which is independent of the potential $V(\bar{r})$. The potential energies $\pm eV(\bar{r})$ of electron and positron cancel each other and do not contribute to the total energy (B.1.8) required for pair production. This energy (B.1.8) is acquired from the binding energy ($Ze^2/\bar{r} > 2mc^2$) by the electron filling into the bound state $1S_{1/2}$. A part of the binding energy becomes the kinetic energy of positron that goes out. This is analogous to the familiar case that a proton ($Z = 1$) catches an electron into the ground state $1S_{1/2}$, and a photon is emitted with the energy not less than 13.6 eV.

In this article, we study classical and semi-classical states of electrons, electron-positron pair production in an electric potential of macroscopic cores with charge $Q = Z|e|$, mass M and macroscopic radius R_c.

B.2. Classical description of electrons in potential of cores

B.2.1. Effective potentials for particle's radial motion

Setting the origin of spherical coordinates (r, θ, ϕ) at the center of such cores, we write the vectorial potential $A_\mu = (\mathbf{A}, A_0)$, where $\mathbf{A} = 0$ and A_0 is the Coulomb potential. The motion of a relativistic electron with mass m and charge e is described by its radial momentum p_r, total angular momenta p_ϕ and the Hamiltonian,

$$H_\pm = \pm mc^2 \sqrt{1 + (\frac{p_r}{mc})^2 + (\frac{p_\phi}{mcr})^2} - V(r), \tag{B.2.1}$$

where the potential energy $V(r) = eA_0$, and $\pm$ corresponds for positive and negative energies. The states corresponding to negative energy solutions are fully occupied. The total angular momentum p_ϕ is conserved, for the potential $V(r)$ is spherically symmetric. For a given angular momentum $p_\phi = mv_\perp r$, where $v_\perp$ is the transverse velocity, the effective potential energy for electron's radial motion is

$$E_\pm(r) = \pm mc^2 \sqrt{1 + (\frac{p_\phi}{mcr})^2} - V(r). \tag{B.2.2}$$

Outside the core ($r \geq R_c$), the Coulomb potential energy $V(r)$ is given by

$$V_{\rm out}(r) = \frac{Ze^2}{r}, \tag{B.2.3}$$

where $\pm$ indicates positive and negative effective energies. Inside the core ($r \leq R_c$), the Coulomb potential energy is given by

$$V_{\rm in}(r) = \frac{Ze^2}{2R_c}\left[3 - \left(\frac{r}{R_c}\right)^2\right], \tag{B.2.4}$$

where we postulate the charged core has a uniform charge distribution with constant charge density $\rho = Ze/V_c$, and the core volume $V_c = 4\pi R_c^3/3$. Coulomb potential energies outside the core (B.2.3) and inside the core (B.2.4) is continuous at $r = R_c$. The electric field on the surface of the core,

$$E_s = \frac{Q}{R_c^2} = \frac{\lambda_e}{R_c} E_c, \quad \beta \equiv \frac{Ze^2}{mc^2 R_c} \tag{B.2.5}$$

where the electron Compton wavelength $\lambda_e = \hbar/(mc)$, the critical electric field $E_c = m^2c^3/(e\hbar)$ and the parameter β is the electric potential-energy on the surface of the core in unit of the electron mass-energy.

B.2.2. Stable classical orbits (states) outside the core.

Given different values of total angular momenta p_ϕ, the stable circulating orbits R_L (states) are determined by the minimum of the effective potential $E_+(r)$ (B.2.2) (see Fig. B.1), at which $dE_+(r)/dr = 0$. We obtain stable orbits locate at the radii R_L,

$$R_L = \left(\frac{p_\phi^2}{Ze^2 m}\right)\sqrt{1 - \left(\frac{Ze^2}{cp_\phi}\right)^2}, \quad R_L \geq R_c, \tag{B.2.6}$$

for different p_ϕ-values. Substituting Eq. (B.2.6) into Eq. (B.2.2), we find the energy of electron at each stable orbit,

$$\mathcal{E} \equiv \min(E_+) = mc^2\sqrt{1 - \left(\frac{Ze^2}{cp_\phi}\right)^2}. \tag{B.2.7}$$

For the condition $R_L \gtrsim R_c$, we have

$$\left(\frac{Ze^2}{cp_\phi}\right)^2 \lesssim \frac{1}{2}\left[\beta(4+\beta^2)^{1/2} - \beta^2\right], \tag{B.2.8}$$

where the semi-equality holds for the last stable orbits outside the core $R_L \to R_c + 0^+$. In the point-like case $R_c \to 0$, the last stable orbits are

$$cp_\phi \to Ze^2 + 0^+, \quad R_L \to 0^+, \quad \mathcal{E} \to 0^+. \tag{B.2.9}$$

Eq. (B.2.7) shows that only positive or null energy solutions (states) to exists in the case of a point-like charge, which is the same as the energy-spectrum Eqs. (B.1.3,B.1.4,B.1.5) in quantum mechanic scenario. While for $p_\phi \gg 1$, radii of stable orbits $R_L \gg 1$ and energies $\mathcal{E} \to mc^2 + 0^-$, classical electrons in these orbits are critically bound for their banding energy goes to zero. We conclude that the energies (B.2.7) of stable orbits outside the core must be smaller than mc^2, but larger than zero, $\mathcal{E} > 0$. Therefore, no energy-level crossing with the negative energy spectrum occurs.

B.2.3. Stable classical orbits inside the core.

We turn to the stable orbits of electrons inside the core. Analogously, using Eqs. (B.2.2,B.2.4) and $dE_+(r)/dr = 0$, we obtain the stable orbit radius $R_L \le 1$ in the unit of R_c, obeying the following equation,

$$\beta^2(R_L^8 + \kappa^2 R_L^6) = \kappa^4; \quad \kappa = \frac{p_\phi}{mcR_c}. \tag{B.2.10}$$

and corresponding to the minimal energy (binding energy) of these states

$$\mathcal{E} = \frac{Ze^2}{R_c}\left[\left(\frac{cp_\phi}{Ze^2}\right)^2 \frac{1}{R_L^4} - \frac{1}{2}(3 - R_L^2)\right]. \tag{B.2.11}$$

There are 8 solutions to this polynomial equation (B.2.10), only one is physical solution R_L that has to be real, positive and smaller than one. As example, the numerical solution to Eq. (B.2.10) is $R_L = 0.793701$ for $\beta = 4.4 \cdot 10^{16}$ and $\kappa = 2.2 \cdot 10^{16}$. In following, we respectively adopt non-relativistic and ultra-relativistic approximations to to obtain analytical solutions.

First considering the non-relativistic case for those stable orbit states whose the kinetic energy term characterized by angular momentum term p_ϕ, see Eq. (B.2.2), is much smaller than the rest mass term mc^2, we obtain the following approximate equation,

$$\beta^2 R_L^8 \simeq \kappa^4, \tag{B.2.12}$$

and the solutions for stable orbit radii are,

$$R_L \simeq \frac{\kappa^{1/2}}{\beta^{1/4}} = \left(\frac{cp_\phi}{Ze^2}\right)^{1/2} \beta^{1/4} < 1, \tag{B.2.13}$$

and energies,

$$\mathcal{E} \simeq \left(1 - \frac{3}{2}\beta + \frac{1}{2}\kappa\beta^{1/2}\right) mc^2. \tag{B.2.14}$$

The consistent conditions for this solution are $\beta^{1/2} > \kappa$ for $R_L < 1$, and $\beta \ll 1$ for non-relativistic limit $v_\perp \ll c$. As a result, the binding energies (B.2.14) of these states are $mc^2 > \mathcal{E} > 0$, are never less than zero. These in fact correspond to the stable states which have large radii closing to the radius R_c of cores and $v_\perp \ll c$.

Second considering the ultra-relativistic case for those stable orbit states whose the kinetic energy term characterized by angular momentum term p_ϕ, see Eq. (B.2.2), is much larger than the rest mass term mc^2, we obtain the following approximate equation,

$$\beta^2 R_L^6 \simeq \kappa^2, \tag{B.2.15}$$

and the solutions for stable orbit radii are,

$$R_L \simeq \left(\frac{\kappa}{\beta}\right)^{1/3} = \left(\frac{p_\phi c}{Ze^2}\right)^{1/3} < 1, \tag{B.2.16}$$

which gives $R_L \simeq 0.7937007$ for the same values of parameters β and κ in above. The consistent condition for this solution is $\beta > \kappa \gg 1$ for $R_L < 1$. The energy levels of these ultra-relativistic states are,

$$\mathcal{E} \simeq \frac{3}{2}\beta\left[\left(\frac{p_\phi c}{Ze^2}\right)^{2/3} - 1\right] mc^2, \tag{B.2.17}$$

and $mc^2 > \mathcal{E} > -1.5\beta mc^2$. The particular solutions $\mathcal{E} = 0$ and $\mathcal{E} \simeq -mc^2$ are respectively given by

$$\left(\frac{p_\phi c}{Ze^2}\right) \simeq 1; \quad \left(\frac{p_\phi c}{Ze^2}\right) \simeq \left(1 - \frac{2}{3\beta}\right)^{3/2}. \tag{B.2.18}$$

These in fact correspond to the stable states which have small radii closing to the center of cores and $v_\perp \lesssim c$.

To have the energy-level crossing to the negative energy continuum, we are interested in the values $\beta > \kappa \gg 1$ for which the energy-levels (B.2.17) of stable orbit states are equal to or less than $-mc^2$,

$$\mathcal{E} \simeq \frac{3}{2}\beta\left[\left(\frac{p_\phi c}{Ze^2}\right)^{2/3} - 1\right] mc^2 \leq -mc^2. \tag{B.2.19}$$

As example, with $\beta = 10$ and $\kappa = 2$, $R_L \simeq 0.585$, $\mathcal{E}_{\rm min} \simeq -9.87mc^2$. The lowest energy-level of electron state is $p_\phi/(Ze^2) = \kappa/\beta \to 0$ with the binding energy,

$$\mathcal{E}_{\rm min} = -\frac{3}{2}\beta mc^2, \tag{B.2.20}$$

locating at $R_L \simeq (p_\phi c/Ze^2)^{1/3} \to 0$, the bottom of the potential energy $V_{\rm in}(0)$ (B.2.4).

B.3. Semi-Classical description

B.3.1. Bohr-Sommerfeld quantization

In order to have further understanding, we consider the semi-classical scenario. Introducing the Planck constant $\hbar = h/(2\pi)$, we adopt the semi-classical Bohr-Sommerfeld quantization rule

$$\int p_\phi d\phi \simeq h(l+\frac{1}{2}), \quad \Rightarrow \quad p_\phi(l) \simeq \hbar(l+\frac{1}{2}), \quad l = 0, 1, 2, 3, \cdots, \tag{B.3.1}$$

which are discrete values selected from continuous total angular momentum p_ϕ in the classical scenario. The variation of total angular momentum $\Delta p_\phi = \pm\hbar$ in th unit of the Planck constant $\hbar$. Substitution

$$\left(\frac{p_\phi c}{Ze^2}\right) \Rightarrow \left(\frac{2l+1}{2Z\alpha}\right), \tag{B.3.2}$$

where the fine-structure constant $\alpha = e^2/(\hbar c)$, must be performed in classical solutions that we obtained in section (B.2).

1. The radii and energies of stable states outside the core (B.2.6) and (B.2.7) become:

$$R_L = \lambda\left(\frac{2l+1}{Z\alpha}\right)\sqrt{1-\left(\frac{2Z\alpha}{2l+1}\right)^2}, \tag{B.3.3}$$

$$\mathcal{E} = mc^2\sqrt{1-\left(\frac{2Z\alpha}{2l+1}\right)^2}, \tag{B.3.4}$$

   where λ is the electron Compton length.

2. The radii and energies of non-relativistic stable states inside the core (B.2.13) and (B.2.14) become:

$$R_L \simeq \left(\frac{2l+1}{2Z\alpha}\right)^{1/2}\beta^{1/4}, \tag{B.3.5}$$

$$\mathcal{E} \simeq \left(1-\frac{3}{2}\beta+\frac{\lambda(2l+1)}{4R_c}\beta^{1/2}\right)mc^2. \tag{B.3.6}$$

3. The radii and energies of ultra-relativistic stable states inside the core

(B.2.16) and (B.2.17) become:

$$
\begin{aligned}
R_L &\simeq \left(\frac{2l+1}{2Z\alpha}\right)^{1/3}, && \text{(B.3.7)} \\
\mathcal{E} &\simeq \frac{3}{2}\beta\left[\left(\frac{2l+1}{2Z\alpha}\right)^{2/3} - 1\right] mc^2. && \text{(B.3.8)}
\end{aligned}
$$

Note that radii R_L in the second and third cases are in unit of R_c.

B.3.2. Stability of semi-classical states

When these semi-classical states are not occupied as required by the Pauli Principle, the transition from one state to another with different discrete values of total angular momentum l (l_1, l_2 and $\Delta l = l_2 - l_1 = \pm 1$) undergoes by emission or absorption of a spin-1 ($\hbar$) photon. Following the energy and angular-momentum conservations, photon emitted or absorbed in the transition have angular momenta $p_\phi(l_2) - p_\phi(l_1) = \hbar(l_2 - l_1) = \pm\hbar$ and energy $\mathcal{E}(l_2) - \mathcal{E}(l_1)$. In this transition of stable states, the variation of radius is $\Delta R_L = R_L(l_2) - R_L(l_1)$.

We first consider the stability of semi-classical states against such transition in the case of point-like charge, i.e., Eqs. (B.3.3,B.3.4) with $l = 0, 1, 2, \cdots$. As required by the Heisenberg indeterminacy principle $\Delta\phi\Delta p_\phi \simeq 4\pi p_\phi(l) \gtrsim h$, the absolute ground state for minimal energy and angular momentum is given by the $l = 0$ state, $p_\phi \sim \hbar/2$, $R_L \sim \lambda(Z\alpha)^{-1}\sqrt{1-(2Z\alpha)^2} > 0$ and $\mathcal{E} \sim mc^2\sqrt{1-(2Z\alpha)^2} > 0$, which corresponds to the last stable orbit (B.2.9) in the classical scenario. Thus the stability of all semi-classical states $l > 0$ is guaranteed by the Pauli principle. This is only case for $Z\alpha \leq 1/2$. While for $Z\alpha > 1/2$, there is not an absolute ground state in the semi-classical scenario. This can be understood by examining how the lowest energy states are selected by the quantization rule in the semi-classical scenario out of the last stable orbits (B.2.9) in the classical scenario. For the case of $Z\alpha \leq 1/2$, equating p_ϕ in Eq. (B.2.9) to $p_\phi = \hbar(l + 1/2)$ (B.3.1), we find the selected state $l = 0$ is only possible solution so that the ground state $l = 0$ in the semi-classical scenario corresponds to the last stable orbits (B.2.9) in the classical scenario. While for the case of $Z\alpha > 1/2$, equating p_ϕ in Eq. (B.2.9) to $p_\phi = \hbar(l + 1/2)$ (B.3.1), we find the selected semi-classical state

$$
\tilde{l} = \frac{Z\alpha - 1}{2} > 0, \tag{B.3.9}
$$

in the semi-classical scenario corresponds to the last stable orbits (B.2.9) in the classical scenario. This state $l = \tilde{l} > 0$ is not protected by the Heisenberg indeterminacy principle from quantum-mechanically decaying in $\hbar$-steps to the states with lower angular momenta and energies (correspondingly smaller radius R_L (B.3.3)) via photon emissions. This clearly shows that the "$Z = 137$-catastrophe" corresponds to $R_L \to 0$, falling to the center of the Coulomb potential and all semi-classical states (l) are unstable.

Then we consider the stability of semi-classical states against such transition in the case of charged cores $R_c \neq 0$. Substituting p_ϕ in Eq. (B.3.1) into Eq. (B.2.8), we obtain the selected semi-classical state $\tilde{l}$ corresponding to the last stable orbit outside the core,

$$\tilde{l} = \sqrt{2}\left(\frac{R_c}{\lambda}\right)\left[\left(\frac{4R_c}{Z\alpha\lambda}+1\right)^{1/2}-1\right]^{-1/2} \approx (Z\alpha)^{1/4}\left(\frac{R_c}{\lambda}\right)^{3/4} > 0. \quad \text{(B.3.10)}$$

Analogously to Eq. (B.3.9), the same argument concludes the instability of this semi-classical state, which must quantum-mechanically decay to states with angular momentum $l < \tilde{l}$ inside the core, provided these semi-classical states are not occupied. This conclusion is independent of $Z\alpha$-value.

We go on to examine the stability of semi-classical states inside the core. In the non-relativistic case $(1 \gg \beta > \kappa^2)$, the last classical stable orbits locate at $R_L \to 0$ and $p_\phi \to 0$ given by Eqs. (B.2.13,B.2.14), corresponding to the lowest semi-classical state (B.3.5,B.3.6) with $l = 0$ and energy $mc^2 > \mathcal{E} > 0$. In the ultra-relativistic case $(\beta > \kappa \gg 1)$, the last classical stable orbits locate at $R_L \to 0$ and $p_\phi \to 0$ given by Eqs. (B.2.16,B.2.17), corresponding to the lowest semi-classical state (B.3.7,B.3.8) with $l = 0$ and minimal energy,

$$\mathcal{E} \simeq \frac{3}{2}\beta\left[\left(\frac{1}{2Z\alpha}\right)^{2/3}-1\right]mc^2 \approx -\frac{3}{2}\beta mc^2. \quad \text{(B.3.11)}$$

This concludes that the $l = 0$ semi-classical state inside the core is an absolute ground state in both non- and ultra-relativistic cases. The Pauli principle assure that all semi-classical states $l > 0$ are stable, provided all these states accommodate electrons. The electrons can be either present inside the neutral core or produced from the vacuum polarization, later will be discussed in details.

We are particular interested in the ultra-relativistic case $\beta > \kappa \gg 1$, i.e., $Z\alpha \gg 1$, the energy-levels of semi-classical states can be profound than $-mc^2$ ($\mathcal{E} < -mc^2$), energy-level crossings and pair-productions occur if these states are unoccupied, as discussed in introductory section. It is even more important to mention that neutral cores like neutron stars of proton number $Z \sim 10^{52}$, the Thomas-Fermi approach has to be adopted to find the configuration of electrons in these semi-classical states, which has the depth of energy-levels $\mathcal{E} \sim -m_\pi c^2$ to accommodate electrons and a supercritical electric field ($E > E_c$) on the surface of the core (1; 48).

B.4. Production of electron-positron pair

When the energy-levels of semi-classical (bound) states $\mathcal{E} \leq -mc^2$ (B.2.19), energy-level crossings between these energy-levels (B.2.17) and negative energy continuum (B.2.2) for $p_r = 0$, as shown in Fig. B.2. The energy-level-crossing indicates that $\mathcal{E}$ (B.2.17) and E_- (B.2.2) are equal,

$$\mathcal{E} = E_-, \tag{B.4.1}$$

where angular momenta p_ϕ in $\mathcal{E}$ (B.3.8) and E_- (B.2.2) are the same for angular-momentum conservation. The production of electron-positron pairs must takes place, provided these semi-classical (bound) states are unoccupied. The phenomenon of pair production can be understood as a quantum-mechanical tunneling process of relativistic electrons. The energy-levels $\mathcal{E}$ of semi-classical (bound) states are given by Eq. (B.3.8) or (B.2.19). The probability amplitude for this process can be evaluated by a semi-classical calculation using WKB method (64):

$$W_{\rm WKB}(|\mathbf{p}_\perp|) \equiv \exp\left\{-\frac{2}{\hbar}\int_{R_b}^{R_n} p_r dr\right\}, \tag{B.4.2}$$

where $|\mathbf{p}_\perp| = p_\phi/r$ is transverse momenta and the radial momentum,

$$p_r(r) = \sqrt{(c|\mathbf{p}_\perp|)^2 + m^2c^4 - [\mathcal{E} + V(r)]^2}. \tag{B.4.3}$$

The energy potential $V(r)$ is either given by $V_{\rm out}(r)$ (B.2.3) for $r > R_c$, or $V_{\rm in}(r)$ (B.2.4) for $r < R_c$. The limits of integration (B.4.2): $R_b = R_L < R_c$ (B.2.16) or (B.3.7) indicating the location of the classical orbit (classical turning point) of semi-classical (bound) state; while another classical turning point R_n is determined by setting $p_r(r) = 0$ in Eq. (B.4.3). There are two cases: $R_n < R_c$ and $R_n > R_c$, depending on β and κ values.

To obtain a maximal WKB-probability amplitude (B.4.2) of pair production, we only consider the case that the charge core is bare and

- the lowest energy-levels of semi-classical (bound) states: $p_\phi/(Ze^2) = \kappa/\beta \to 0$, the location of classical orbit(B.2.16) $R_L = R_b \to 0$ and energy (B.2.17) $\mathcal{E} \to \mathcal{E}_{\rm min} = -3\beta mc^2/2$ (B.2.20);
- another classical turning point $R_n \leq R_c$, since the probability is exponentially suppressed by a large tunneling length $\Delta = R_n - R_b$.

In this case ($R_n \leq R_c$), Eq. (B.4.3) becomes

$$p_r = \sqrt{(c|\mathbf{p}_\perp|)^2 + m^2c^4}\sqrt{1 - \frac{\beta^2 m^2 c^4}{4[(c|\mathbf{p}_\perp|)^2 + m^2c^4]}\left(\frac{r}{R_c}\right)^4}, \tag{B.4.4}$$

and $p_r = 0$ leads to

$$\frac{R_n}{R_c} = \left(\frac{2}{\beta mc^2}\right)^{1/2} [(c|\mathbf{p}_\perp|)^2 + m^2c^4]^{1/4}. \tag{B.4.5}$$

Using Eqs. (B.4.2,B.4.4,B.4.5), we have

$$\begin{aligned} W_{\rm WKB}(|\mathbf{p}_\perp|) &= \exp\left\{-\frac{2^{3/2}[(c|\mathbf{p}_\perp|)^2 + m^2c^4]^{3/4}R_c}{c\hbar(mc^2\beta)^{1/2}}\int_0^1\sqrt{1-x^4}dx\right\} \\ &= \exp\left\{-0.87\frac{2^{3/2}[(c|\mathbf{p}_\perp|)^2 + m^2c^4]^{3/4}R_c}{c\hbar(mc^2\beta)^{1/2}}\right\}. \end{aligned} \tag{B.4.6}$$

Dividing this probability amplitude by the tunneling length $\Delta \simeq R_n$ and time interval $\Delta t \simeq 2\hbar\pi/(2mc^2)$ in which the quantum tunneling occurs, and integrating over two spin states and the transverse phase-space $2\int d\mathbf{r}_\perp d\mathbf{p}_\perp/(2\pi\hbar)^2$, we approximately obtain the rate of pair-production per the unit of time and volume,

$$\Gamma_{\rm NS} \equiv \frac{d^4N}{dtd^3x} \simeq \frac{1.15}{6\pi^2}\left(\frac{Z\alpha}{\tau R_c^3}\right)\exp\left\{-\frac{2.46}{(Z\alpha)^{1/2}}\left(\frac{R_c}{\lambda}\right)^{3/2}\right\}, \tag{B.4.7}$$

$$= \frac{1.15}{6\pi^2}\left(\frac{\beta}{\tau\lambda R_c^2}\right)\exp\left\{-\frac{2.46R_c}{\beta^{1/2}\lambda}\right\}, \tag{B.4.8}$$

$$= \frac{1.15}{6\pi^2}\left(\frac{1}{\tau\lambda^2R_c}\right)\left(\frac{E_s}{E_c}\right)\exp\left\{-2.46\left(\frac{R_c}{\lambda}\right)^{1/2}\left(\frac{E_c}{E_s}\right)^{1/2}\right\} \tag{B.4.9}$$

where $E_s = Ze/R_c^2$ being the electric field on the surface of the core and the Compton time $\tau = \hbar/mc^2$.

To have the size of this pair-production rate, we compare it with the Sauter-Euler-Heisenberg-Schwinger rate of pair-production in a constant field E (16; 34; 35),

$$\Gamma_{\rm S} \equiv \frac{d^4N}{dtd^3x} \simeq \frac{1}{4\pi^3\tau\lambda^3}\left(\frac{E}{E_c}\right)^2\exp\left\{-\pi\frac{E_c}{E}\right\}. \tag{B.4.10}$$

When the parameter $\beta \simeq (R_c/\lambda)^2$, Eq. (B.4.8) becomes

$$\Gamma_{\rm NS} \equiv \frac{d^4N}{dtd^3x} \simeq \frac{1.15}{6\pi^2}\left(\frac{1}{\tau\lambda^3}\right)\exp\{-2.46\} = 1.66\cdot 10^{-3}/(\tau\lambda^3), \tag{B.4.11}$$

which is close to the Sauter-Euler-Heisenberg-Schwinger rate (B.4.10) $\Gamma_{\rm S} \simeq 3.5\cdot 10^{-4}/(\tau\lambda^3)$ at $E \simeq E_c$. Taking a neutron star with core mass $M = M_\odot$ and radius $R_c = 10$km, we have $R_c/\lambda = 2.59\cdot 10^{16}$ and $\beta = 3.86\cdot 10^{-17}Z\alpha$, leading to $Z \simeq 2.4 \cdot 10^{51}$ and the electric field on the core surface $E_s/E_c = Z\alpha(\lambda/R_c)^2 \simeq 2.6 \cdot 10^{16}$. In this case, the charge-mass radio $Q/(G^{1/2}M) = 2 \cdot 10^{-6}|e|/(G^{1/2}m_p) = 2.2 \cdot 10^{12}$, where where G is the Newton constant and proton's charge-mass radio $|e|/(G^{1/2}m_p) = 1.1 \cdot 10^{18}$.

Let us consider another case that the electric field on the core surface E_s (B.2.5) is about the critical field ($E_s \simeq E_c$). In this case, $Z = \alpha^{-1}(R_c/\lambda)^2 \simeq 9.2 \cdot 10^{34}$, $\beta = Z\alpha\lambda/R_c = R_c/\lambda \simeq 2.59 \cdot 10^{16}$, and the rate (B.4.8) becomes

$$\Gamma_{\rm NS} \equiv \frac{d^4N}{dtd^3x} \simeq \frac{1.15}{6\pi^2}\left(\frac{1}{\tau\lambda^3}\right)\left(\frac{\lambda}{R_c}\right)\exp\left\{-2.46\left(\frac{R_c}{\lambda}\right)\right\}, \tag{B.4.12}$$

which is exponentially smaller than Eq. (B.4.11) for $R_c \gg \lambda$. In this case, the charge-mass radio $Q/(G^{1/2}M) = 8.46 \cdot 10^{-5}$.

It is interesting to compare this rate of electron-positron pair-production with the rate given by the Hawking effect. We take $R_c = 2GM/c^2$ and the charge-mass radio $Q/(G^{1/2}M) \simeq 10^{-19}$ for a naive balance between gravitational and electric forces. In this case $\beta = \frac{1}{2}(Q/G^{1/2}M)(|e|/G^{1/2}m) \simeq 10^2$, the rate (B.4.8) becomes,

$$\Gamma_{\rm NS} \;=\; \frac{1.15}{6\pi^2}\left(\frac{25}{\tau\lambda^3}\right)\left(\frac{1}{mM}\right)\exp\left\{-0.492(mM)\right\}, \tag{B.4.13}$$

where $mM = R_c/(2\lambda)$. This is much larger than the rate of electron-positron emission by the Hawking effect (65),

$$\Gamma_{\rm H} \;\sim\; \exp\left\{-8\pi(mM)\right\}, \tag{B.4.14}$$

since the exponential factor $\exp\{-0.492(mM)\}$ is much larger than $\exp\{-8\pi(mM)\}$, where $2mM = R_c/\lambda \gg 1$.

B.5. Summary and remarks

In this letter, analogously to the study in atomic physics with large atomic number Z, we study the classical and semi-classical (bound) states of electrons in the electric potential of a massive and charged core, which has a uniform charge distribution and macroscopic radius. We have found negative energy states of electrons inside the core, whose energies can be smaller than $-mc^2$, and the appearance of energy-level crossing to the negative energy spectrum. As results, quantum tunneling takes place, leading to electron-positron pairs production, electrons then occupy these semi-classical (bound) states and positrons are repelled to infinity. Assuming that massive charged cores are bare and non of these semi-classical (bound) states are occupied, we analytically obtain the maximal rate of electron-positron pair production in terms of core's radius, charge and mass, and we compare it with the Sauter-

Euler-Heisenberg-Schwinger rate of pair-production in a constant field. We have seen that even for very small charge-mass radio of the core that is given by the the naive balance between gravitational and electric forces, this rate is much larger than the rate of electron-positron pair-production by the Hawking effect.

Any electron occupations of these semi-classical (bound) states must screen core's charge and the massive core is no longer bare. The electric potential potential inside the core is changed. For the core consists of a large number of electrons, the Thomas-Fermi approach has to be adopted. We recently study (1; 48) the electron distribution inside and outside the massive core, i.e., the distribution of electrons occupying stable states of the massive core, and find the electric field on the surface of the massive core is overcritical.

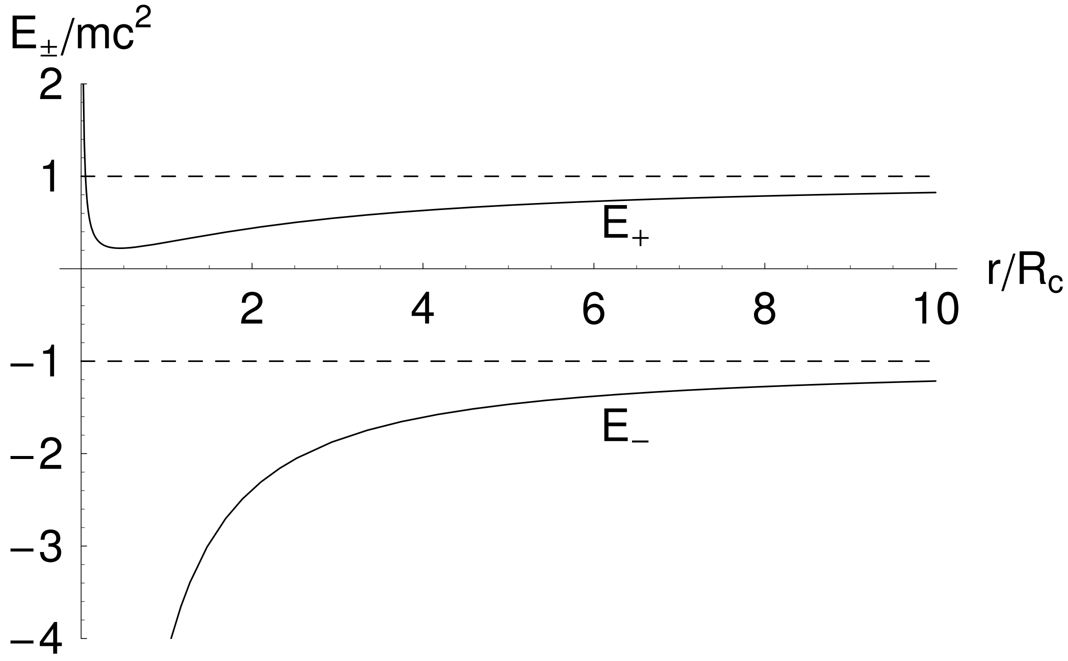

Figure B.1.: In the case of point-like charge distribution, we plot the positive and negative effective potential energies $E_\pm$ (B.2.2), $p_\phi/(mcR_c) = 2$ and $Ze^2 = 1.95mc^2R_c$, to illustrate the radial location R_L (B.2.6) of stable orbits where E_+ has a minimum (B.2.7). All stable orbits are described by $cp_\phi > Ze^2$. The last stable orbits are given by $cp_\phi \rightarrow Ze^2 + 0^+$, whose radial location $R_L \rightarrow 0$ and energy $\mathcal{E} \rightarrow 0^+$. There is no any stable orbit with energy $\mathcal{E} < 0$ and the energy-level crossing with the negative energy spectrum E_- is impossible.

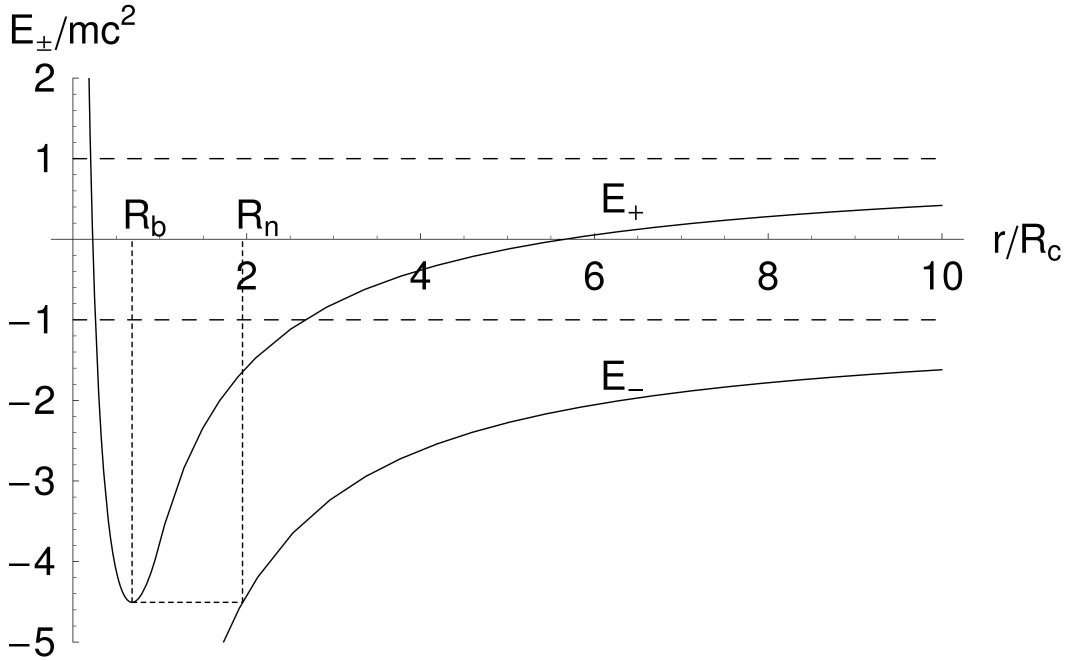

Figure B.2.: For the core $\kappa = 2$ and $\beta = 6$, we plot the positive and negative effective potentials $E_\pm$ (B.2.2) , in order to illustrate the radial location (B.2.16) $R_L < R_c$ of stable orbit, where E_+'s minimum (B.2.17) $\mathcal{E} < mc^2$ is. All stable orbits inside the core are described by $\beta > \kappa > 1$. The last stable orbit is given by $\kappa/\beta \to 0$, whose radial location $R_L \to 0$ and energy $\mathcal{E} \to \mathcal{E}_{\rm min}$ (B.2.20). We indicate that the energy-level crossing between bound state (stable orbit) energy at $R_L = R_b$ and negative energy spectrum E_- (B.2.17) at the turning point R_n.

C. On the Generalization of the Oppenheimer–Volkoff Model of Neutron Stars

The Einstein–Maxwell Field Equations.

The metric for a spherically symmetric spacetime can be written as

$$ds^2 = -e^{\nu} c^2 dt^2 + e^{\lambda} dr^2 + r^2 d\theta^2 + r^2 \sin^2 d\phi^2 \,, \tag{C.0.1}$$

where ν and λ are functions of r. We denote $x^{\alpha} \equiv (x^0, x^1, x^2, x^3) = (c\,t, r, \theta, \phi)$.

The energy–momentum tensor for an isotropic fluid endowed with electric field can be written as

$$T_{\alpha\beta} = (\bar{\varepsilon} + \bar{p}) u_{\alpha} u_{\beta} + \bar{p} g_{\alpha\beta} + \Pi^{em}_{\alpha\beta} \,, \tag{C.0.2}$$

$$\Pi^{em}_{\alpha\beta} = 2p^{em} (h_{\alpha\beta} - 3\chi_{\alpha}\chi_{\beta}) \,, \tag{C.0.3}$$

where

$$\bar{\varepsilon} = \varepsilon + \varepsilon^{em} \,, \qquad \bar{p} = p + p^{em} \,, \qquad \varepsilon^{em} = 3p^{em} = \frac{e^{-(\nu+\lambda)}(\varphi')^2}{8\pi} \,,$$

being ε and p the energy density and pressure of the fluid, φ the Coulomb potential, u_{α} is a future directed time–like vector ($u_{\alpha}u^{\alpha} = -c^2$, $u^0 > 0$), χ_{α} is a space–like vector ($\chi_{\alpha}\chi^{\alpha} = c^2$) and $h_{\alpha\beta} = u_{\alpha}u_{\beta} + g_{\alpha\beta}$ is the projection tensor.

Thus the Einstein–Maxwell Field equations read

$$e^{-\lambda} \left(\frac{\lambda'}{r} - \frac{1}{r^2} \right) + \frac{1}{r^2} = \frac{8\pi G}{c^4} \bar{\varepsilon} \,, \tag{C.0.4}$$

$$e^{-\lambda} \left(\frac{\nu'}{r} + \frac{1}{r^2} \right) - \frac{1}{r^2} = \frac{8\pi G}{c^4} (p - 3p^{em}) \,, \tag{C.0.5}$$

$$p' = -\frac{\nu'}{2} (\varepsilon + p) - e^{-\nu/2} \varphi' \rho_{ch} \,, \tag{C.0.6}$$

$$\varphi'' + \left[\frac{2}{r} - \frac{(\lambda' + \nu')}{2} \right] \varphi' = -4\pi e^{\nu/2} e^{\lambda} \rho_{ch} \,, \tag{C.0.7}$$

where ρ_{ch} is the charge density.

The Eq.(C.0.6) is the generalization of the TOV equation for charged fluids and Eq.(C.0.7) is the general relativistic version of the Poisson equation.

The TOV Equation and the Equilibrium Conditions for the Gas.

In this section we derive the relation between the TOV equation and the equilibrium condition for the gas.

We consider a gas of electrons, protons and neutrons which is governed for the relativistic degenerate equation of state

$$\varepsilon = k_n \tilde{\varepsilon} , \qquad p = k_n \tilde{p} , \qquad k_n \equiv \frac{m_n c^2}{8\pi^2 \lambda_n^3} , \qquad \lambda_i = \frac{\hbar}{m_i c} , \tag{C.0.8}$$

$$\tilde{\varepsilon} = \sum_{i=e,p,n} \rho_i , \qquad \tilde{p} = \sum_{i=e,p,n} p_i , \qquad \varepsilon_i = \bar{k}_i \Phi_i , \qquad p_i = \bar{k}_i \Psi_i , \qquad \bar{k}_i \equiv (m_i/m_n)^4 , \tag{C.0.9}$$

$$\Phi_i = x_i(1+2x_i^2)\sqrt{1+x_i^2} - \ln(x_i + \sqrt{1+x_i^2}) , \quad \Psi_i = \frac{8}{3} x_i^3 \sqrt{1+x_i^2} - \Phi_i , \tag{C.0.10}$$

where $x_i \equiv \frac{P_i^F}{m_i c} = \lambda_i (3\pi^2 n_i)^{1/3}$, being m_i the rest–mass of the particle, P_i^F its Fermi momentum, λ_i its Compton wavelength and n_i its number density.

By definition, the above EOS follows the first law of the thermodynamics for a gas at zero temperature

$$\varepsilon_i + p_i = n_i \, \mu_i , \qquad p_i' = n_i \, \mu_i' , \tag{C.0.11}$$

where $\mu_i = m_i c^2 \sqrt{1+x_i^2}$ is the chemical potential, so using it the the TOV equation (C.0.6) becomes

$$\sum_{i=e,p,n} n_i \, (\mu_i' + \frac{\nu'}{2} \mu_i + q_i e^{-\nu/2} \varphi') = 0 . \tag{C.0.12}$$

Using the General Relativistic Fermi energy of a gas at $T = 0$ (68)

$$E_i^F = \sqrt{-g_{00}} \mu_i + q_i A_\alpha u^\alpha , \tag{C.0.13}$$

where A_α is the electromagnetic four potential, which in the present case becomes

$$E_i^F = e^{\nu/2} \mu_i + q_i \varphi , \tag{C.0.14}$$

the TOV equation (C.0.12) can be written as

$$\sum_{i=e,p,n} n_i \frac{dE_i^F}{dr} = 0 . \tag{C.0.15}$$

Therefore, the TOV equation is, indeed, an equilibrium equation for the Fermi energy when we deal with one-component gases because it reduces to E^F = constant. We recall that the above definition of Fermi energy contains the rest energy of the system, so if we want conserve analogy with the classical and special relativistic case we must redefine it as follows

$$\varepsilon_e^F = E_e^F - e^{\nu_s/2} m_e c^2 \,, \tag{C.0.16}$$

which obviously does not change the TOV equation (C.0.15). The subscript 's' means that we have redefined the Fermi energy up to a constant, which we have taken as its value on the surface of the configuration assuming global neutrality ($\varphi_s = 0$).

Assuming the general relativistic Thomas-Fermi equilibrium condition for the electron gas and the $\beta-$ equilibrium condition

$$\varepsilon_e^F = 0 \,, \qquad \varepsilon_n^F = \varepsilon_p^F \,, \tag{C.0.17}$$

the TOV equation (C.0.15) reduces to

$$\varepsilon_e^F = \varepsilon_p^F = \varepsilon_n^F = 0 \,. \tag{C.0.18}$$

It is worth to note that the above equations represent just the conditions of thermodynamic equilibrium of the gas, so we can extract enormous information from them. In fact, we will use them to demonstrate that local charge neutrality ($n_e = n_p$) does not represent a self-consistent solution to the system.

Let us rewrite Eqs.(C.0.18) in the form

$$\sqrt{1+x_e^2} = \frac{e^{\nu_s/2} + e\varphi/(m_e c^2)}{e^{\nu_s/2} - e\varphi/(m_p c^2)} \sqrt{1+x_p^2} \,, \tag{C.0.19}$$

$$\sqrt{1+x_n^2} = \frac{e^{\nu_s/2}}{e^{\nu_s/2} - e\varphi/(m_p c^2)} \sqrt{1+x_p^2} \,. \tag{C.0.20}$$

From the above equations we can see there is an upper limit for the Coulomb potential, i.e.

$$e\varphi < e^{\nu_s/2} m_p c^2 \,. \tag{C.0.21}$$

In addition, if we take the case of local neutrality $\varphi \equiv 0$, the thermodynamic equilibrium conditions reduce to

$$x_e = x_p \qquad x_n = x_p \,. \tag{C.0.22}$$

The first equation contradicts the local neutrality condition $n_e = n_p$, which in terms of the normalized Fermi momentum reads

$$m_e\, x_e = m_p\, x_p\,, \tag{C.0.23}$$

while the second one appears to be impossible to achieve due to the difference between the neutron mass and the proton one. Therefore, the only possible solution to this case is

$$n_e = n_p = n_n = 0\,. \tag{C.0.24}$$

Numerical Integration of the Equations.

Using the Eqs. (C.0.19) the normalized Fermi momenta x_i can be written as a function of the Coulomb potential φ and the metric function ν, thus we need to integrate only the equations regarding the functions λ, ν and φ.

We perform the numerical integration of the Einstein-Maxwell system (C.0.4-C.0.7) up to the point where the mass density reaches the so-called melting density ($\rho_m \approx 2 \times 10^{14}$ g cm^{-3}) (69), below which the system cannot be considered as a liquid of electrons, protons and neutrons, and another EOS should be considered (25; 26).

As we have seen from the equilibrium equations, the system will have a net charge at every point of the configuration, also at the melting point, so up to this point we have a charged core. In order to obtain a globally neutral core, we will apply the procedure of Ruffini *et al.* (1). From the melting point we perform an integration on a very small scale, of the order of the electron Compton wavelength, where obviously gravity does not play any role. On this small region we maintain the proton number density constant at its value on the melting density point. In this region the electric field increases due to the charge separation (the electron number density decreases while the proton one holds constant). After certain radius the proton number density is dropped to zero while the electron one is integrated with continuity until global neutrality is reached.

It is worth noticing that if we drop immediately the proton number to zero at the melting density point and continue the integration with the electron gas is impossible to reach global neutrality, because the boundary conditions are not satisfied (a small change in the electron density of the external shell produce a large electric field while the electric field at the melting point would be very small, producing a discontinuity in the first derivative of the Coulomb potential).

Below we show the numerical results for the central conditions $\rho_c \approx 1.32 \times 10^{14}\, g\, cm^{-3}$ and $P_c \approx 6.5 \times 10^{34}\, dyn\, cm^{-2}$. The red line corresponds to the melting density point.

Results.

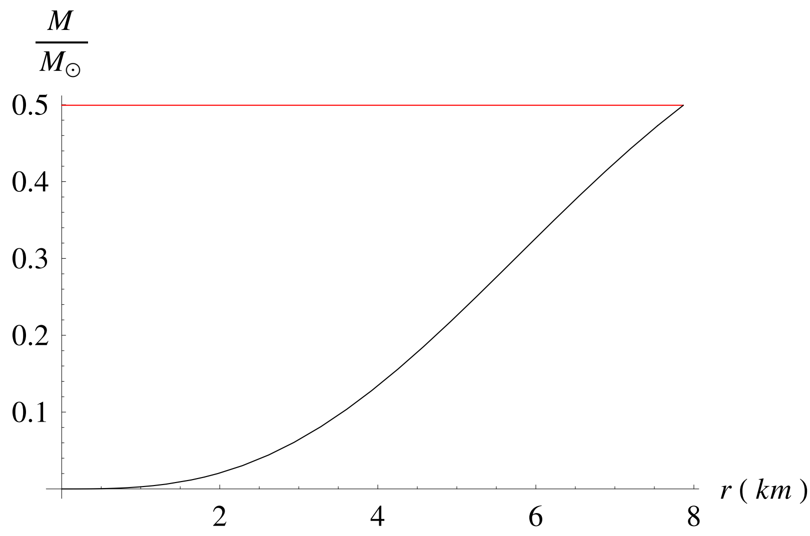

Figure C.1.: Mass of the Core as function of the radius.

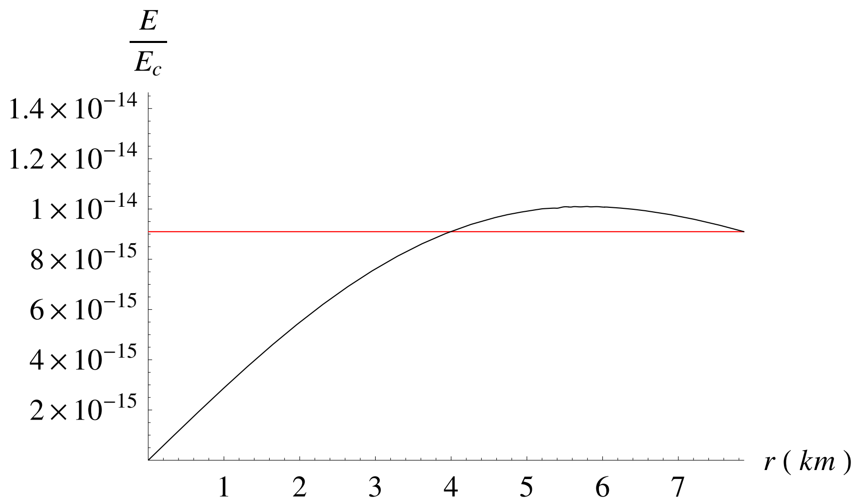

Figure C.2.: Electric Field in the Core as function of the radius.

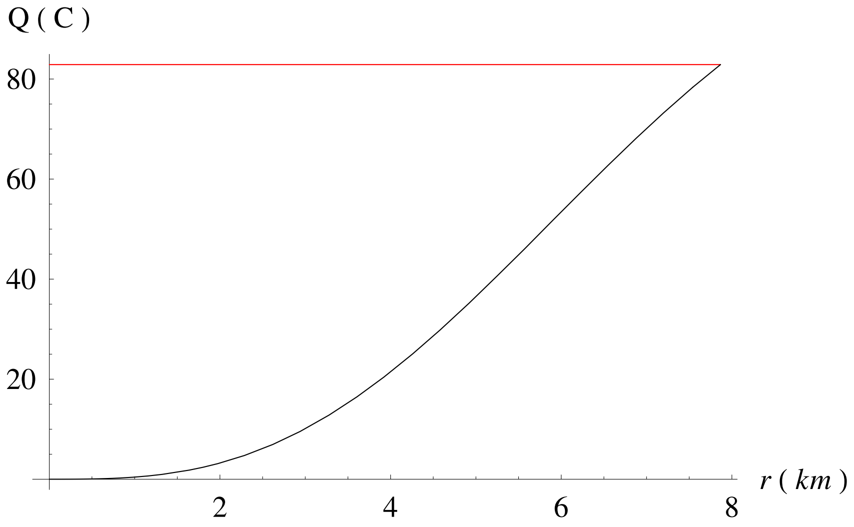

Figure C.3.: Charge of the Core as function of the radius.

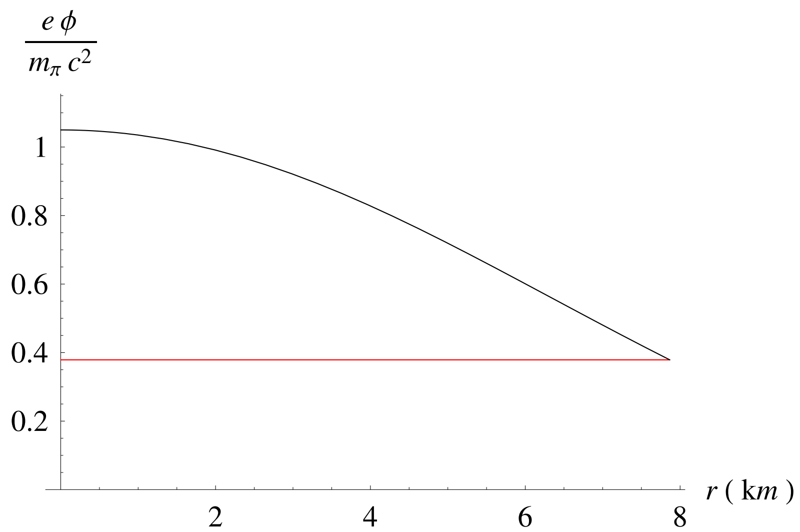

Figure C.4.: Coulomb potential energy of the Core as function of the radius.

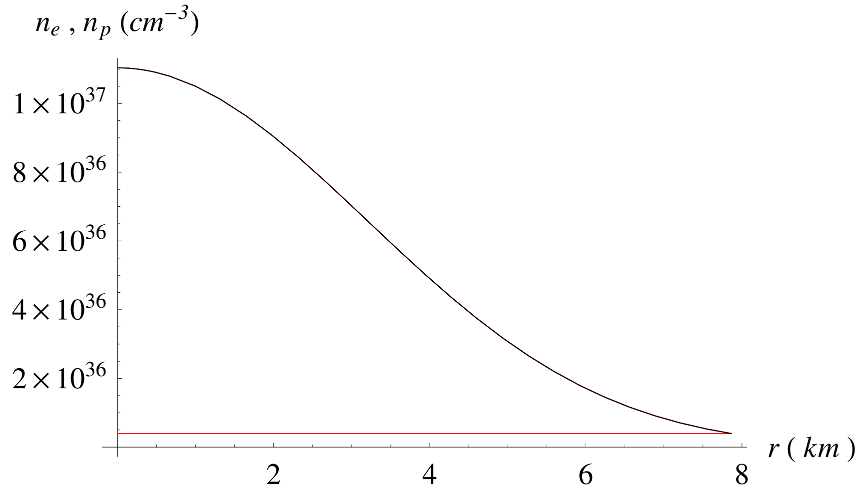

Figure C.5.: Number density of electrons and protons in the Core as function of the radius.

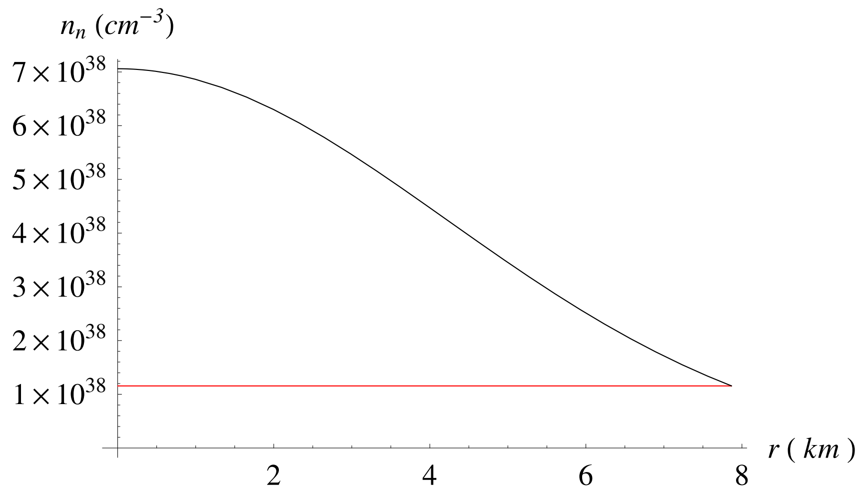

Figure C.6.: Number density of neutrons in the Core as function of the radius.

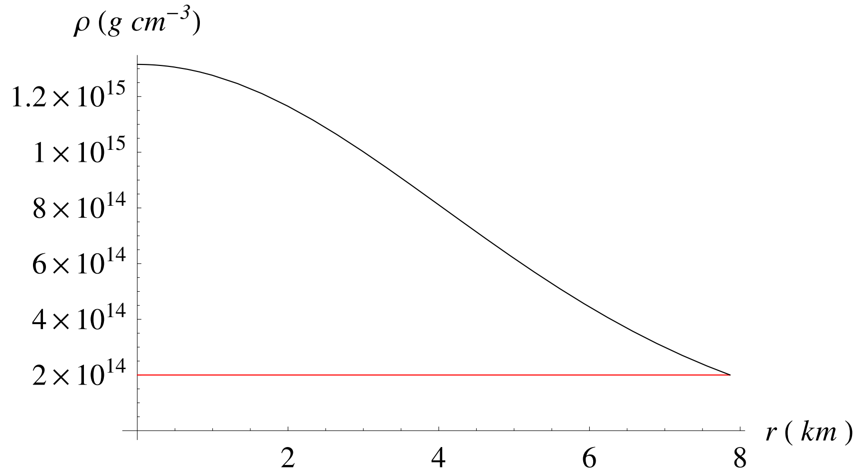

Figure C.7.: Mass density of the Core as function of the radius.

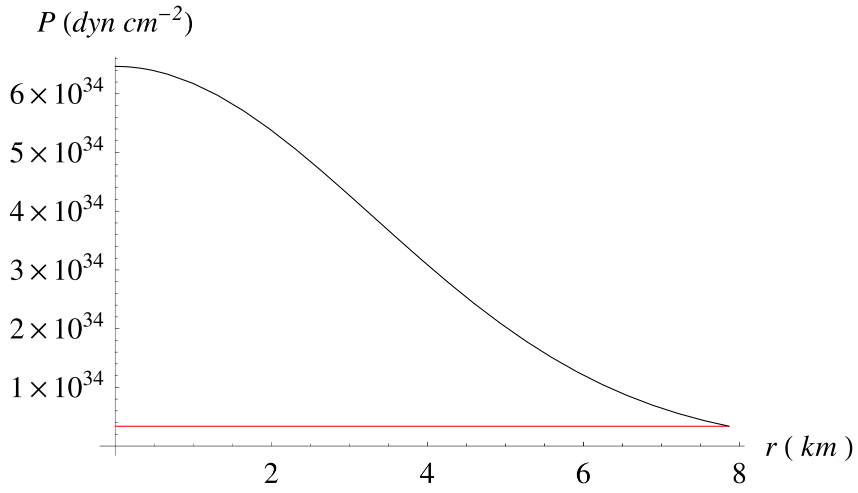

Figure C.8.: Pressure of the Core as function of the radius.

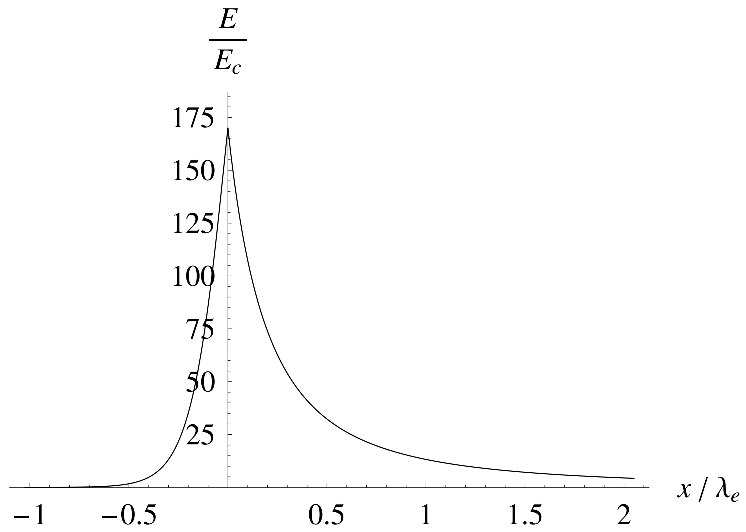

Figure C.9.: Electric Field of the Shell as function of the radius.

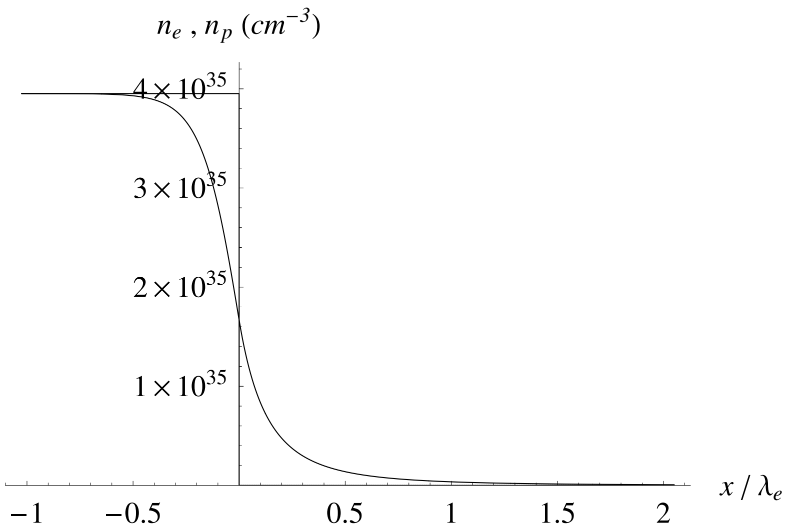

Figure C.10.: Number density of electrons and protons in the Shell as function of the radius.

D. The Outer Crust of Neutron Stars

The General Relativistic Model. The Outer Crust of Neutron Stars is the region of Neutron Stars characterized by a mass density less than the "neutron drip" density $\rho_{drip} = 4.3 \cdot 10^{11} g\, cm^{-3}$ (69) and composed by White Dwarf - like material (fully ionized nuclei and free electrons). Its internal structure can be described by the Tolman-Oppenheimer-Volkoff (TOV) equation

$$\frac{dP}{dr} = -\frac{G\left(\rho + \frac{P}{c^2}\right)\left(m + \frac{4\pi r^3 P}{c^2}\right)}{r^2\left(1 - \frac{2Gm}{rc^2}\right)}, \tag{D.0.1}$$

together with the equation

$$\frac{dm}{dr} = 4\pi r^2 \rho, \tag{D.0.2}$$

where m, ρ and P are the mass, the density and the pressure of the system. We have determined M_{crust} and ΔR_{crust} by integrating eq. (D.0.1) and (D.0.2) from $r_{in} = R_{is}$, where R_{is} is the radius of the inner part of the star (the base of the Outer Crust).
The pressure and the mass density of the system are

$$P \approx P_e, \tag{D.0.3}$$

$$\rho \approx \mu_e m_n n_e. \tag{D.0.4}$$

P_e is the pressure of electrons, given by (70)

$$P_e = k_e\, \phi_e, \tag{D.0.5}$$

where

$$k_e = \frac{m_e c^2}{8\pi^2 \lambda_e^3}, \tag{D.0.6}$$

$$\phi_e = \tag{D.0.7}$$

$$\xi_e\left(\frac{2}{3}\xi_e^2 - 1\right)\sqrt{\xi_e^2 - 1} + \log\left(\xi_e + \sqrt{\xi_e^2 - 1}\right), \tag{D.0.8}$$

with λ_e the Compton wavelenght of electrons, $\xi_e = \sqrt{1+x_e^2}$ and x_e the Fermi momentum of electrons normalized to $(m_e c)$. μ_e is the mean molecular weight per electron that, for a completely ionized element of atomic weight A and number Z, is equal to A/Z (for simplicity, we assume $\mu_e = 2$), m_n is the mass of neutrons and n_e is the number density of electrons

$$n_e = \frac{x_e^3}{3\pi^2 \lambda_e^3}. \tag{D.0.9}$$

In eq. (D.0.4) we have assumed the local charge neutrality of the system.

The mass and the thickness of the crust. We have integrated eq. (D.0.1) and (D.0.2) for different sets of initial conditions; in fig. D.1 are shown the results obtained assuming

$$10\,km \leq R_{is} \leq 20\,km,$$
$$1M_\odot \leq M_{is} \leq 3M_\odot$$

and an initial pressure equal to $1.6\,10^{30} dyne\,cm^{-2}$, that corresponds to a mass density equal to ρ_{drip}.
It can be seen that M_{crust} has values ranging from $10^{-6}M_\odot$ to $10^{-3}M_\odot$; both M_{crust} and ΔR_{crust} increase by increasing R_{is} and decreasing M_{is} (see fig. D.1, D.2).

It's important to note that the values estimated for M_{crust} strongly depend on the values of M_{is} and R_{is} used; in particular, the values of M_{is} considered are greater that the maximum mass calculated for neutrons stars with a core of degenerate relativistic electrons, protons and neutrons in local charge neutrality ($M_{max} = 0.7M_\odot$ (22)). The outstanding theoretical problem to address is to identify the physical forces influencing such a strong departure; the two obvious candidate are the electromagnetic structure in the core and/or the strong interactions.

The Fireshell Model of GRBs. In the Fireshell Model (8) GRBs are generated by the gravitational collapse of the star progenitor to a charged black hole. The electron–positron plasma created in the process of black hole (BH) formation expands as a spherically symmetric "fireshell". It evolves and encounters the *baryonic remnant* of the star progenitor of the newly formed BH, then is loaded with baryons and expands until the trasparency condition is reached and the Proper - GRB is emitted. The afterglow emission starts due to the collision between the remaining optically thin fireshell and the Circum-Burst Medium. A schematization of the model is shown in fig. D.3.
The baryon loading is measured by the dimensionless quantity

$$B = \frac{M_B c^2}{E_{dya}}, \tag{D.0.10}$$

GRB	$M_B/M_\odot$
970228	5.0×10^{-3}
050315	4.3×10^{-3}
061007	1.3×10^{-3}
991216	7.3×10^{-4}
011121	9.4×10^{-5}
030329	5.7×10^{-5}
060614	4.6×10^{-6}
060218	1.3×10^{-6}

Table D.1.: GRBs and correspondent values of M_B used to reproduce the observed data within the Fireshell Model (71), in units of solar masses.

where M_B is the mass of the baryonic remnant and E_{dya} is the energy of the dyadosphere, the region outside the horizon of a BH where the electric field is of the order of the critical value for electron positron pair creation (16), (34) and (35)

$$E_c = \frac{m_e^2 c^3}{e\hbar} \approx 10^{16}\, V\, cm^{-1}. \tag{D.0.11}$$

B and E_{dya} are the two free parameters of the model.

The mass of the crust and M_B. Using the values of B and E_{dya} constrained by the observational data of several GRBs (71) and eq. (D.0.10), we have obtained the correspondent values of M_B (see table D.1). It can be seen that these values are compatible with the ones of M_{crust}.

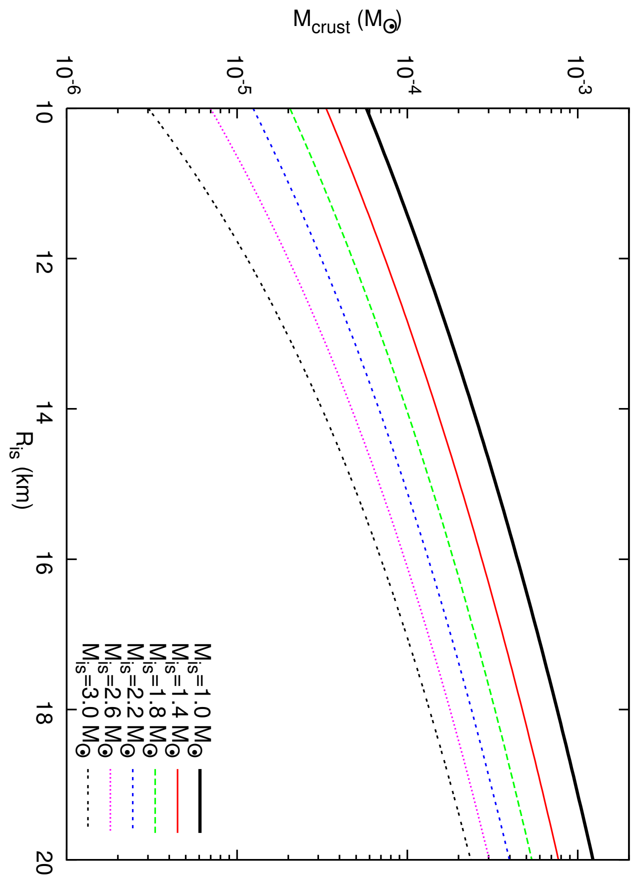

Figure D.1.: Values of M_{crust} in units of solar masses, as function of R_{is}, for different values of M_{is} (see legend).

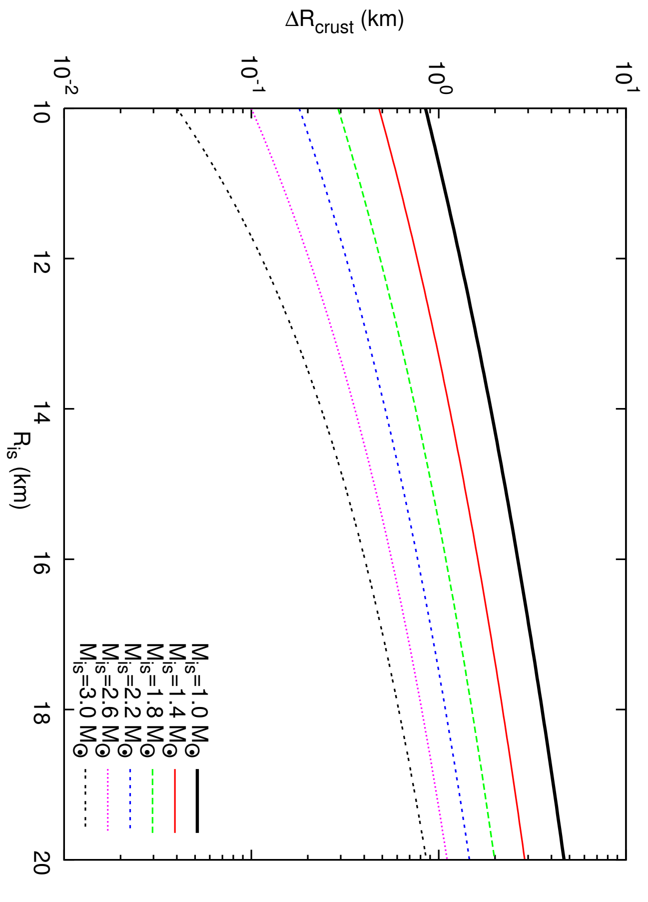

Figure D.2.: Values of thickness of the Outer Crust ΔR_{crust} in km, as function of R_{is}, for different values of M_{is} (see legend).

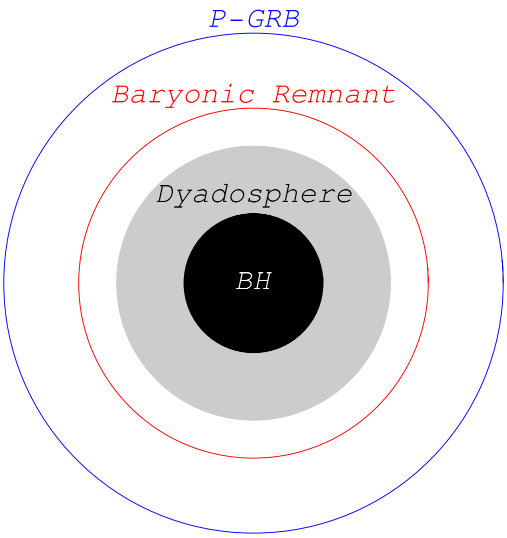

Figure D.3.: Schematization of the Fireshell Model of GRBs.

E. The Role of Thomas - Fermi approach in Neutron Star Matter

.

Introduction.

We first recall how certainly one of the greatest success in human understanding of the Universe has been the research activity started in 1054 by Chinese, Korean and Japanese astronomers by the observations of a "Guest Star"(see e.g. Shklovsky (72)), followed by the discovery of the Pulsar $NPO532$ in the Crab Nebula in 1967, (see e.g. Manchester and Taylor (73)), still presenting challenges in the yet not identified physical process originating the expulsion of the remnant in the Supernova explosion (see e.g. Mezzacappa and Fuller (7) and Fig. E.1(a)). We are currently exploring the neutron star equilibrium configuration for a missing process which may lead to the solution of the above mentioned astrophysical puzzle.

We also recall an additional astrophysical observation which is currently capturing the attention of Astrophysicists worldwide: the Gamma ray Bursts or for short GRBs. Their discovery was accidental and triggered by a very unconventional idea proposed by Yacov Borisovich Zel'dovich (see e.g. (74)). It is likely that this idea served as an additional motivation for the United States of America to put a set of four Vela Satellites into orbit, 150,000 miles above the Earth. They were top-secret omnidirectional detectors using atomic clocks to precisely record the arrival times of both X-rays and γ-rays (see Fig. E.1(b)). When they were made operational they immediately produced results (see Fig. E.1(b)). It was thought at first that the signals originated from nuclear bomb explosions on the earth but they were much too frequent, one per day! A systematic analysis showed that they had not originated on the earth, nor even in the solar system. These Vela satellites had discovered GRBs! The first public announcement of this came at the AAAS meeting in San Francisco in a special session on neutron stars, black holes and binary X-ray sources, organized by Herb Gursky and myself (75).

A few months later, Thibault Damour and myself published a theoretical framework for GRBs based on the vacuum polarization process in the field of a Kerr–Newman black hole (19). We showed how the pair creation predicted by the Heisenberg–Euler–Schwinger theory (16; 35) would lead to a transformation of the black hole, asymptotically close to reversibility. The electron–positron pairs created by this process were generated by what we now call the blackholic energy (74). In that paper we concluded that this “naturally leads to a very simple model for the explanation of the recently discovered GRBs”. Our theory had two very clear signatures. It could only operate for black holes with mass M_{BH} in the range 3.2–10^6 $M_\odot$ and the energy released had a characteristic value of

$$E = 1.8 \times 10^{54} M_{BH}/M_\odot \,\text{ergs}\,. \tag{E.0.1}$$

Since nothing was then known about the location and the energetics of these sources we stopped working in the field, waiting for a clarification of the astrophysical scenario.

The situation changed drastically with the discovery of the “afterglow” of GRBs (77) by the joint Italian-Dutch satellite BeppoSAX (see Fig. E.1(b)). This X-ray emission lasted for months after the “prompt” emission of a few seconds duration and allowed the GRB sources to be identified much more accurately. This then led to the optical identification of the GRBs by the largest telescopes in the world, including the Hubble Space Telescope, the KECK telescope in Hawaii and the VLT in Chile (see Fig. E.1(b)). Also, the very large array in Socorro made the radio identification of GRBs possible. The optical identification of GRBs made the determination of their distances possible. The first distance measurement for a GRB was made in 1997 for GRB970228 and the truly enormous of isotropical energy of this was determined to be 10^{54} ergs per burst. This proved the existence of a single astrophysical system emitting as much energy during its short lifetime as that emitted in the same time by all other stars of all galaxies in the Universe![a] It is interesting that this “quantum” of astrophysical energy coincided with the one Thibault Damour and I had already predicted, see Eq. (E.0.1). Much more has been learned on GRBs in recent years confirming this basic result (see e.g. (8)). The critical new important step now is to understand the physical process leading to the critical fields needed for the pair creation process during the gravitational collapse process from a Neutron Stars to a Black Hole.

As third example, we recall the galactic ’X-ray bursters’ as well as some observed X-ray emission precursor of supernovae events (78). It is our opinion that the solution of: **a)** the problem of explaining the energetics of the emission of the remnant during the collapse to a Neutron Star, **b)** the problem of formation of the supercritical fields during the collapse to a Black Hole, **c)** the less energetics of galactic ’X-ray bursters’ and of the precursor of the supernovae explosion event, will find their natural explanation from a yet unexplored field: the electro-dynamical structure of a neutron star. We will outline a few crucial ideas of how a Thomas-Fermi approach to a neutron star

[1]Luminosity of average star = 10^{33} erg/s, Stars per galaxy = 10^{12}, Number of galaxies = 10^9. Finally, $33 + 12 + 9 = 54$!

can indeed represent an important step in identify this crucial new feature.

Thomas-Fermi model.

We first recall the basic Thomas-Fermi non relativistic Equations (see e.g. Landau and Lifshitz (79)). They describe a degenerate Fermi gas of N_{el} electrons in the field of a point-like nucleus of charge Ze. The Coulomb potential $V(r)$ satisfies the Poisson equation

$$\nabla^2 V(r) = 4\pi e n, \tag{E.0.2}$$

where the electron number density $n(r)$ is related to the Fermi momentum p_F by $n = p_F^3/(3\pi^2\hbar^3)$. The equilibrium condition for an electron, of mass m, inside the atom is expressed by $\frac{p_F^2}{2m} - eV = E_F$. To put Eq. (E.0.2) in dimensionless form, we introduce a function ϕ, related to Coulomb potential by $\phi(r) = V(r) + \frac{E_F}{e} = Ze\frac{\chi(r)}{r}$. Assuming $r = bx$, with $b = \frac{(3\pi)^{3/2}}{2^{7/3}}\frac{1}{Z^{1/3}}\frac{\hbar^2}{me^2}$, we then have the universal equation (41; 42)

$$\frac{d^2\chi(x)}{dx^2} = \frac{\chi(x)^{3/2}}{x^{1/2}}. \tag{E.0.3}$$

The first boundary condition for this equation follows from the request that approaching the nucleus one gets the ordinary Coulomb potential therefore $\chi(0) = 1$. The second boundary condition comes from the fact that the number of electrons N_{el} is $1 - \frac{N_{el}}{Z} = \chi(x_0) - x_0\chi'(x_0)$.

White dwarfs and Neutron Stars as Thomas-Fermi systems.

It was at the 1972 Les Houches organized by Bryce and Cecille de Witt summer School (see Fig. E.2(a) and (80)) that, generalizing a splendid paper by Landau (81), I introduced a Thomas-Fermi description of both White Dwarfs and Neutron Stars within a Newtonian gravitational theory and describing the microphysical quantities by a relativistic treatment. The equilibrium condition for a self-gravitating system of fermions, in relativistic regime is $c\sqrt{p_F^2 + m_n^2c^2} - m_nc^2 - m_nV = -m_nV_0$, where p_F is the Fermi momentum of a particle of mass m_n, related to the particle density n by $n = \frac{1}{3\pi^2\hbar^3}p_F^3$. $V(r)$ is the gravitational potential at a point at distance r from the center of the configuration and V_0 is the value of the potential at the boundary R_c of the configuration $V_0 = \frac{GNm_n}{R_c}$. N is the total number of particles. The Poisson equation is $\nabla^2 V = -4\pi G m_n n$. Assuming $V - V_0 = GNm_n\frac{\chi(r)}{r}$ and $r = bx$, with $b = \frac{(3\pi)^{2/3}}{2^{7/3}}\frac{1}{N^{1/3}}\left(\frac{\hbar}{m_nc}\right)\left(\frac{m_{Planck}}{m_n}\right)^2$ we obtain the gravitational Thomas-Fermi equation

$$\frac{d^2\chi}{dx^2} = -\frac{\chi^{3/2}}{\sqrt{x}}\left[1 + \left(\frac{N}{N^*}\right)^{4/3}\frac{\chi}{x}\right]^{3/2}, \tag{E.0.4}$$

where $N^* = \left(\frac{3\pi}{4}\right)^{1/2}\left(\frac{m_{Planck}}{m_n}\right)^3$. Eq.(E.0.4) has to be integrated with the boundary conditions $\chi(0) = 0, \quad -x_b\left(\frac{d\chi}{dx}\right)_{x=x_b} = 1$. Eq. (E.0.4) can be applied as well to the case of white dwarfs.

It is sufficient to assume

$$b = \frac{(3\pi)^{2/3}}{2^{7/3}}\frac{1}{N^{1/3}}\left(\frac{\hbar}{m_e c}\right)\left(\frac{m_{Planck}}{\mu m_n}\right)^2,$$
$$N^* = \left(\frac{3\pi}{4}\right)^{1/2}\left(\frac{m_{Planck}}{\mu m_n}\right)^3,$$
$$M = \int_0^{R_c} 4\pi r^2 n_e(r)\mu m_n dr.$$

For the equilibrium condition $c\sqrt{p_F^2 + m^2c^2} - mc^2 - \mu m_n V = -\mu m_n V_0$, in order to obtain for the critical mass the value $M_{crit} \approx 5.7 M_{sun}\mu_e^{-2} \approx 1.5 M_{sun}$.

The relativistic Thomas-Fermi equation.

In the intervening years my attention was dedicated to an apparently academic problem: the solution of a relativistic Thomas-Fermi Equation and extrapolating the Thomas-Fermi solution to large atomic numbers of $Z \approx 10^4 - 10^6$. Three new features were outlined: **a)** the necessity of introducing a physical size for the nucleus, **b)** the penetration of the electrons in the nucleus, **c)** the definition of an effective nuclear charge (15; 18). The electrostatic potential is given by $\nabla^2 V(r) = 4\pi e n$, where the number density of electrons is related to the Fermi momentum p_F by $n = \frac{p_F^3}{3\pi^2\hbar^3}$. In order to have equilibrium we have $c\sqrt{p_F^2 + m^2c^2} - mc^2 - eV(r) = E_F$. Assuming $\phi(r) = V(r) + \frac{E_F}{e} = Ze\frac{\chi(r)}{r}$, $Z_c = \left(\frac{3\pi}{4}\right)^{1/2}\left(\frac{\hbar c}{e^2}\right)^{3/2}$, and $r = bx$, with $b = \frac{(3\pi)^{3/2}}{2^{7/3}}\frac{1}{Z^{1/3}}\frac{\hbar^2}{me^2}$, the Eq. (E.0.3) becomes

$$\frac{d^2\chi(x)}{dx^2} = \frac{\chi(x)^{3/2}}{x^{1/2}}\left[1 + \left(\frac{Z}{Z_c}\right)^{4/3}\frac{\chi(x)}{x}\right]^{3/2}. \tag{E.0.5}$$

The essential role of the non-pointlike nucleus.

The point-like assumption for the nucleus leads, in the relativistic case, to a non-integrable expression for the electron density near the origin. We assumed a uniformly charged nucleus with a radius r_{nuc} and a mass number A given by the following semi-empirical formulae

$$r_{nuc} = r_0 A^{1/3}, \quad r_0 \approx 1.5 \times 10^{-13} cm, \tag{E.0.6}$$

$$Z \simeq \left[\frac{2}{A} + \frac{3}{200}\frac{1}{A^{1/3}}\right]^{-1}, \tag{E.0.7}$$

Eq.(E.0.5) then becomes

$$\frac{d^2\chi(x)}{dx^2} = \frac{\chi(x)^{3/2}}{x^{1/2}}\left[1 + \left(\frac{Z}{Z_c}\right)^{4/3}\frac{\chi(x)}{x}\right]^{3/2} - \frac{3x}{x_{nuc}^3}\theta(x_{nuc} - x), \tag{E.0.8}$$

where $\theta = 1$ for $r < r_{nuc}$, $\theta = 0$ for $r > r_{nuc}$, $\chi(0) = 0$, $\chi(\infty) = 0$.

Eq.(E.0.8) has been integrated numerically for selected values of Z (see Fig. E.2(b) and (15; 18)). Similar results had been obtained by Greiner and his school and by Popov and his school with special emphasis on the existence of critical electric field at the surface of heavy nuclei. Their work was mainly interested in the study of the possibility of having process of vacuum polarization at the surface of heavy nuclei to be possibly achieved by heavy nuclei collisions (see for a review (83)). Paradoxically at the time we were not interested in this very important aspect and we did not compute the strength of the field in our relativistic Thomas-Fermi model which is indeed of the order of the Critical Field $E_c = m^2c^3/e\hbar$.

Nuclear matter in bulk: $A \approx 300$ or $A \approx (m_{Planck}/m_n)^3$.

The situation clearly changed with the discovery of GRBs and the understanding that the process of vacuum polarization unsuccessfully sought in earthbound experiments could indeed be observed in the process of formation of a Black Hole from the gravitational collapse of a neutron star (83). The concept of a Dyadosphere, (84; 85), was introduced around an already formed Black Hole and it became clear that this concept was of paramount importance in the understanding the energy source fo GRBs. It soon became clear that the initial conditions for such a process had to be found in the electrodynamical properties of neutron stars. Similarly manifest came the crucial factor which had hampered the analysis of the true electro dynamical properties of a neutron star; the unjustified imposition of local charge neutrality as opposed to the global charge neutrality of the system. We have therefore proceeded to make a model of a nuclear matter core of $A \approx (m_{Planck}/m_n)^3$ nucleons (1). We generalized to this more general case the concept introduced in their important work by W. Greiner and V. Popov (see Fig. E.3(a) and Fig. E.3(b)) as follows.

I have assumed that the proton number density is constant inside the core $r \leq R_c$ and vanishes outside the core $r > R_c$:

$$n_p = \frac{1}{3\pi^2\hbar^3}(P_p^F)^3 = \frac{3N_p}{4\pi R_c^3}\theta(R_c - r), \quad R_c = \Delta\frac{\hbar}{m_\pi c}N_p^{1/3},$$

where P_p^F is the Fermi momentum of protons, $\theta(R_c - r)$ is the step-function and Δ is a parameter. The proton Fermi energy is

$$\mathcal{E}_p(P_p^F) = [(P_p^F c)^2 + m_p^2 c^4]^{1/2} - m_p c^2 + eV, \tag{E.0.9}$$

where e is the proton charge and V is the Coulomb potential. Based on the Gauss law, $V(r)$ obeys the Poisson equation $\nabla^2 V(r) = -4\pi e \left[n_p(r) - n_e(r)\right]$ and boundary conditions $V(\infty) = 0, \quad V(0) = finite$, where the electron number density $n_e(r)$ is given by

$$n_e(r) = \frac{1}{3\pi^2\hbar^3}(P_e^F)^3, \tag{E.0.10}$$

being P_e^F the electron Fermi momentum. The electron Fermi energy is

$$\mathcal{E}_e(P_e^F) = [(P_e^F c)^2 + m^2 c^4]^{1/2} - mc^2 - eV. \tag{E.0.11}$$

The energetic equation for an electrodynamic equilibrium of electrons in the Coulomb potential $V(r)$ is $\mathcal{E}_e(P_e^F) = 0$, hence the Fermi momentum and the electron number density can be written as

$$n_e(r) = \frac{1}{3\pi^2\hbar^3 c^3}\left[e^2 V^2(r) + 2mc^2 eV(r)\right]^{3/2}.$$

Introducing the new variable $x = r/(\hbar/m_\pi c)$ (the radial coordinate in unit of pion Compton length $(\hbar/m_\pi c)$, $x_c = x(r = R_c)$), I have obtained the following relativistic Thomas-Fermi Equation ((86; 66)):

$$\frac{1}{3x}\frac{d^2\chi(x)}{dx^2} = -\alpha\left\{\frac{1}{\Delta^3}\theta(x_c - x) - \frac{4}{9\pi}\left[\frac{\chi^2(x)}{x^2} + 2\frac{m}{m_\pi}\frac{\chi}{x}\right]^{3/2}\right\}, \tag{E.0.12}$$

where χ is a dimensionless function defined by $\frac{\chi}{r} = \frac{eV}{c\hbar}$ and α is the fine structure constant $\alpha = e^2/(\hbar c)$. The boundary conditions of the function $\chi(x)$ are $\chi(0) = 0 \quad , \quad \chi(\infty) = 0$ and $N_e = \int_0^\infty 4\pi r^2 dr n_e(r)$. Instead of using the phenomenological relation between Z and A, given by Eqs. (E.0.6) and (E.0.7), we determine directly the relation between A and Z by requiring the β-equilibrium

$$\mathcal{E}_n = \mathcal{E}_p + \mathcal{E}_e. \tag{E.0.13}$$

The number-density of degenerate neutrons is given by $n_n(r) = \frac{1}{3\pi^2\hbar^3}(P_n^F)^3$, where P_n^F is the Fermi momentum of neutrons. The Fermi energy of degenerate neutrons is

$$\mathcal{E}_n(P_n^F) = [(P_n^F c)^2 + m_n^2 c^4]^{1/2} - m_n c^2, \tag{E.0.14}$$

where m_n is the neutron mass. Substituting Eqs. (E.0.9, E.0.11, E.0.14) into

Eq. (E.0.13), we obtain $[(P_n^F c)^2 + m_n^2 c^4]^{1/2} - m_n c^2 = [(P_p^F c)^2 + m_p^2 c^4]^{1/2} - m_p c^2 + eV$. These equations and boundary conditions form a close set of non-linear boundary value problem for a unique solution for Coulomb potential $V(r)$ and electron distribution (E.0.10), as functions of the parameter Δ, i.e., the proton number-density n_p. The solution is given in Fig. E.4(a). A relevant quantity for exploring the physical significance of the solution is given by the number of electrons within a given radius r, $N_e(r) = \int_0^r 4\pi(r')^2 n_e(r')dr'$. This allows to determine, for selected values of the $A = N_p + N_n$ parameter, the distribution of the electrons within and outside the core and follow the progressive penetration of the electrons in the core at increasing values of A (see Fig. E.4(b)). We can then evaluate, generalizing the results in (15; 18) , the net charge inside the core $N_{\rm net} = N_p - N_e(R_c) < N_p$, and consequently determine of the electric field at the core surface, as well as within and outside the core (see Fig. E.5).

The energetically favorable configurations.

Introducing the new function ϕ defined by $\phi = \Delta \left[\frac{4}{9\pi}\right]^{1/3} \frac{\chi}{x}$, and putting $\hat{x} = \Delta^{-1}\sqrt{\alpha}\,(12/\pi)^{1/6}\,x$, $\xi = \hat{x} - \hat{x}_c$ the ultra-relativistic Thomas-Fermi equation can be written as

$$\frac{d^2\hat{\phi}(\xi)}{d\xi^2} = -\theta(-\xi) + \hat{\phi}(\xi)^3, \tag{E.0.15}$$

where $\hat{\phi}(\xi) = \phi(\xi + \hat{x}_c)$. The boundary conditions on $\hat{\phi}$ are: $\hat{\phi}(\xi) \to 1$ as $\xi \to -\hat{x}_c \ll 0$ (at massive core center) and $\hat{\phi}(\xi) \to 0$ as $\xi \to \infty$. We must also have the continuity of the function $\hat{\phi}$ and the continuity of its first derivative $\hat{\phi}'$ at the surface of massive core $\xi = 0$.

Eq. (E.0.15) admits an exact solution

$$\hat{\phi}(\xi) = \begin{cases} 1 - 3\left[1 + 2^{-1/2}\sinh(a - \sqrt{3}\xi)\right]^{-1}, & \xi < 0, \\ \frac{\sqrt{2}}{(\xi+b)}, & \xi > 0, \end{cases} \tag{E.0.16}$$

where integration constants a and b are: $\sinh a = 11\sqrt{2}$, $a = 3.439$; $b = (4/3)\sqrt{2}$.

We than have for the Coulomb potential energy, in terms of the variable ξ, $eV(\xi) = \left(\frac{1}{\Delta^3}\frac{9\pi}{4}\right)^{1/3} m_\pi c^2 \hat{\phi}(\xi)$, and at the center of massive core $eV(0) = \hbar c(3\pi^2 n_p)^{1/3} = \left(\frac{1}{\Delta^3}\frac{9\pi}{4}\right)^{1/3} m_\pi c^2$, which plays a fundamental role in order to determine the stability of the configuration.

It is possible to compare energetic properties of different configurations satisfying the different neutrality conditions $n_e = n_p$ and $N_e = N_p$, with the same core radius R_c and total nucleon number A. The total energy in the case

$n_e = n_p$ is

$$\mathcal{E}^{\mathrm{loc}}_{\mathrm{tot}} = \sum_{i=e,p,n} \mathcal{E}^i_{\mathrm{loc}},$$
$$\mathcal{E}^i_{\mathrm{loc}} = 2\int \frac{d^3r d^3p}{(2\pi\hbar)^3}\epsilon^i_{\mathrm{loc}}(p) =$$
$$\frac{cV_c}{8\pi^2\hbar^3}\left\{\bar{P}^F_i[2(\bar{P}^F_i)^2 + (m_i c)^2][(\bar{P}^F_i)^2 + (m_i c)^2]^{1/2} - (m_i c)^4 \mathrm{Arsh}\left(\frac{\bar{P}^F_i}{m_i c}\right)\right\}$$

The total energy in the case $N_e = N_p$ is

$$\mathcal{E}^{\mathrm{glob}}_{\mathrm{tot}} = \mathcal{E}_{\mathrm{elec}} + \mathcal{E}_{\mathrm{binding}} + \sum_{i=e,p,n} \mathcal{E}^i_{\mathrm{glob}}$$
$$\mathcal{E}_{\mathrm{elec}} = \int \frac{E^2}{8\pi} d^3r \approx \frac{3^{3/2}\pi^{1/2}}{4}\frac{N_p^{2/3}}{\sqrt{\alpha}\Delta c} m_\pi \int_{-\kappa R_c}^{+\infty} dx\,[\phi'(x)]^2$$
$$\mathcal{E}_{\mathrm{binding}} = -2\int \frac{d^3r d^3p}{(2\pi\bar{h})^3} eV(r) \approx -\frac{V_c}{3\pi^2\hbar^3}(P^F_e)^3 eV(0)$$
$$\mathcal{E}^i_{\mathrm{glob}} = 2\int \frac{d^3r d^3p}{(2\pi\bar{h})^3}\epsilon^i_{\mathrm{glob}}(p) =$$
$$\frac{cV_c}{8\pi^2\hbar^3}\left\{P^F_i[2(P^F_i)^2 + (m_i c)^2][(P^F_i)^2 + (m_i c)^2]^{1/2} - (m_i c)^4 \mathrm{Arsh}\left(\frac{P^F_i}{m_i c}\right)\right\}.$$

We have indicated with $\bar{P}^F_i$ $(i = n, e, p)$ the Fermi momentum in the case of local charge neutrality ($V = 0$) and with P^F_i ($i = n, e, p$) the Fermi momentum in the case of global charge neutrality ($V \neq 0$). The energetic difference between local neutrality and global neutrality configurations is positive, $\Delta\mathcal{E} = \mathcal{E}^{loc}_{tot} - \mathcal{E}^{\mathrm{glob}}_{\mathrm{tot}} > 0$, so configurations which obey to the condition of global charge neutrality are energetically favorable with respect to one which obey to the condition of local charge neutrality (86; 87). For a core of 10 Km the difference in binding energy reaches 10^{49} ergs which gives an upper limit to the energy emittable by a neutron star, reaching its electrodynamical ground state.

The current work is three fold: **a)** generalize our results considering the heavy nuclei as special limiting cases of macroscopic nuclear matter cores (66), **b)** describe a macroscopic nuclear matter core within the realm of General Relativity fullfilling the generalized Tolman, Oppenheimer, Volkoff equation (88), **c)** Generalyze the concept of a Dyadosphere to a Kerr-Newman Geometry (89).

Conclusions.

It is clear that any neutron star has two very different components: the core with pressure dominated by a baryonic component and the outer crust with pressure dominated by a leptonic component and density dominated by the nuclear species. The considerations that we have presented above apply to the first component where the baryonic pressure dominates. It is clear that when the density increases and baryons become ultra-relativistic is this baryonic component which undergoes the process of gravitational collapse and its dynamics is completely dominated by the electrodynamical process which we have presented in this talk.

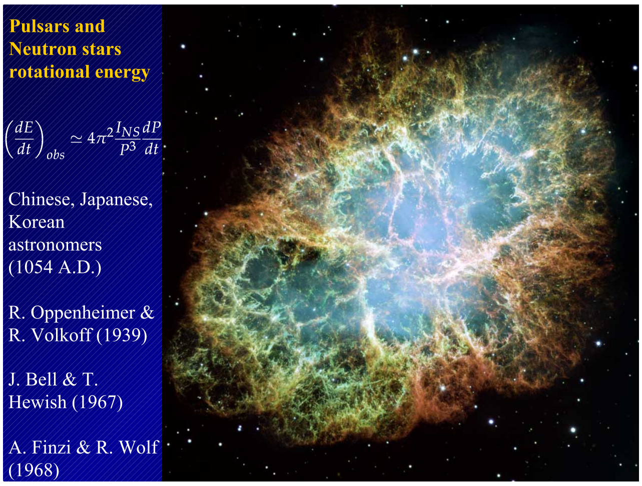

(a)

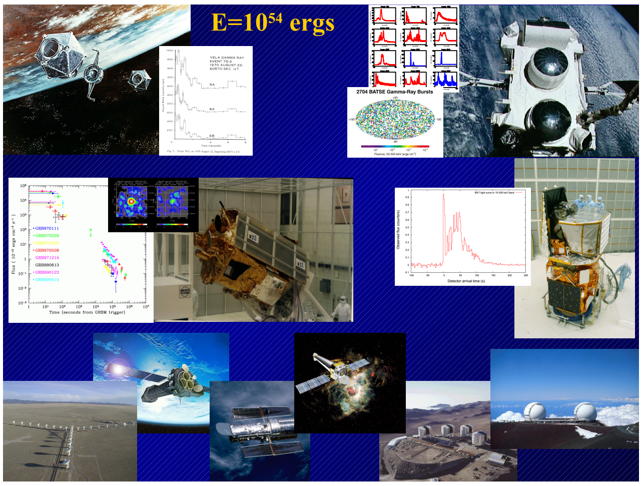

(b)

Figure E.1.: (a) The expanding shell of the remnant of the Crab Nebulae as observed by the Hubble Space Telescope. Reproduced from Hubble Telescope web site with their kind permission (News Release Number: STScl-2005-37). (b) On the upper left the Vela 5A and 5B satellites and a typical event as recorded by three of the Vela satellites; on the upper right the Compton satellite and the first evidence of the isotropy of distribution of GRB in the sky; on the center left the Beppo Sax satellite and the discovery of the after glow; on the center right a GRB from Integral satellite; in the lower part the Socorro very large array radiotelescope ,the Hubble, the Chandra and the XMM telescopes, as well as the VLT of Chile and KECK observatory in Hawaii. All these instruments are operating for the observations of GRBs (76).

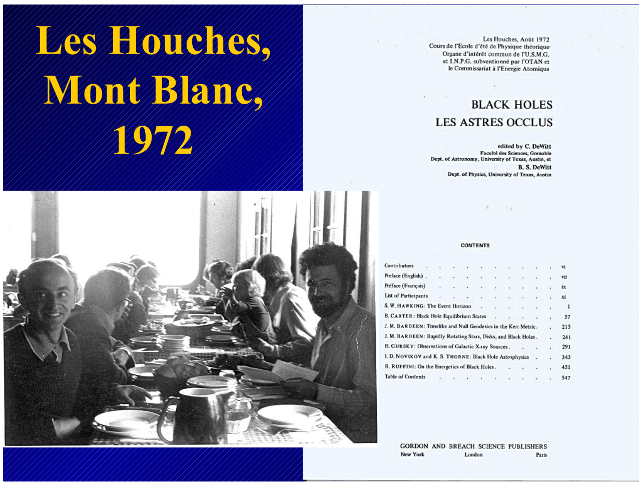

(a)

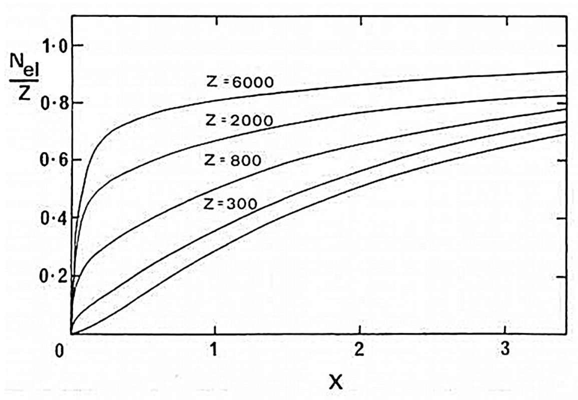

(b)

Figure E.2.: (a) Lunch at Les Louces summer school on 'Black Holes'. In front, face to face, Igor Novikov and the author; in the right the title of the book in English and in French. It is interesting that in that occasion Cecile de Witt founded the French translation of the word 'Back Hole' in 'Trou Noir' objectionable and she introduced instead the even more objectionable term 'Astres Occlus'. The French neverthless happily adopted in the following years the literally translated word 'Trou Noir' for the astrophysical concept I introduced in 1971 with J.A. Wheeler ((82)). (b) The number of electrons contained within a distance x of the origin, as a function of the total number Z for a neutral atom. The lowest curve is that given by the solution of the non-relativistic Thomas-Fermi equation.

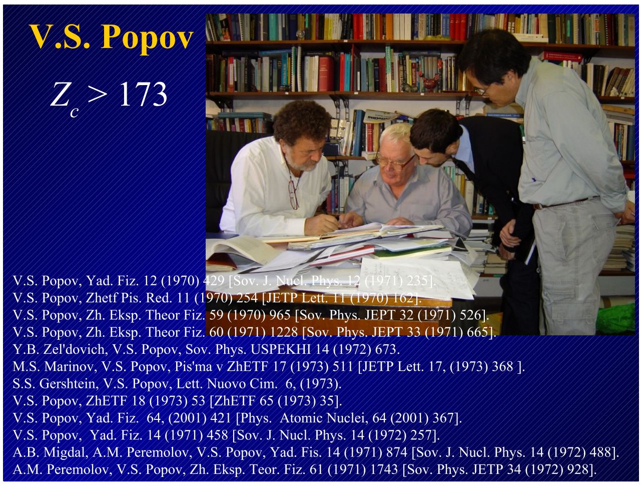

(a)

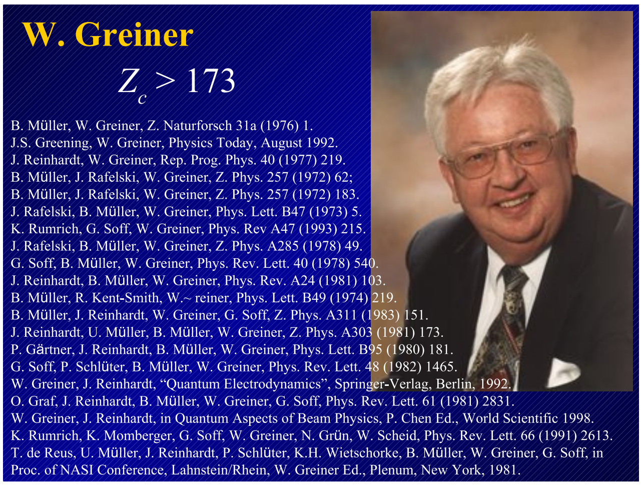

(b)

Figure E.3.: (a) Vladimir Popov discussing with the author and Professors She Sheng Xue and Gregory Vereshchagin (Roma 2007). Also quoted the classical contributions of Popov and his school. (b) Walter Greiner and the citation of classical papers by him and his school.

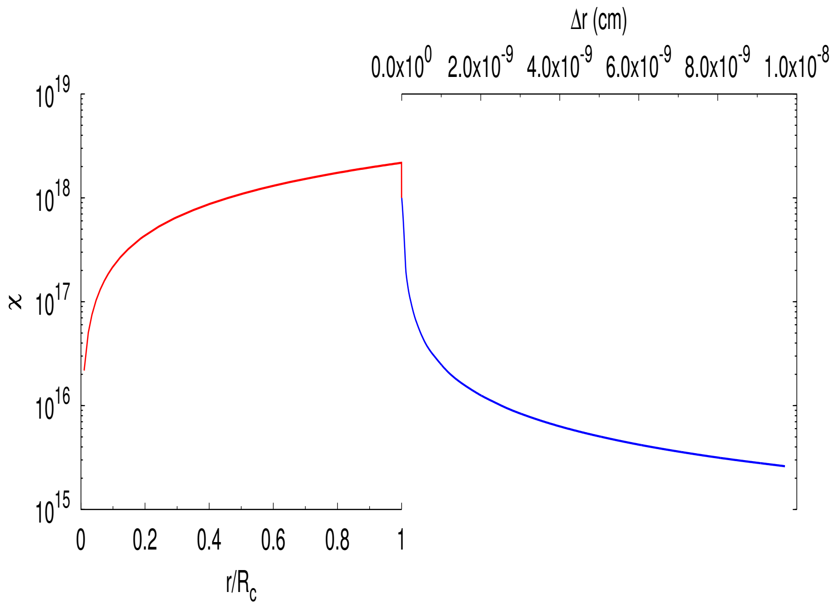

(a)

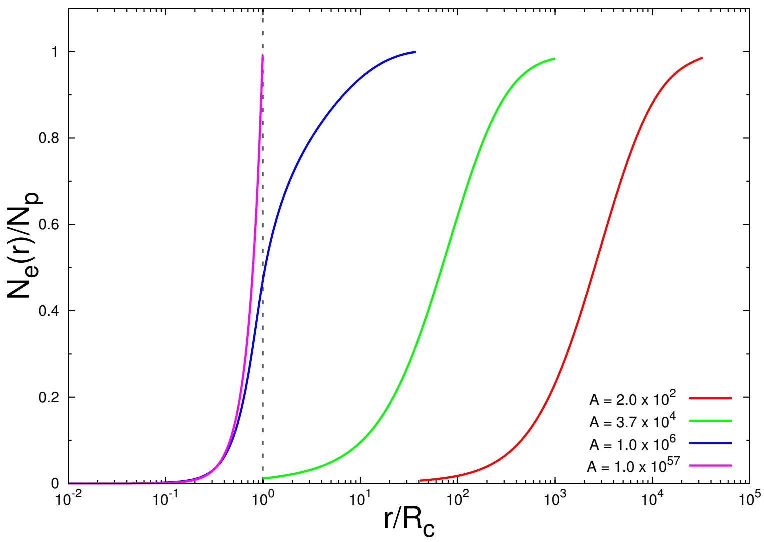

(b)

Figure E.4.: (a) The solution χ of the relativistic Thomas-Fermi Equation for $A = 10^{57}$ and core radius $R_c = 10$km, is plotted as a function of radial coordinate. The left solid line corresponds to the internal solution and it is plotted as a function of radial coordinate in unit of R_c in logarithmic scale. The right dotted line corresponds to the solution external to the core and it is plotted as function of the distance Δr from the surface in the logarithmic scale in centimeter. (b) The electron number in the unit of the total proton number N_p, for selected values of A, is given as function of radial distance in the unit of the core radius R_c, again in logarithmic scale. It is clear how by increasing the value of A the penetration of electrons inside the core increases.

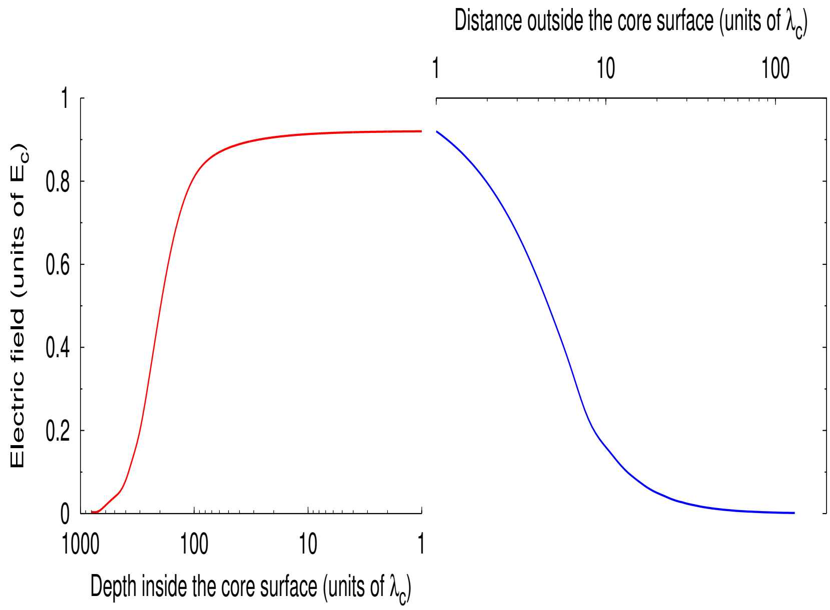

Figure E.5.: The electric field in the unit of the critical field E_c is plotted around the core radius R_c. The left (right) solid (dotted) diagram refers to the region just inside (outside) the core radius plotted logarithmically. By increasing the density of the star the field approaches the critical field.

Bibliography

[1] R. Ruffini, M. Rotondo and S.-S. Xue, Int. J. Mod. Phys. D **16**, 1 (2007).

[2] J. Madsen, Phys. Rev. Lett. **100**, 151102 (2008).

[3] P. C. C. Freire et al., `arXiv:0711.2028v1`.

[4] P. C. C. Freire et al., ApJ, **679**, 1433 (2008).

[5] C.E. Rhoades and R. Ruffini, Phys. Rev. Lett. **28**, 1235 (1972).

[6] J.M. Lattimer and M. Prakash, Phys. Rep. **442**, 109 (2007).

[7] A. Mezzacappa and G.M. Fuller, "Open Issues in Core Collapse Supernova Theory," World Scientific 2005.

[8] R. Ruffini, in *Proceedings of the Eleventh Marcel Grossman Meeting*, R. Jantzen, H. Kleinert, R. Ruffini (eds.), (World Scientific, Singapore, 2008).

[9] W. Pieper and W. Greiner, Z. Phys. **218**, 327 (1969).

[10] J. S. Greenberg and W. Greiner, Physics Today, August, **24** (1982).

[11] B. Müller, H. Peitz, J. Rafelski and W. Greiner, Phys. Rev. Lett. **32**, 324 (1974).

[12] V. S. Popov, Sov. Phys. JETP **32**, 526 (1971).

[13] Ya. B. Zeldovich and V. S. Popov, Sov. Phys. USP. **14**, 673 (1972).

[14] A. B. Migdal, D. N. Voskresenskii and V. S. Popov, Sov. Phys. JETP Lett. **24**, 186 (1976).

[15] J. Ferreirinho, R. Ruffini and L. Stella, Phys. Lett. B **91**, 314 (1980).

[16] W. Heisenberg and H. Euler, Z. Phys. **98**, 714 (1936).

[17] E. Segré, "Nuclei and Particles", Second Edition, W. A. Benjamin 1977.

[18] R. Ruffini and L. Stella, Phys. Lett. B **102**, 442 (1981).

[19] T. Damour and R. Ruffini, Phys. Rev. Lett. **35**, 463 (1975).

[20] R. P. Kerr, Phys. Rev. Lett. **11**, 273 (1963).

[21] A. G. Aksenov, R. Ruffini and G. V. Vereshchagin, Phys. Rev. Lett. **99**, 125003 (2007).

[22] R. Oppenheimer and G. M. Volkoff, Phys. Rev. **55**, 374 (1939).

[23] B. K. Harrison et al., "Gravitational theory and gravitational collapse," (University of Chicago Press, Chicago, 1965).

[24] G. Baym, H. A. Bethe and C. J. Pethick, Nuc. Phys. A **175**, 225 (1971).

[25] B. Patricelli, M. Rotondo, J. A. Rueda H. and R. Ruffini., in *Proceedings of the Fifth Italian-Sino Workshop*, D. Lee, W. Lee, S.-S. Xue (eds.), AIP Conf. Proc., Vol. 1059, pp. 68-71 (2008).

[26] B. Patricelli, J. A. Rueda H. and R. Ruffini, in *Proceedings of the Third Stueckelberg Workshop*, G. Montani and G. W. Vereshchagin (eds.), (World Scientific, 2008, in preparation).

[27] J. A. Rueda H., B. Patricelli, M. Rotondo, R. Ruffini and S. S. Xue, in *Proceedings of the Third Stueckelberg Workshop*, G. Montani and G. W. Vereshchagin (eds.), (World Scientific, 2008, in preparation).

[28] H. Andréasson, `arXiv:0804.1882v1`.

[29] E. Lieb and B. Simon, Phys. Rev. Lett. 31, (1973) 681.

[30] I. Pomeranchuk and Ya. Smorodinsky, J. Phys., USSR 9, (1945) 97.

[31] S. S. Gershtein and Ya. B. Zeldovich, Soviet Physics JETP, Vol. 30, (1970) 385.

[32] B. Muller and J. Rafelski, Phys. Rev. Lett., Vol. 34, (1975) 349.

[33] A. B. Migdal, D. N. Voskresenskii and V. S. Popov, JETP Letters, Vol. 24, No. 3 (1976) 186.

[34] F. Sauter, Z. Phys. 69 (1931) 742.

[35] J. Schwinger, Phys. Rev. 82 (1951) 664; J. Schwinger, Phys. Rev. 93 (1954) 615; J. Schwinger, Phys. Rev. 94 (1954) 1362.

[36] G. Gamow, "Constitution of Atomic Nuclei and Radioactivity", Clarendon Press, Oxford, 1931.

[37] J. R. Oppenheimer and G. Volkoff, Phys. Rev. D55, 374 (1939).

[38] R. Ruffini and S. Bonazzola, Phys. Rev. D187, (1969) 1767.

[39] H. A. Bethe, G. Börner and K. Sato, Astron. & Astrophys. 7, (1970) 279.

[40] A. G. W. Cameron Annual Reviews Inc. (1970) 179.

[41] L. H. Thomas, Proc. Cambridge Phil. Society, 23, (1927) 542-548.

[42] E. Fermi, Rend. Accad. Lincei 6, (1927) 602-607.

[43] G. Scorza-Dragoni, Rend. Accad. Lincei 8, (1928) 301; 9, (1929) 378 .

[44] A. Sommerfeld, Z. Physik 78, (1932) 283 .

[45] C. Miranda, Mem. Accad. Italia 5, (1934) 285-322.

[46] E. Lieb, Rev. Mod. Physics 53, (1981) 603-642.

[47] L. Spruch, Rev. Mod. Physics 63, (1991) 151-209.

[48] R. Ruffini, M. Rotondo and S.-S. Xue, submitted to Phys. Rev. Lett. .

[49] P. A. M. Dirac, Proc. Roy. Soc. 117 (1928) 610; P. A. M. Dirac, Proc. Roy. Soc. 118 (1928) 341.

[50] P. A. M. Dirac, "Principles of Quantum Mechanics", Clarendon Press, Oxford, 1958.

[51] W. Gordon, Z. Phys. 48 (1928) 11.

[52] C. G. Darwin, Proc. Roy. Soc. A118 (1928) 654.

[53] A. Sommerfeld, Atomau und Spektrallinien, 4. Aufl. ,6. Kap.

[54] N. Case, Phys. Rev. 80 (1950) 797.

[55] F. G. Werner and J. A. Wheeler, Phys. Rev. 109 (1958) 126.

[56] V. Vorankov and N. N. Kolesinkov, Sov. Phys. JETP 12 (1961) 136.

[57] V. S. Popov, Yad. Fiz. 12 (1970) 429 [Sov. J. Nucl. Phys. 12 (1971) 235].

[58] V. S. Popov, Zhetf Pis. Red. 11 (1970) 254 [JETP Lett. 11 (1970) 162]; V. S. Popov, Zh. Eksp. Theor Fiz. 59 (1970) 965 [Sov. Phys. JEPT 32 (1971) 526].

[59] V. S. Popov, Zh. Eksp. Theor Fiz. 60 (1971) 1228 [Sov. Phys. JEPT 33 (1971) 665].

[60] M. S. Marinov and V. S. Popov, Pis'ma v ZhETF 17 (1973) 511 [JETP Lett. 17, (1973) 368]; G. Siff, B. Müller and J. Rafelski, Zeits. Naturforsch 292 (1974) 1267.

[61] V. S. Popov, Yad. Fiz. 64, (2001) 421 [Phys. Atomic Nuclei, 64 (2001) 367].

[62] Review article: J. Rafelski, L.P. Fulcher and A. Klein, Phys. Reps. 38 (1978) 227.

[63] Review article: W. Greiner, B. Müller and J. Rafelski, “Quantum Electrodynamics of Strong Fields” Monograph in Physics, ISBN 3-540-13404-2 Springer-Verlag Berlin Heidelberg (1985) (references there in).

[64] H. Kleinert, R. Ruffini and S.-S. Xue, to appear in Phys. Rev. D (2008).

[65] S. W. Hawking, Nature 238 (1974) 30; S. W. Hawking, Commun. Math. Phys. 43, 199 (1975); G. W. Gibbons and S. W. Hawking, Phys. Rev. D 15 2752 (1977).

[66] B. Patricelli, M. Rotondo and R. Ruffini, “On the Charge to Mass Ratio of Neutron Cores and Heavy Nuclei, AIP Conference Proceedings”, Vol. 966 (2008), pp. 143-146.

[67] R. Eisberg, R. Resnick, “Quantum Physics of Atoms, Molecules, Solids, Nuclei, and Particles”, Second Edition, J. Wiley & Sons, 1985

[68] E. Olson, M. Bailyn, Phys. Rev. D, Vol. 18, pp. 6, 1978

[69] G. Baym, C. Pethick and P. Sutherland, Astrophysical Journal, Vol. 170, pp. 299, 1971

[70] S. L. Shapiro, S. A. Teukolsky, “Black Holes, White Dwarfs, and Neutron Stars - The Physics of Compact Objects”, WILEY - VCH, 2004

[71] M. G. Dainotti et al., in preparation

[72] I. S. Shlkvoskii, *Supernovae*, (Wiley, New York, 1968).

[73] R. N. Manchester and J. H. Taylor, *Pulsars*, (Freeman and Co., San Francisco, CA, 1977).

[74] R. Ruffini, From the ergosphere to the dyadosphere in *Festschrift in Honor of Roy Kerr*, D. Wildshire (ed.), (Cambridge University Press, 2008).

[75] H. Gursky and R. Ruffini, *Neutron Stars, Black Holes and Binary X-Ray Sources*, (Springer, 1975).

[76] R. Ruffini, M. G. Bernardini, C. L. Bianco, L. Caito, P. Chardonnet, M. G. Dainotti, F. Fraschetti, R. Guida, M. Rotondo, G. Vareshchagin, L. Vitagliano and S. S. Xue, in *Cosmology and Gravitation: XII th Brazilian School of Cosmology and Gravitation* , M. Novello, S. E. Perez Bergliaffa (eds.), AIP Conf. Proc., 910, 55 (2007).

[77] E. Costa et al., *Nature* **387**, 783 (1997).

[78] A. M. Soderberg et al., `arXiv:0802.1712v1`.

[79] L. D. Landau and E. M. Lifshitz, *Non-Relativistic Quantum Mechanics*, (Pergamon Press, Oxford, 1975).

[80] R. Ruffini, On the energetics of Black Holes in *Black Holes - Les astres occlus*, C. and B.S. De Witt (eds.) , (Gordon and Breach, New York, 1972).

[81] L. D. Landau, *Phys. Z. Sowjetunion* **1**, 285 (1932).

[82] R. Ruffini and J. A. Wheeler, *Phys. Today* **24**, 30 (1971).

[83] R. Ruffini, G. Vereshchagin and S. S. Xue , Progress Report, in preparation, (2008).

[84] R. Ruffini, in *Black Holes and High Energy Astrophysics*, H. Sato and N. Sugiyama (eds.), 167 (Universal Academic Press, Tokyo, 1998).

[85] G. Preparata , R. Ruffini and S. S. Xue, *Astron. Astroph.* 338, L87 (1998).

[86] M. Rotondo, R. Ruffini and S. S. Xue, in *Relativistic Astrophysics: 4th Italian-Sino Workshop*, C.L. Bianco, S.S. Xue (eds.) , AIP Conf. Proc., 966, 147 (2007).

[87] R. Ruffini, M. Rotondo and S. S. Xue, in preparation, (2008).

[88] J. Rueda, M. Rotondo and R. Ruffini, in preparation, (2008).

[89] C. Cherubini, A. Geralico, J. A. H. Rueda and R. Ruffini, in *Relativistic Astrophysics: 4th Italian-Sino Workshop*, C.L. Bianco, S.S. Xue (eds.) , AIP Conf. Proc., 966, 123 (2007).